Integrated Thermal and Daylight Performance Comparison of Single and Double Glass Skin Façade for Hot Climate Conditions

By: Naif Altahlawi

Committee Members:

Chairman: James Jones

Elizabeth Grant

Adnan Adas

Robert Schubert

General Audience Abstract

Improving the quality of indoor environments is a main goal in today's architecture. Towards this goal, the use of glass and curtain walls is common in office buildings. The building façade is a key factor for the amount of energy consumed to reach comfort levels in the building. That is, because facades influence lighting, glare, heat gain, noise safety and energy usage. Therefore, the use of glass improves transparency which can interfere with comfort levels inside the building due to solar heat gain. The Double Skin façade system is widely adopted in Europe and has been shown to reduce energy used for heating in cold weather. In winter, heat losses can be reduced as the system's intermediate cavity acts as a thermal buffer. However, there is no clear understanding of how the system will perform in hot arid climate conditions where cooling is the dominant operating mode. A Double Skin Façade can provide shading during the overheating period, while having the desired glass elevations sought by designers. This is due to ventilation and solar control devices located inside the system's cavity. Being placed between the interior and the exterior glass panels, solar control devices are protected from the weather, which in return decreases its size. Furthermore, the additional glass panel allows windows in the system's inner layer to be opened for natural ventilation. Unfortunately, the performance of the Double Skin Façade system for hot arid climate is not well documented. Therefore, the primary goal of this research is to compare the thermal and light performance of the Double Skin Façade system to a single façade system for hot weather conditions.

Academic Abstract

Visual integration of the building interior and exterior is one of the charms of today's architecture. The Double-Skin facade system is a technology that can reduce the drawbacks of using glass in a building's elevation. In fact, the double-skin façade (DSF) offers transparency while reducing energy consumption when compared to single-skin systems in cold and moderate weather conditions. However, there is no clear evidence of how the system will perform in hot climate conditions. In this research, a testing procedure was established to experimentally evaluate the performance of the double-skin façade system, data was collected to create multiple regression models, and then evaluate the double-skin façade's performance and compare it to a single-skin system in hot arid climate conditions.

Dedication

My dissertation is proudly and wholeheartedly dedicated to my beloved parents. My dear mother, thank you for your endless love, prayers and support through this journey. To my father who was my source of inspiration, advice and encouragement. With both of you believing in this dissertation, I was able to be strongly motivated to achieve such success and honor.

To my lovely wife, Alwaleedah Murad; who stood by me through this journey and continually inspired me with her hope, love and support. To my daughters, Ruby and Lulya, and our new born son, Tarek; for your care, patience and unyielding love that has inspired me to pursue and complete this research.

I would also like to offer my gratitude to my advisor, Dr. James Jones, for his insightful guidance, educational insights and support while conducting my research. Thank you for your early inspiration, coaching and enthusiasm from the beginning of this journey.

I am further grateful to thank all the members of my committee. Dr. Elizabeth Grant, Dr. Adnan Adas and Mr. Robert Schubert, for your continuing support, guidance, and sharing your kind words of advice and encouragement to complete this dissertation.

Lastly, to my dear family, my brothers Fahad, Meshal and Turki, my sister Naifa, and to my friends, thank you for all of your constant boosts of encouragement, and support.

Table of Contents

1. Introduction

1.1 General information

Buildings directly impact both manmade and outdoor environments. With today's growing global population, the building industry has rapidly become one of the largest market sectors. According to Baden (2006), "As of 2001, buildings used 40 percent of the energy consumed both in the US and the European Union" (p.8). A study by the US Department of Energy (2006) also noted that "39 percent of the total amount of carbon dioxide in the United States can be attributed to buildings" (p. 346). Clearly, the building industry merits consideration in efforts to conserve natural resources. The architect's responsibility is to become aware of the impact buildings have on the natural environment and adopt strategies toward sustainable "green" buildings. One system with a promising future is the double-skin façade, one well utilized in European architecture. Implementing this system reportedly has reduced the energy needed for heating, cooling and lighting. Case studies show that double-skin façades usually increase indoor environmental quality and occupant satisfaction.

1.2 Role of the façade in building energy use

Building façades are no longer integral to today's structural system, but are more like skins that protect building interiors. A façade covers the sides of the building as an external layer and is highly visible. Its materials and textures, as well as chosen colors, shape a building's very character. As Compagno (2000) noted, "façades to a certain extent are the letter of introduction to the architectural work, the first thing we see. They may seduce us or make us despair, and through their reading one can imagine the nature of what is hidden behind them" (p.9). The oldest principle in architecture is to create a shelter to protect from solar radiation, wind, rain, and temperature. A façade's duty reaches far beyond providing shelter. It must also react to mixed weather conditions in offering personal comfort. Thus, in modern architecture, new façade systems and technologies are being adopted to meet such requirements.

Of course, HVAC technologies help buildings meet comfort requirements. Yet, the better the skin performs, the less energy consumed in achieving a consistent level of comfort. Recently, designers and researchers have shown interest in the role the façade plays in a building's energy usage.

Growing awareness of global warming and its environmental impacts have led architects and policymakers around the globe to find solutions to reduce building energy consumption. Since façades influence lighting, heat gain, sound protection, safety, glare and energy usage, the external skin is a key factor in the level of energy consumed by any given building.

The type of building façade must be selected after careful consideration. Many planning and analysis methods should be studied before adopting a particular system for a building. According to Mostaedi (2002), "any serious inquiry must address the following; 1) Function: what is the practical purpose of the building / the building skin? 2) Construction: what are the elements / components of the building / building skin, and how are these elements assembled into a whole? 3) Form: what does the building / building skin look like? 4) Ecology: what is the energy consumption of the building / building skin during construction, use, and demolition?" (p.29). All of the preceding questions should be considered when determining the type of system that will perform best in certain environmental conditions. Additionally, the energy consumed to achieve a consistent comfort level is highly influenced by all of these aspects.

1.3 Desire for transparency and window usage

Visual integration of the building interior and exterior is one of the charms of today's architecture. To soften the indoor-outdoor boundary, "glass curtain walls" are prized for enhancing environmental quality and transparency. A wide variety of glazing systems are available today to achieve this goal. In the past, concern over energy consumption constrained window area and transparency for a building. As a result, daylight available for indoor space was very minimal. Today's glass curtain wall determines the levels of light and heat entering the building to significantly affect comfort levels and influence the quality of the interior. The 2010 ASHRAE Standard 90.1 limit for the window-to-wall ratio has been reduced from 40 to 30 percent for US buildings. The use of shading, active day-lighting and window coating can reverse this percentage decline in window area.

Conventional masonry architecture has consisted of large volumes of solid masonry with small window areas. Centuries ago, construction glass was limited to avoid heat loss. Windows were cherished building elements with high heat transfer rates that increased energy consumption. This persisted until construction technologies advanced to allow larger openings typical in structures today. After the Industrial Revolution, the ratio of solids to

voids developed in favor of the voids in façades of low- and high-rise structures. Today, physical transparency is prolific in various buildings, and the desire to showcase transparent elevations is now possible using modern design.

Architects have designed in concert with the glass industry new, simpler glass elevations. These new systems aim to maximize glass area by limiting non-transparent support elements like mullions. This collaboration has produced a new curtain wall several stories high with no visible structure. Such modern glass systems now require coatings to control solar radiation admission into buildings. Compagno (2000) said, "many systems are now available for the use of glass in façades, all aimed at achieving maximum transparency by reducing the non-transparent support structure" (p.15). Experimental studies and simulations have shown that even wintertime solar radiation can produce undesirable heat gain inside the building. Precise design and proper consideration becomes crucial when selecting a system for given environmental conditions. Solar control, heat flow, and glass coatings should be exploited to favor large glass openings in towers.

1.4 Double-skin system as a solution

The double-skin system is a technology that can reduce the drawbacks of using glass in a building elevation. In fact, the double-skin façade (DSF) offers transparency while reducing energy consumption when compared to single-skin systems. The DSF comprises several layers working together to control both light and heat admission: an exterior glass layer, a cavity housing a solar-control device, and an internal glass layer. DSF usage is suitable for reducing energy use and outdoor noise transmission while maintaining the option of natural ventilation.

Significant reduction in energy consumption may be achieved by proper use of the double-skin system versus single-skin systems. Since double-skin façade performance is profoundly influenced by weather conditions, it is crucial to craft a robust system that exploits the surrounding environment. For the downtown office building, sound insulation offered by double-skin systems can be significant. The outer layer acts as a sound-insulating wall that protects the building from unwanted noise, lowering the need for sound reduction by inner façade layers. Of course, the level of external-layer sound insulation depends on the size and location of the openings.

The system can be adopted in both high- and low-rise structures. In high-rise buildings, the extra layer of glass can limit structural wind pressures. Furthermore, the additional glass panel allows windows to be opened

even on these upper floors. Such natural ventilation can prove essential in reducing both the cost and energy consumption of air conditioning.

Sick building syndrome (SBS) is a growing health issue where building users suffer ill health and discomfort after spending extended periods indoors. This issue arises from a lack of fresh air circulation. Compagno (1995) said, "Natural ventilation of offices by fresh air is much more acceptable to the building's users, and it has the additional benefits of reducing investment in air handling systems and also reducing energy consumption" (p.94).

Another advantage of the double-skin façade system is that it provides shade using cavity-housed solar-control devices during periods of overheating. To cut maintenance costs, the solar control devices are placed between the interior and the exterior glass panels to protect the devices from weather conditions. As solar radiation heats the outer glass panes, cavity air temperature increases such that the air rises for upper vent extraction to remove the heat. Overheating should be avoided in the cavity during the summer months by forcibly increasing the airflow inside the cavity.

Wintertime heat loss can be reduced as the central cavity insulates as a thermal buffer. Air between the two panes of glass helps form a warmer inner layer so that less heat is lost through the glass, and less heating energy is thus needed during winter. Here, rooms near windows are better insulated and require less energy to achieve thermal comfort. Advantages of the DSF system will be explained in depth in Chapter 2.

In conclusion, double-skin façades have great potential to reduce energy consumption and cost. According to Oesterle (2001), "Taking account of investment and ongoing cost, a comparison of the two alternatives showed that the combination of a two-layered façade with supporting ventilation was ultimately more economical than a single-layer façade with internal air conditioning" (p.26). Even though an extra glass layer adds to the cost of construction, studies have shown that the double-skin system can prove economically viable in high- and low-rise constructions.

1.5 Reported benefits using the double-skin system

Many reported benefits are associated with double-skin system usage.

- Transparency: the glass skin improves space quality by enhancing transmitted light and scenery.

- Energy cost reduction: 1) Energy savings were reported owing to the extra thermal barrier against winter heat loss.

  2) DSF acts as a semi-external shading layer.

  3) Cavity vents the heat and allows daylight.

  4) Depending on the climate, DSFs can limit the size of mechanical cooling systems for direct savings in the installation cost.

- Natural ventilation: the system controls pressures, particularly for upper floors of the building while acting as a layer attenuating lower-floor urban noise.

- Enhanced thermal comfort: improvement in thermal comfort was reported when using double-skin systems since the inner pane surface temperature is closer to room temperature. Furthermore, natural night-time ventilation allows for the removal of heat radiated by indoor furniture and fixtures.

- Heat recovery: when coupled with active airflow, the DSF creates the opportunity for heat recovery and transfer.

1.6 Issues driving the need for this study

Since the double-skin system offers reduced building energy consumption, it has been adopted recently in developed lands after these countries have suffered decades of inefficient building systems and materials. Earlier, fully glazed buildings were highly wasteful with single panes experiencing huge heat gains and losses. Thus, they required excessive operation of the heating or air-conditioning system to maintain comfort. Before the mid-1970s energy price inflation, there was little concern for efficiency. In the early 1970s, a worldwide oil embargo forced the building industry to reconsider glass use in façades. Now, new technologies and low-E glass materials have become popular. While these new glass technologies have reduced energy consumption, it is recognized that the façade system has further potential to reduce energy usage. The double glass façade is among these technologies.

When compared to a single-glass façade, the double-skin system typically incurs higher installation and maintenance cost. This arises from the extra glass and skill level of installers needed to build as well as to more often

maintain and service the system. Still, the cost of additional engineering, labor, and material may yet be offset by the reduction in energy needed to operate the facility's HVAC system. The need for skilled labor to build and service the DSF is a major concern when adopting the DSF.

Today's developing countries are recognizing the importance of energy-efficient buildings in general, and the enclosure system in particular. Case-in-point is the Middle East: new facilities in that region have modern designs copied from Western countries, and most use glass curtain walls that admit heat. Due to its location, the weather is hot every day. Buildings with large window-to-wall ratios, in turn, must be cooled all year. Furthermore, clients fear designing a sustainable building that they deem expensive and unnecessary. Also, clients are skeptical of the payback period and the profitability of sustainable investment, an attitude that consequently hinders consideration of systems like the double-skin system.

1.7 Problem statement

The double-skin system enjoys wide acceptance in England, Germany, and other parts of Europe. The United States and developing countries have limited numbers of buildings that use this system. With the growing demand for sustainable buildings, further studies are needed to show the amount of savings that the system can provide. DSF cost-effectiveness is not well established for Saudi Arabia, and this requires further research. Adopting DSF technology for newer European buildings has shown much promise as a solution to reduce facility energy consumption, but this has applied primarily in cold and moderate climates.

While the system might also have value in hot weather conditions, the potential savings are unclear. In hot climates, the cavity may rise in temperature to the point of requiring increased airflow to minimize heat transfer into the inner layer. In this case, mechanical ventilated systems offer the best potential to conserve energy for lower HVAC costs. Purposeful adjustments to the system may optimize cavity heat removal. Natural ventilation may also help reduce nighttime HVAC system usage. Added electricity to drive the mechanically ventilated double-skin system is also a factor since fan operation counters the benefit of DSF somewhat. Fan maintenance is costly, and improper operation and servicing of the system may yield underperformance that increases energy consumption.

Little research has asked how the system will perform in hot climate conditions such as in the Middle East. Further investigation is needed to know how well the system will act in hot, arid climates. Cavity temperature may escalate in these conditions. Consequently, it is vital to know if cavity temperatures will exceed desirable limits affecting the inner glass surfaces.

This study will compare two different systems: the single base layer versus a mechanically ventilated double-skin façade system using eQUEST energy simulation and statistical equations that will be described in later chapters. Since there is not yet a precise procedure to evaluate the system, this study will determine the appropriate methods by which the double-skin façade may be assessed for hot, arid climates. Furthermore, this research will specify the desirable façade configuration of each system for the hot climate condition.

1.8 Approach and method description

The use of double-skin façades has the potential to reduce energy consumption when compared to traditional construction approaches. According to Bailey (1997), "a double-skin system and building management system is expected to reduce between half and two-thirds of energy cost compared to conventional buildings." However, there is no clear evidence to support this claim. The double-skin façade system performance depends on interacting variables. This research focused on studying the behavior of the double envelope system, seeking to evaluate the energy performance of the system by collecting experimental data for use in numerical simulations. An experiment was conducted to study the thermal and light performance of the DSF versus window system for real weather and solar conditions.

Thermal performance of a double-skin façade system depends on a number of variables described in Chapter 3. Energy savings of this system are not well established, and further research must quantify the double-skin façade system's impact on facility energy consumption, particularly in hot, arid climates. The double-skin system will next be assessed against current systems using data from eQUEST simulations against calculations of the DSF performance in the city of Riyadh, Saudi Arabia. The research objectives are:

1) Experimentally test a double-skin envelope system.
2) Collect on-site data for a range of sun and weather conditions.
3) Statistically analyze light and thermal performances in regression form.
4) Create a statistical model of performance for use in heat removal rate calculations for a double skin façade system.
5) Simulate a representative building in hot, arid climate conditions.
6) Use weather data of the city of Riyadh, Saudi Arabia to calculate heat removal rate for a double skin façade system,
7) Summarize the energy-related findings.
8) Summarize the analysis procedure.

Results of this work are expected to make two specific contributions to the body of knowledge:

1) A new analysis procedure will be designed to determine the energy-related performance of double-skin façades in hot, arid climates.

2) Through this new analysis, the applicability of double-skin façades in a hot, arid climate will be inferred via simulation of a typical office tower.

Chapter 2 Literature Review

2.1 Introduction

Chapter 2 presents a brief history of the double-skin façade system and describes its typical system layers and materials. System operation modes are next defined and compared. Then the double-skin system's numerous advantages are described with documented examples in the literature. Thermal-acoustic insulation benefits are detailed with supporting data to explain the system's operating capacity for cutting energy consumption. DSF shading is deemed one of the key advantages in using a double skin. A case study for venetian blinds showcases the benefits a shading device brings to a facility's day-lighting strategy. Chapter 2 concludes describing different types of double-skin systems, chronicling previous research, and offering conclusions.

2.2 System description

2.2.1 History of the double-skin system

The idea of the double-skin system is not new. These systems evolved from an early concept of creating a thermal buffer between inside and outside layers of glass. Early examples can be found in old Swiss farmhouses. Those traditional buildings were oriented to the sun by being built into south-facing slopes with double glass "box-type" windows. This type of window had two layers of glass adjustable during the summer so that the inside layer could be opened and the external layer removed for air to enter the building. In winter, both layers were kept in place for passive air heating in the buffer space to reduce the need for supplemental heating.

In modern architecture, the same concept is adopted to reduce energy usage by countering heat gain in the summer and heat loss in the winter, to minimize indoor lamps and muffle outdoor noise. An early version of a double-skin building system was first proposed by Jean-Baptiste in 1849 for an industrial museum that was described as two layers of glass encasing a cavity to contain hot air during the winter and cool air during the summer.

In the early 1900s, interest in the system blossomed. Paul Sheerbeart described in 1914 a concept similar to the double-envelope system in his book Glass Architecture (Scheerbeart, 1914). In 1929, Le Corbusier devised a system circulating air at the interior temperature through a cavity in the envelope of the building. Le Corbusier believed that heat gain and loss through the wall could be reduced, even though system performance was poorer than expected. His early experiments proved unsuccessful heating air in the winter and cooling the air in summer (Banham, 1969).

As the 1950s began, new airflow studies were conducted and published in Scandinavia with the purpose of improving energy efficiency in buildings. In the late 1960s, the first office building using the double envelope (box-plot window) was built in Helsinki, Finland (Brandle and Boehm, 1982; Ripatti, 1984; and Park et al., 1989). One early example inspiring architects to use double-skin systems to limit heat transmission through the building skin was the Sugar Company in Peterborough, UK (Crowely, 1975).

Following the oil embargo of the 1970s, the need for using energy-efficient technologies became fundamental in the building industry. The use of mechanically ventilated windows to reduce energy has continued to grow across Europe. The goal has remained to reduce heat loss in the winter and to minimize solar and heat gains in the summer. In the United States, however, very few buildings were adopting this technology with the goal of saving energy. The Occidental building at Niagara Falls and the Coca-Cola facility in Charlotte were rare examples.

2.2.2 System Layers

A typical double-skin envelope system incorporates three layers of glass. According to Kragh (2000), the double-skin façade is "a system that consists of an external screen, a ventilated cavity, and an internal screen. Solar shading is typically positioned in the ventilated cavity. The external and internal screens can be single glass or double glazed units. The depth of the cavity and the type of ventilation depend on environmental conditions, the desired envelope performance and the overall design of the building including environmental systems" (p.49). The relative positions of the single- and double-glazed units depend on the cavity ventilation strategy, passive versus mechanical, and the concern for condensation. The layers of the system and their descriptions appear next.

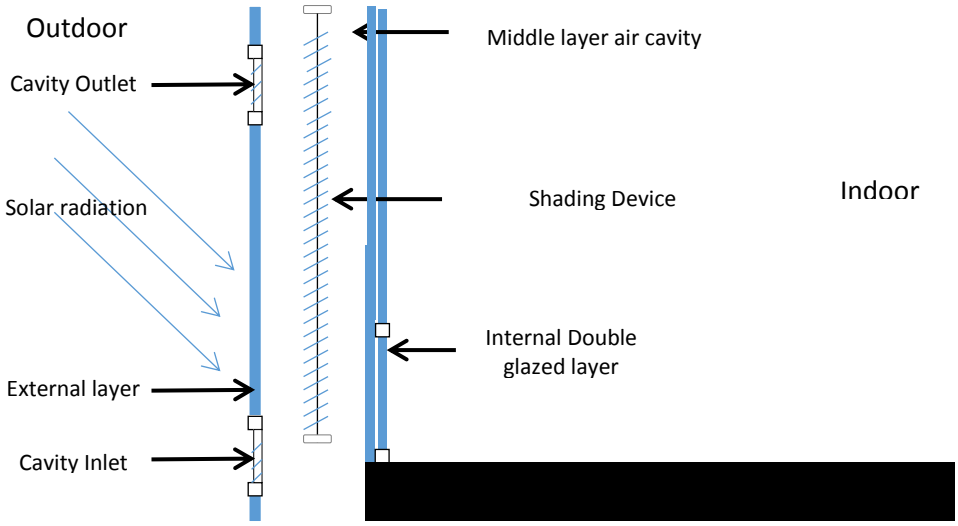

Figure 2.1 Double-skin layers diagram (naturally vented with external ports)

- External layer: the exterior façade of the building. Usually, this part of the system is a naturally vented cavity that includes single glass panels that offer protection from weather as well as reduction in sound transmission.
- Middle layer: usually up to a two-meter-wide air channel between the exterior and interior layers. This part of the system allows air to be heated by solar energy and ventilated naturally through outer window openings or by using exhaust fans. Furthermore, solar shading devices can be integrated into this layer and automatically controlled to adjust the amount of light passing into the building.
- Internal layer: the internal layer for the naturally ventilated system is a double layer of low-E glass that engages the supporting framework.

Solar properties for the glass used in the double-skin system are not much different from that of the single-skin façade. Nevertheless, the additional skin works as a thermal buffer to reduce heat loss and capture passive solar gain. During the winter, heated cavity air can be used for warming the inside of the building. On the other hand, during hot summer months, expelling hot cavity air can buffer heat gains. By exploiting adaptable configurations, the system works well in different climates and locations.

2.2.3 Glass as a building material

Glass is usually defined as supercooled liquid or transparent material that is cooled without crystallizing. Mostaedi (2002) noted, "various chemical substances can form glass: among the inorganic ones are principally the oxide of silicon, boron, germanium, phosphorus, and arsenic" (p.11). Glazing performance is influenced by its structure and composition.

Transparency is what makes this material desirable. Light transmission and transparency make glass one of the most important materials adopted in buildings today. Glass properties admit light rays without losing focus while protecting occupants from weather conditions.

The human eye can see only part of the solar radiation spectrum, with the visible portion range in the 380 to 780 nm wavelength band. Radiation in the wavelength band of 315-3000 nm can pass through glazing with some absorption by the glass. Much of the light passing through the glass is converted to longwave (infrared) radiation that cannot transmit back out – a phenomenon known as the greenhouse effect.

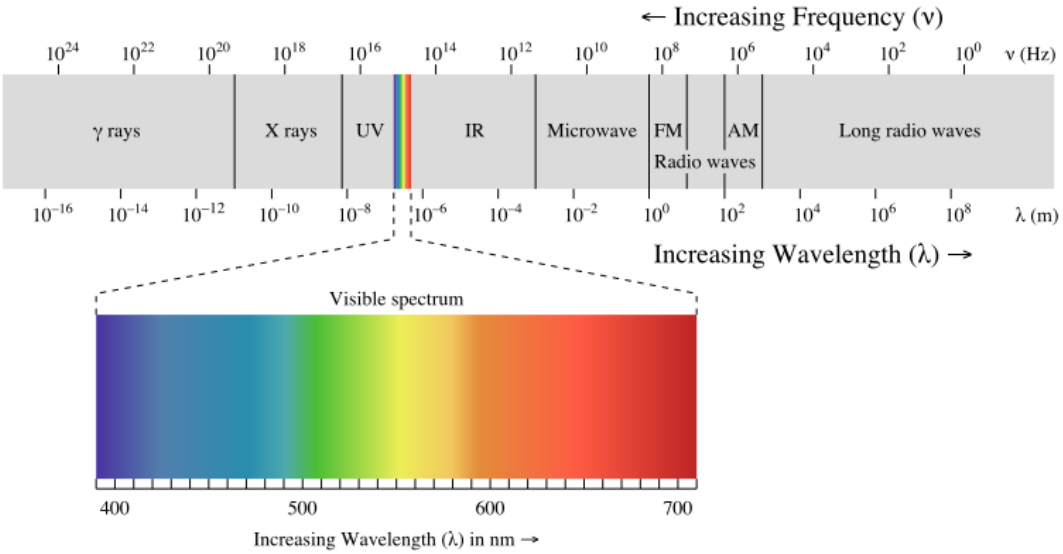

Figure 2.2 According to Brainard (2010) "Visible light waves"

The quality of light in any room is influenced by levels of light and glare. As for incoming light, Compagno (2000) advised, "the lighting intensity should be approximately 2/3 to 1/10 of the interior field lighting intensity. Hence, it is important to select and position glare protection elements in a manner that provides evenly distributed daylight without glare, while avoiding unnecessary cooling loads in the interior space" (p.31).

Total solar energy transmission, or "G-factor" energy passing through the glass, is the aggregate heat transferred to the interior as radiation, convection, and conduction. Thin glass conducts more than thick glass. New coating technologies can alter radiation transfer, while convection can be controlled by modifying the construction. Surface coatings such as low-E films are thin layers of metal-oxide on the glazing. The metal layer acts to reflect much solar radiation in cutting transmission and absorption. As mentioned in the ASHRAE Handbook of Heat Fundamentals, the overall heat admission through the glass material depends on the amount of the heat flow inward by convection plus radiation admitted through the glass. Heat flow can be expressed as:

$$Q_a = E_{td} + E_{tg} + Q_{RCI}$$

Q_a = Instantaneous heat admission due to fenestration, Btu/h-ft²
E_{td} = Transmitted direct solar radiation, Btu/h-ft²
E_{tg} = Heat radiated inward from hot glass, Btu/h-ft²
Q_{RCI}= Rate of heat convection inward, Btu/h-ft²

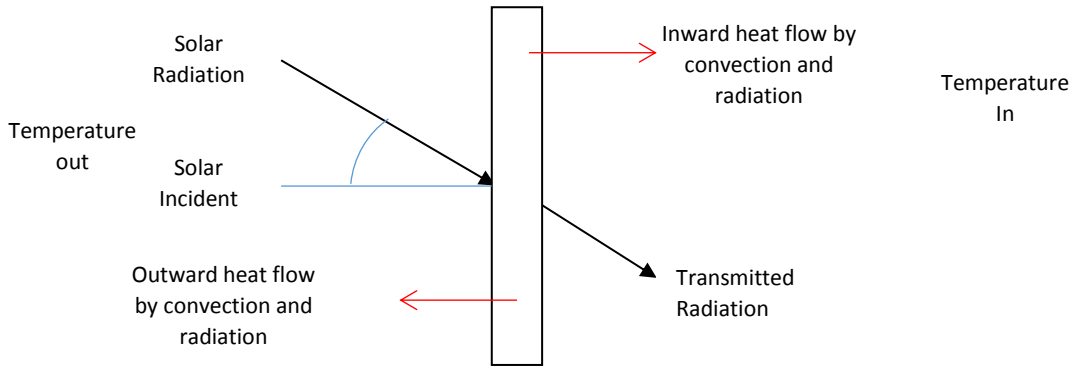

Figure 2.3 Instantaneous heat balance for sunlit glazing material

Admitted solar radiation can accumulate in the room by heating objects with large thermal mass storing this energy for release back into the room. The angle of the incoming solar radiation affects all levels of heat passing through, reflected, and absorbed by the glass in the radiant heat budget. Heat from hot glass introduced to the room is known as "inward heat flow by convection and radiation."

In the summer, minimizing inward heat flow is significant to the building's energy consumption. Reducing heat gain can reduce the amount of energy needed for air conditioning.

One factor that affects the glass system performance is the temperature difference between the air indoors and outdoors. Heat conduction rises with this temperature difference: the greater the temperature spread, the more heat is conducted through the glass. Conduction can be important during extreme weather with very hot or frigid winds. Conductive heat transfer rates can be estimated using the window's U-value in units of heat transfer per hour per area for a given temperature difference.

On the other hand, minimizing outward heat flow in winter is significant to reducing energy needed for heating. The difference between the indoor room temperature and the outdoor temperature drives heat loss as governed by the U-value of the glass. According to Compagno (1996), "thermal conductance, U-value, is the rate of loss of heat per square meter, for a temperature difference of one degree Kelvin between the inner and the outer environments separated by glass" (p.14). Thus, new technologies enlisting glass films, double glazing, and systems like the double envelope are gaining favor since they lower the effective U-value.

Building Regulations Approved Document L1 – Conservation of fuel and power in dwellings (2002 edition) is an approved document written by the government of the UK. Among requirements listed in *Building Regulations* are the following U-value reference tables reprinted on the next page.

Table A1 Indicative U-values (W/m²·K) for windows and rooflights with wood or PVC-U frames, and doors

	Gap between panes			Adjustment for rooflights in dwellings[5]
	6mm	12mm	16mm or more	
Single glazing		4.8		+0.3
Double glazing (air filled)	3.1	2.8	2.7	
Double glazing (low-E, ε_n = 0.2)[1]	2.7	2.3	2.1	
Double glazing (low-E, ε_n = 0.15)	2.7	2.2	2.0	
Double glazing (low-E, ε_n = 0.1)	2.6	2.1	1.9	
Double glazing (low-E, ε_n = 0.05)	2.6	2.0	1.8	
Double glazing (argon filled)[2]	2.9	2.7	2.6	
Double glazing (low-E ε_n = 0.2, argon filled)	2.5	2.1	2.0	
Double glazing (low-E ε_n = 0.1, argon filled)	2.3	1.9	1.8	
Double glazing (low-E ε_n = 0.05, argon filled)	2.3	1.8	1.7	+0.2
Triple glazing	2.4	2.1	2.0	
Triple glazing (low-E, ε_n = 0.2)	2.1	1.7	1.6	
Triple glazing (low-E, ε_n = 0.1)	2.0	1.6	1.5	
Triple glazing (low-E, ε_n = 0.05)	1.9	1.5	1.4	
Triple glazing (argon filled)	2.2	2.0	1.9	
Triple glazing (low-E ε_n = 0.2, argon filled)	1.9	1.6	1.5	
Triple glazing (low-E ε_n = 0.1, argon filled)	1.8	1.4	1.3	
Triple glazing (low-E ε_n = 0.05, argon filled)	1.7	1.4	1.3	
Solid wooden door[4]		3.0		

L1 TABLES OF U-VALUES

A2 Indicative U-values (W/m²·K) for windows with metal frames (4mm thermal break)

	gap between panes		
	6mm	12mm	16mm or more
Single glazing		5.7	
Double glazing (air filled)	3.7	3.4	3.3
Double glazing (low-E, ε_n = 0.2)	3.3	2.8	2.6
Double glazing (low-E, ε_n = 0.1)	3.2	2.6	2.5
Double glazing (low-E, ε_n = 0.05)	3.1	2.5	2.3
Double glazing (argon filled)	3.5	3.3	3.2
Double glazing (low-E, ε_n = 0.2,argon filled)	3.1	2.6	2.5
Double glazing (low-E, ε_n = 0.1, argon filled)	2.9	2.4	2.3
Double glazing (low-E, ε_n = 0.05, argon filled)	2.8	2.3	2.1
Triple glazing	2.9	2.6	2.5
Triple glazing (low-E, ε_n = 0.2)	2.6	2.2	2.0
Triple glazing (low-E, ε_n = 0.1)	2.5	2.0	1.9
Triple glazing (low-E, ε_n = 0.05)	2.4	1.9	1.8
Triple glazing (argon-filled)	2.8	2.5	2.4
Triple glazing (low-E, ε_n = 0.2, argon filled)	2.4	2.0	1.9
Triple glazing (low-E, ε_n = 0.1, argon filled)	2.2	1.9	1.8
Triple glazing (low-E, ε_n = 0.05, argon filled)	2.2	1.8	1.7

Note
For windows and rooflights with metal frames incorporating a thermal break other than 4mm, the following adjustments should be made to the U-values given in Table A2.

Figure 2.4 According to Building Regulations Approved Document L1 - Conservation of fuel and power in dwellings (2002 edition) "Table of U-Values"

2.2.4 System operating modes

2.2.4.1 Natural ventilation

The performance of the double envelope depends mostly on the design and operation of the interstitial cavity vented naturally or mechanically. Naturally ventilated cavities depend on air temperature differences to drive thermal buoyancy. Solar radiation enters the cavity, causing the air to rise in temperature and decline in density toward the upper openings for outdoor exhaust. The system is both easy and simple, but it poses risks. If the cavity is not well designed, solar heat gain in the system cavity may accumulate to the point of cavity overheating.

In the naturally ventilated system, air is suctioned into the heated cavity and exhausted by the stack effect. The stack effect alone can ventilate the system in low- or no-wind conditions. Solar radiation absorbed inside the cavity increases the air temperature while thus reducing its density. Less dense air rises and vents naturally through the port to remove heat.

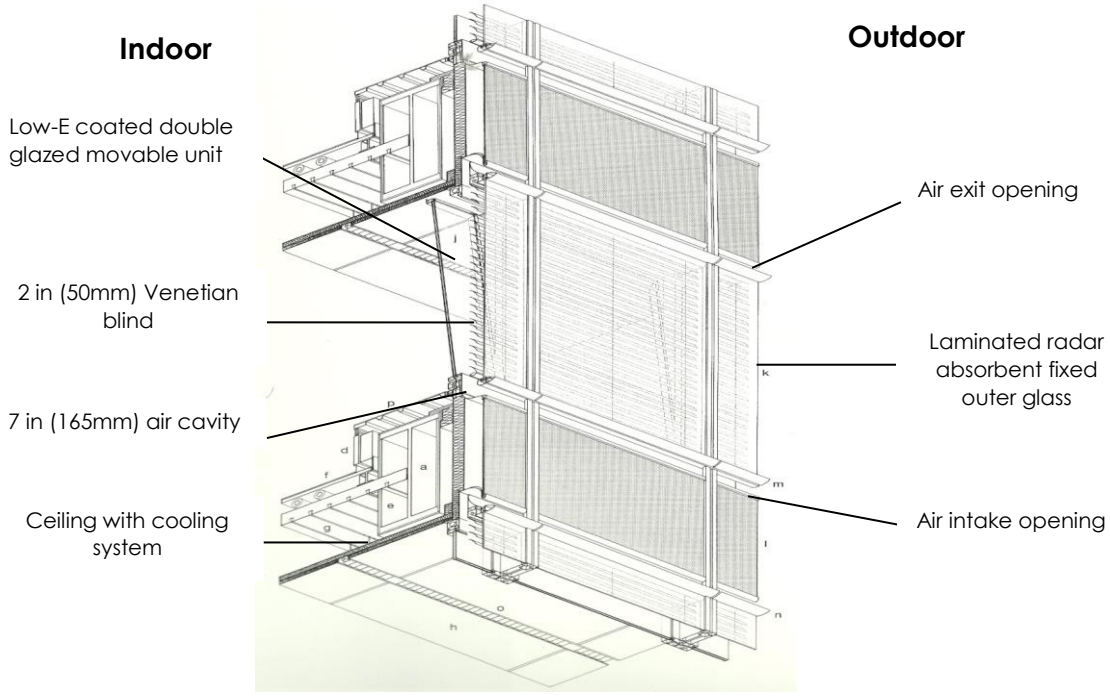

Figure 2.5 According to Fischer (1997), "Commerzbank naturally ventilated double-skin section" (p.27)

Also in play is any wind flowing over the building façade that can develop a pressure difference between ports in the cavity. Care must be taken to ensure that stack-driven and wind-driven pressures are not counteractive.

Air inside the cavity may overheat, driving more heat to the indoor space. Of course, hot cavity air rules out opening the inner pane for ventilation.

Under certain conditions, natural ventilation may experience issues like sound transmission and overheating that may disturb indoor environments. Therefore, a natural ventilation double-skin system seems better suited for winter applications where captured cavity heat maintains its temperature closer to the indoor air temperature.

A good building example of using a natural ventilated double-skin system is the Commerzbank headquarters in Frankfurt, Germany designed by Norman Foster, well recognized for his adoption of modern technologies. Outer offices are ventilated directly from the outdoors. Though high-rise buildings such as this one usually have upper-floor windows that cannot be opened and exposed to high-speed winds, the Commerzbank facility is entirely ventilated naturally. Adopting the double-skin system permits windows to be opened in this building for natural ventilation. Reportedly, Commerzbank Headquarters is one of Europe's most efficient buildings.

Here, the external layer is a fixed single pane of glass, and the inner layer is an openable double-glazed, low-E window. Outdoor air enters the lower opening of the window and moves up the cavity by the stack effect, removing hot air from office spaces when the inner windows are open. The cavity is 7" (165mm) wide. In the cavity are venetian blinds controlled automatically by a computer reacting to weather conditions and sunlight. The management system tilts the blinds to reflect sunlight deeper into the building or closes them to block excessive heat. Strategies adopted in the facility, including the sky-garden, double-skin and building management systems, are estimated to save from half to two-thirds of the energy used in typical offices (Bailey, 1997).

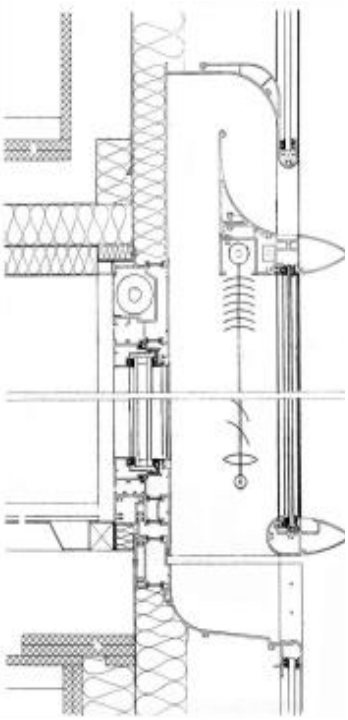

Figure 2.6 According to Davies and Lambot (1997), "Section view of the Commerzbank"

The unique design of the building with a three-floor winter garden positions the fourth floor to act as a sunroom with a single-skin glass façade. In winter, the office area with double-skin layers can be naturally ventilated, and hot air from the cavity can be mechanically vented into the building to reduce

the need for heating. The natural ventilation in offices neighboring the winter garden works better than for outer-edge offices since the garden acts as a thermal buffer warming the whole tower.

For spring and fall seasons when outdoor temperatures are not frigid, mechanical ventilation is not necessary. During summer nights, the heat stored inside the building is removed with external air, thus lowering the need for cooling during the day. The building is also cooled by a static water cooling system located in the ceiling panels. Water is chilled by refrigerating machines. The design of the Commerzbank Headquarters meets the goal of reduced energy consumption by adopting a unique garden space, atrium areas and a double envelope system that operates under control of an electronic building management system.

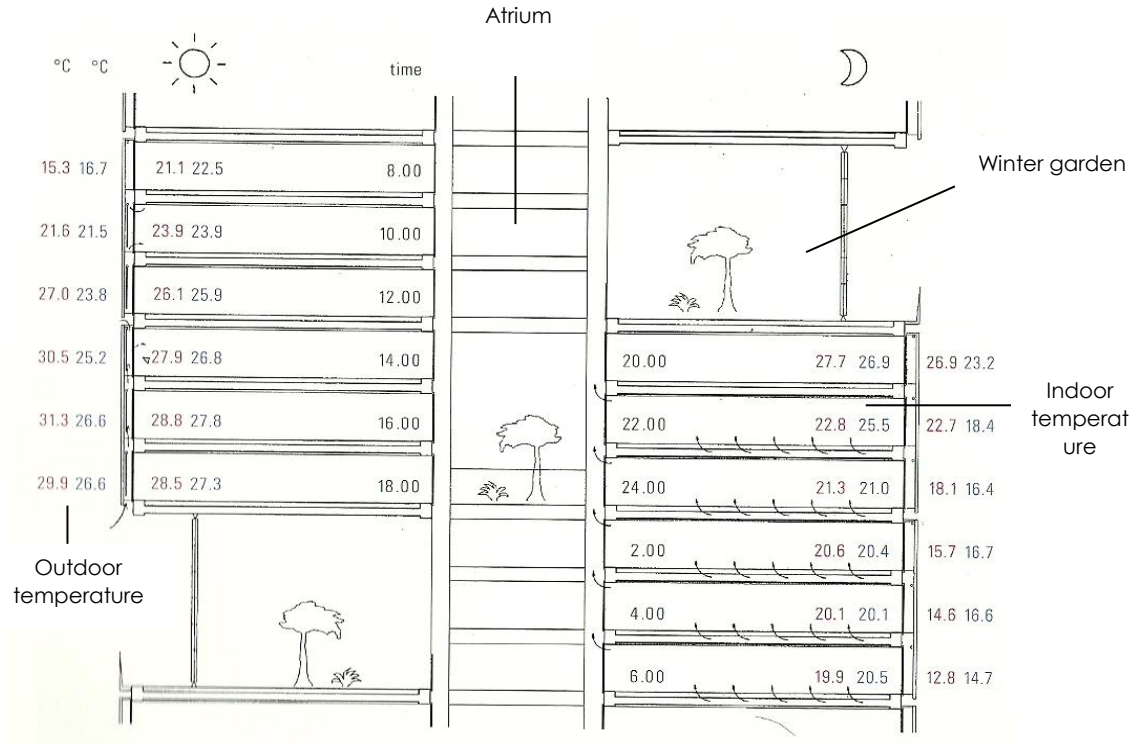

Figure 2.7 According to Daniels (1997), "Temperature simulations (24 hours) in offices, external and room temperatures over the course of one day: left column day, right column night" (p.95)

2.2.4.2 Mechanical ventilation

Mechanical ventilation systems generally use electric fans located on the top of the window cavity to exhaust hot air using suction. In winter, fans are off to allow air inside the cavity to rise in temperature. In summer, the fans activate to exhaust air outdoors for air temperature in the cavity to remain lower than for the naturally ventilated system. More moderate cavity temperatures lessen inner-layer heat gain. Since each system has its own advantages, the optimal choice should be based on location, air quality, and cost to determine which system will be most useful. Mechanically ventilated double-skin systems allow sealing the building, thus providing more protection from sound and air pollution than naturally ventilated systems. In addition, for locations with severe weather conditions and poor outdoor air quality, the MV-DSF system allows for a better indoor environment. Recirculating the air may also lower the risk of condensation and pollution in the cavity as well as in the building itself.

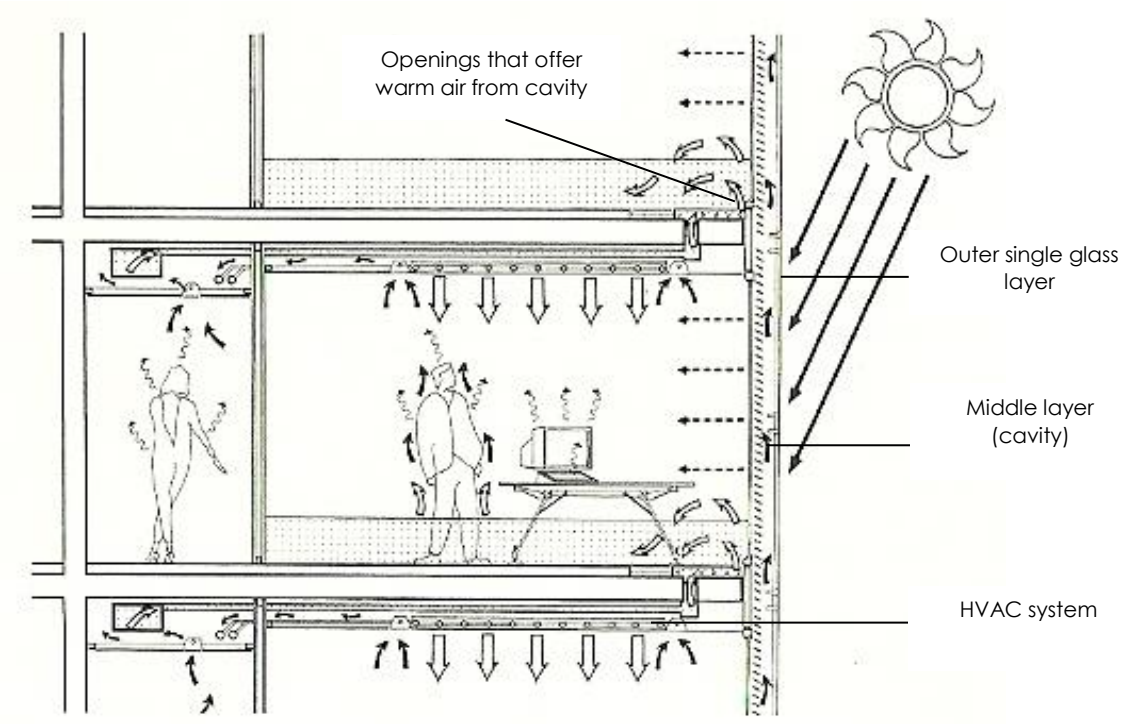

Figure 2.8 According to Compagno (1996), "Mechanically ventilated system"

The Business Promotion Center located in Duisburg, Germany is a good example of a mechanically ventilated double-skin façade. Designed by Norman Foster, the building is seven stories, or 30 meters, tall. The building fulfills "German codes that are very strict and regulate the detailing of exterior cladding" (Barreneche, 1995). This double-skin envelope of the building enlists single-glazed outer panels fixed by aluminum tension rods, low-e, double-glazed inner glass panels, and an 8"- wide (200 mm) cavity. Located inside the cavity are venetian blinds that provide solar control. The ventilation system in the building uses mechanical fans to supply and exhaust cavity air to ensure proper distribution.

Air driven into the cavity by mechanical fans removes heat gain in the cavity. Air continues upward to either be exhausted in summer or introduced inside for winter heating. Air is not directly from outside, thus offering less potential risk of condensation and pollution in the cavity (Barreneche, 1995).

Furthermore, the mechanically ventilated system allows an airtight building, thus securing more protection from outside weather and street noise.

Air rises through the continuous cavity by the stack effect for expulsion through openings on the top of the cavity. In summer, the increased airflow removes more heat, reducing heat gain through the inner glass layer. In winter, cavity air heated by solar radiation functions as a buffer and provides warm air for office areas inside. Architects examined this facility's function and site prior to optimizing the curtain wall design.

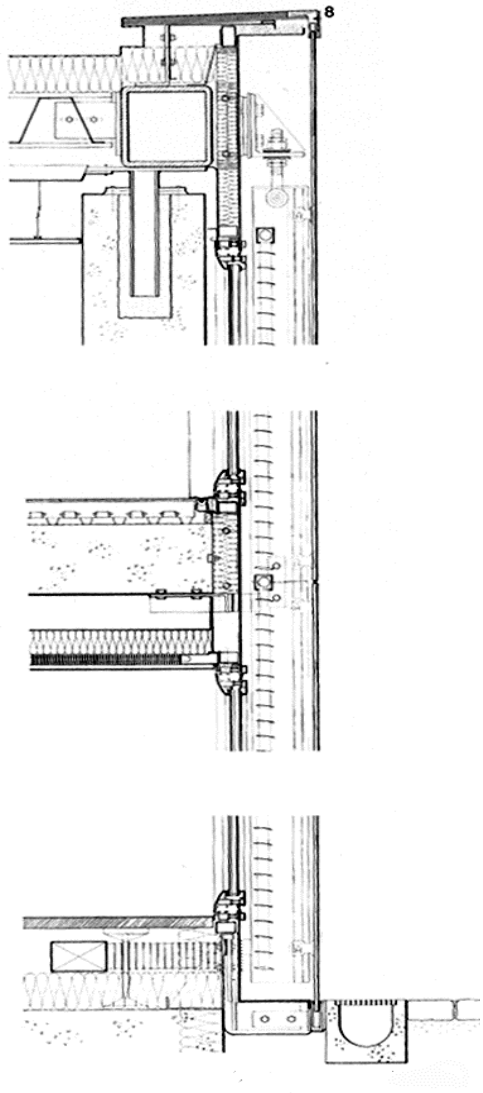

Figure 2.9 Shou-li (2000), "The section view of the Business Promotion Center" (p.8)

2.3 Benefits and advantages of the double envelope

It has become increasingly vital that building skins be thermally efficient. One primary function of the building skin is to respond to the environment and weather conditions to ensure comfortable interiors. The building skin should minimize the energy required for the mechanical systems to satisfy comfort needs inside the building. The double-envelope façade reacts to external conditions in ways providing numerous advantages that make the system beneficial. The following pages detail the DSF advantages in terms of sound, heat, and light.

2.3.1 Acoustic insulation

Sound insulation can be an important reason to use double-skin façades. External sound pollution, like heavy traffic, can affect the comfort levels in occupied space. Reducing external noise transmitted into the building can be crucial for good indoor environmental quality. The reduction in noise transmission is particularly important when the system is designed to support natural ventilation.

Road traffic, railway lines, and industrial areas are the main causes of noise pollution in our cities. According to Oesterle, E, & Lieb, R. (2001), "The constantly increasing volume of road traffic is one of the main causes of noise pollution. The noise level is determined by factors such as the following: proximity of the road to the façade of the building, distance from the nearest traffic lights, nature of road surface, number of vehicles per hour, speed of the vehicles, and the proportion of heavy vehicles" (p.35). With an additional layer of glass in the double envelope system, a considerable amount of sound can be reduced. The external layer acts as an acoustic screen put before the actual building internal elevation. Sound transmission in this case is reflected back to its source. However, the noise cannot be reflected where holes in the external layer aid natural ventilation. The number and size of openings, and the type of glass used, play a key role in the system's acoustic insulation. The extra outer layer also makes opening windows in the inner layer for natural ventilation possible without exposure to outside noise.

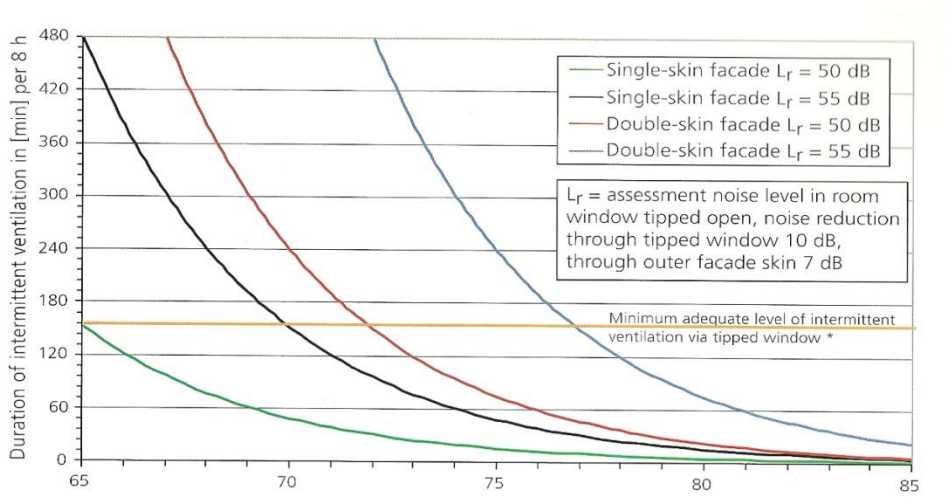

Figure 2.10 According to Oesterle, E, & Lieb, R. (2001) "Relevant external level in (dB)" (p.40)

Noise can impair the health and concentration of people in the building. To design an appropriate double-skin system to insulate external noise, system designers should take into consideration a number of factors that can influence system performance. For instance, the orientation of the façade to the street can determine system dimensions and properties. Further factors to be taken into account include road surface, traffic density, and speed. These factors impacting sound levels will determine insulation needs. The double-skin system offers an appropriate response to the noise pollution facing urban properties.

To calculate the amount of sound insulation needed in a building, we first distinguish areas that are subject to noise from those being protected and define the maximum acceptable noise levels for the areas insulated. Next, standards and codes that classify sound insulation required for the building should be followed. The resistance of sound insulation (R), referred to as frequency-related sound insulation, describes the insulation of the layout's separating elements (walls, floors, windows, doors, etc.). Assigning a value (R) to each building element, a series of tests are done to compute a mean value that is applied to acoustical design planning. Building elements are then chosen to yield acceptable room noise levels. For example, in many countries, noise levels in a working space should not exceed Lr = 55 dB. Thus, acoustic planning of an office building should not violate this admissible noise level.

The amount of sound insulation needed depends on the level of external noise at the site. The greater the noise, the more insulation the external layer should provide. In double-skin systems, the outer skin reduces the sound insulation needed for the inner skin of the system. The amount of insulation provided by the external skin must be known and considered to avoid unnecessary expenses insulating the inner layer of the building skin. The improvement in sound insulation provided by the outer layer should be quantified prior to determining the degree of inner insulation needed.

One disadvantage is that, in some situations, sound is echoed back into the interior space owing to DSF reflections. The air cavity between the two layers of internal and external panes may form a pathway for sound. This may pose unwanted sound propagation from one room to another. Thus, it is crucial to pay special heed to sound transmission in the system. Noise volume is not the only concern. Noise with informational content is more likely to further disturb the working environment.

According to Lieb, R. (2001), "the constant humming of the ventilation plant or the buzz of street noises is more likely to be tolerated than other noises at the same level such as conversation, a prolonged sound at a single frequency, or clearly identifiable working noises" (p.37). The middle layer of the double-skin system can promote information travel through the building, triggering more disturbance in the workspace. Office studies have indicated that employee productivity rises when there is less noise in the working environment. Distance from 'information noise' may reduce its disturbance level. From a sociological point of view, sounds that enter through doors are more tolerated than sounds entering through windows. The more noise fluctuates through the system, the less productive the work environment and the less chance of opening a window for ventilation. Thus, the acoustical planning of the double-skin façade merits careful consideration of sounds with informational content within the workspace.

Table 2.1 According to according to Oesterle, E, & Lieb, R. (2001), "Table by Schmidt shows how a spoken text can be understood and affect the working environment" (p.37)

Distance from ambient noise	Degree of disturbance	Comprehensibility	Productivity
10 dB	Great	Good, effortless	0%
5 dB	Small	Good/familiar text	50%
0 dB	Scarcely heard	Difficult/familiar text	
-5 dB	Minimal	Fragment/unknown text	95%
-10 dB	None	Fragments impossible	

2.3.2 Thermal insulation

Using double-skin façades can provide greater thermal insulation than traditional single glass systems. This greater thermal insulation is due to the extra outer layer that further resists heat transfer. Though simple in theory, heat transfer and glass temperature distributions can be quite complex. All materials that transfer heat, whether it is a gas, solid or liquid, can emit or absorb heat. Heat conducts or convects from high temperature to low at different rates depending on material properties, thickness and area. Heat energy can also radiate through empty space to interact with surfaces and objects that reflect, absorb, emit or transmit based again on material traits and geometric orientation, especially angles of incidence.

In summer, warm cavity air in the double-skin façade can be expelled naturally or mechanically by exhaust fans to remove the captured heat. It is critical to design the system carefully to avoid overheating the cavity. The design of the cavity is significant in terms of the width and height of the cavity along with the size of the openings to support airflow.

During hot summer days, solar radiation passing through all window layers heats the room air, adding to the HVAC system's load during the daytime. Shading devices can be installed in the cavity for manual or automatic control of the amount of light and heat entering a building using a system that reacts to sun angle. Shading devices are protected from wind and rain when they reside in the encased cavity of the DSF. In this case, simply constructed devices work, costing less and requiring less maintenance.

Shading devices play a critical role in double-skin system performance. They capture solar radiation entering the cavity to minimize heat gain and enhance the stack-effect airflow. The smaller the cavity space, the faster it will heat. Thus, shading device properties such as size, color, shape, type and location may impact system performance. Shading devices should be located away from the inner layer to avoid hot radiant pockets.

Overnight, it is conceivable that the interior of a building could overheat. Room furniture, walls, and ceilings rise in temperature during the daytime, only to store and re-emit that heat during the night. The amount of heat absorbed and stored by an indoor object depends on its mass and thermal storage capacity. When a building's air conditioning system is off with windows and doors closed, prior heat absorbed in objects will radiate air trapped inside the room. As a result, room air will overheat, which will increase the energy needed for cooling the building the next morning.

One countermeasure is to pre-cool the building using natural ventilation. Double-skin façade systems can help. Even during hot summer seasons, the outdoor temperature drops at night below the indoor air temperature. Double-skin systems can lower the temperature inside the building by allowing air exchange through secure openings overnight. Since the ports are located in the inner layer, the outer layer restricts unwanted access. Furthermore, the double-envelope outer skin protects the building from adverse weather to permit open-window options for the inner layer.

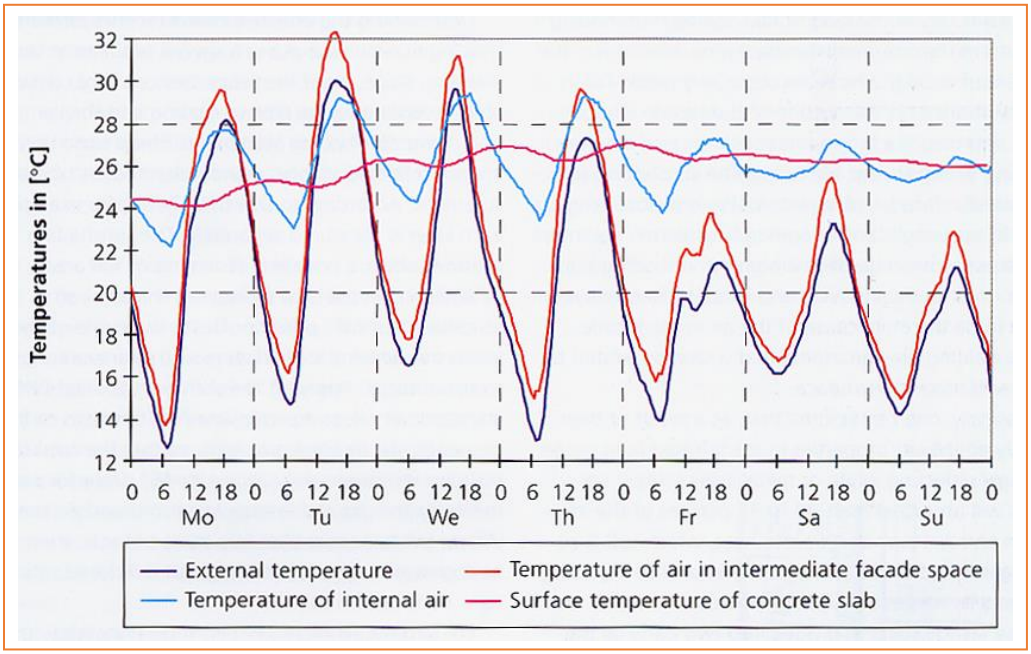

Figure 2.11 Oesterle, E, & Lieb, R. (2001), "Temperature curves for a week: externally, within the façade (mean temperature), within the room, and on the surface of the heat storage slab" (p.76)

In the winter, the external layer of glass serves as additional insulation to help resist heat loss. For any double-skin system, the U-value should be properly specified. According to ASHRAE (2001), "The U-value is the reciprocal of the sum of the R values in a system, including the resistance of the inside and outside air films. The resistance of the outside air film, and therefore the U-value of the system, will depend on the wind speed and convective heat transfer at the outer layer" (p.17). Lower U-values for the double-skin system signify more heat resistance. Furthermore, the extra layer forms a barrier against heat loss due to radiation. The exterior glass panel also helps warm the air temperature in the cavity. On cold days, solar radiation heats the cavity air to keep the inner layer surface warm. As a result, less heat is lost through the glass, thus securing comfort levels.

Temperature is also a factor in heat flow. The difference between indoor and outdoor air temperatures drives heat conduction through the DSF. Admitted solar radiation, though, can warm furnishings inside the office, increasing thermal comfort inside the building to reduce heating costs.

According to Oesterle and Lieb (2001), "through the phenomenon of thermal radiation, the surrounding surfaces have a considerable influence on a person's overall perception of temperature. In rooms where the surface temperatures of walls and ceiling are low, human beings react unconsciously to the influence by turning up heating and thus increasing the air temperature" (p.69). In addition, having cold surfaces on one side of a room can result in greater discomfort. Asymmetrical heat exchange may result in more heating demand for the room. For example, in a room with a single glass façade, asymmetrical heat exchange on one side of the room will result in occupants needing warmer room air temperatures to maintain comfort. Thus, the more alike temperatures of surfaces in the front, rear, floor or ceiling of the room are, the more comfortable room occupants will feel. A double-skin envelope with a low U-value and warm glass temperature will create a more comfortable ambiance at a lower temperature setting than will a single-glass system. Thus, thermal radiation from object surfaces can wield significant influence on the overall sense of comfort.

Cavity air heating is controllable by the building's management system. On a sunlit winter day with the cavity vents closed, the temperature of the cavity air will rise in this passive heating strategy. Proper design of a double-skin façade must specify geometry, position of shading devices, and whether or not the system can be opened for natural ventilation. According to Barakat (1987), "the air flow through the window cavity recovered a large portion of heat loss. This represented about half of the energy needed to heat the air inside the building. If compared to a conventional window, the effective steady state U-value of the air flow window was found to be in the order of 0.5 W/sq.m. The overall reduction in purchased energy of the supply-air window unit relative to a similar double-glazed window unit or a triple-glazed window unit is about 25% and 20%, respectively" (p.152-156).

2.3.3 Light and shading

Natural daylight might be the most important feature of any workspace. According to Kragh (2000), "transparency in architecture has always been desirable, and the problem has always been to realize a transparent building envelope without compromising energy performance and indoor climate. For years, the development of advanced façades and environmental systems has aimed at creating fully glazed buildings with low energy consumption and high levels of occupant comfort" (p.132). Direct sunlight, however, is intense and should be avoided in any building's design. A sky dome better serves as a source of day-lighting in a facility.

Sky conditions are qualified as clear, partly cloudy, or overcast. Clear sky illumination varies depending on sun location, turbidity, and humidity. Partly cloudy is the most common condition where days are neither fully cloudy nor perfectly clear. Partly cloudy skies share some characteristics of the clear sky regarding sun position and its influence on the building. The overcast sky is a condition of cloud cover, and the location of the sun cannot be identified. According to Brown (2001), "the overcast sky is three times brighter at the zenith than at the horizon, and the illumination is evenly distributed around the zenith. Therefore, the top of the sky dome is the source of the most illumination" (p.27).

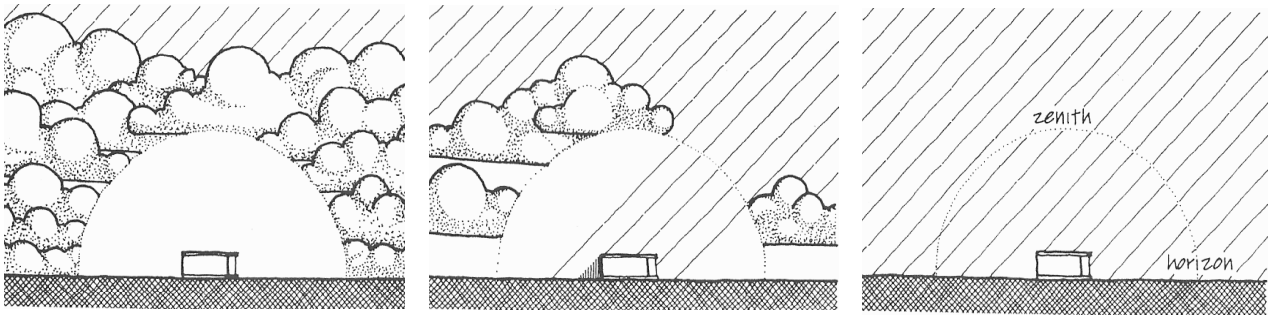

Figure 2.12 According to Brown (2001),"Sky cover types" (p.27)

Daylight is a useful factor reducing energy consumption in most buildings. Nevertheless, there are always challenges providing natural light without high heat gain through windows. New technologies similar to double envelope systems might address this trade-off. Providing daylight into a space reduces the need for electric lighting. Further studies indicate that daylight increases both productivity and workspace quality in an office.

A small reduction in the amount of light has been seen with the extra glass layer in the double-skin system when compared to a single glass façade. Yet, the double-skin system is not so different from the single glass façade in terms of the level of light transmitted to the space. In terms of quality, the DSF offers better quality light with less heat gain. The extra glass layer does reduce the *quantity* of light passing through by about 10 percent. This reduction might increase slightly if the glass is thickened for safety or structural reasons. To estimate the quantity of light in a space, we use daylight factor T_Q. Oesterle and Lieb (2001) remarked, "the daylight factor describes the relationship between the lighting intensity on a horizontal plane in an internal space and that on a horizontal plane outdoors" (p.80). Outdoor lighting intensity lies typically between 5000 to 10000 lux. In a workspace, light intensity of 300 to 500 lux is typically required to achieve a comfortable level. In any case, when daylight is provided to a workspace, especially if the light travels farther into the room, then there is less need for artificial light, and DSF lighting *quality* does not deteriorate.

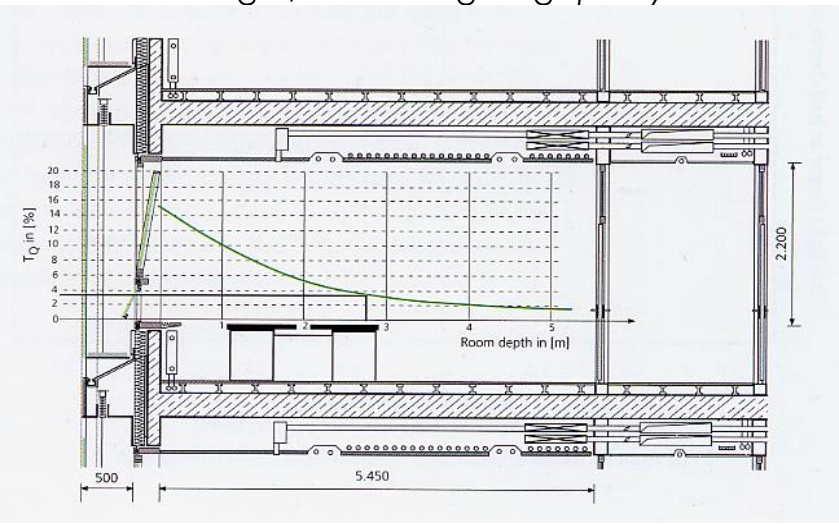

Figure 2.13 Oesterle, E, & Lieb, R. (2001), "Daylight factor curve versus room depth for double-skin façade" (p.81)

Providing daylight more evenly enhances lighting quality in a room and is more important than the amount of light. To ensure the quality of room lighting, a workspace generally requires evenly distributed illumination.

The window size in a room strongly influences the amount of light in the space. The bigger the window, the more lighting typically provided to the room. Widening a window increases the amount of light allowed into the room. The depth of the room may change the minimum requirement of light needed in the space. The longer the distance from the window to a desk in the room, the more likely it is that electric lighting is needed at the desk.

In any case, the use of double-skin systems favors maximum window area to provide more light into the space. Another advantage of the double-skin system is that, with proper shading/reflecting elements, the system can project daylight deeper into a room with better quality. In double-skin systems, all reflecting/shading devices reside in the cavity, keeping them protected from weather conditions. Clean, dust-free surfaces are crucial to performance. Therefore, housing these devices in the cavity lowers maintenance and cleaning efforts. Usually, the reflecting devices are coated with light-colored paint to reflect light up toward the ceiling. Light-colored ceilings can then reflect light back down to enhance light inside the space. Of course, light intensity declines with each reflection.

Special consideration should be made regarding the design of the blinds. The system must adjust and respond to the sun angle to reflect the maximum light into the space. Since the "daylight factor" is based on the diffused overcast sky, simple horizontal reflecting surfaces will not suffice. The system must reflect from all directions. Furthermore, the brightness of a room's surfaces should be adapted to fully exploit a system's reflectivity. Glare is also important to lighting quality. The less discrepancy in light level from a window to an interior desk, the better the quality of lighting.

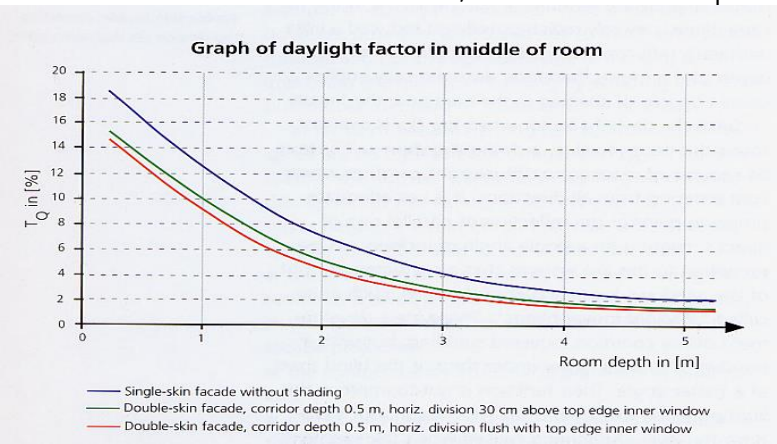

Figure 2.14 Oesterle, & Lieb (2001), "Comparison of daylight factor curves in middle of room" (p.82)

A great example using daylight through a double façade comes from the Groz GmbH Head offices in Wurzburg, Germany, designed by Welber + Geisler. The building has a unique shading device system enlisting venetian blinds located in the cavity. Each floor has two types of blinds controlled independently by a computer system. Upper blinds are made of reflective material to reflect daylight to the ceiling and deeper inside the room. The ceiling painted with brightly colored reflective paint then helps light travel farther inside the room.

The lower blinds are darkly painted with absorbent coating to capture solar heat. This helps raise the temperature inside the cavity for increased thermal buoyancy and its natural stack effect. The lower blinds are also designed to offer glare-free scenery when the blinds are open.

The cavity is ventilated through ports at the lower end of the system (inlets) and near the top (outlets). The system is mechanically ventilated by fans to boost cavity airflow that removes excess heat. Warm air can be sent inside the building to reduce heating cost, or exhausted outside in summer. The inner layer glass can open into the cavity for fresh air.

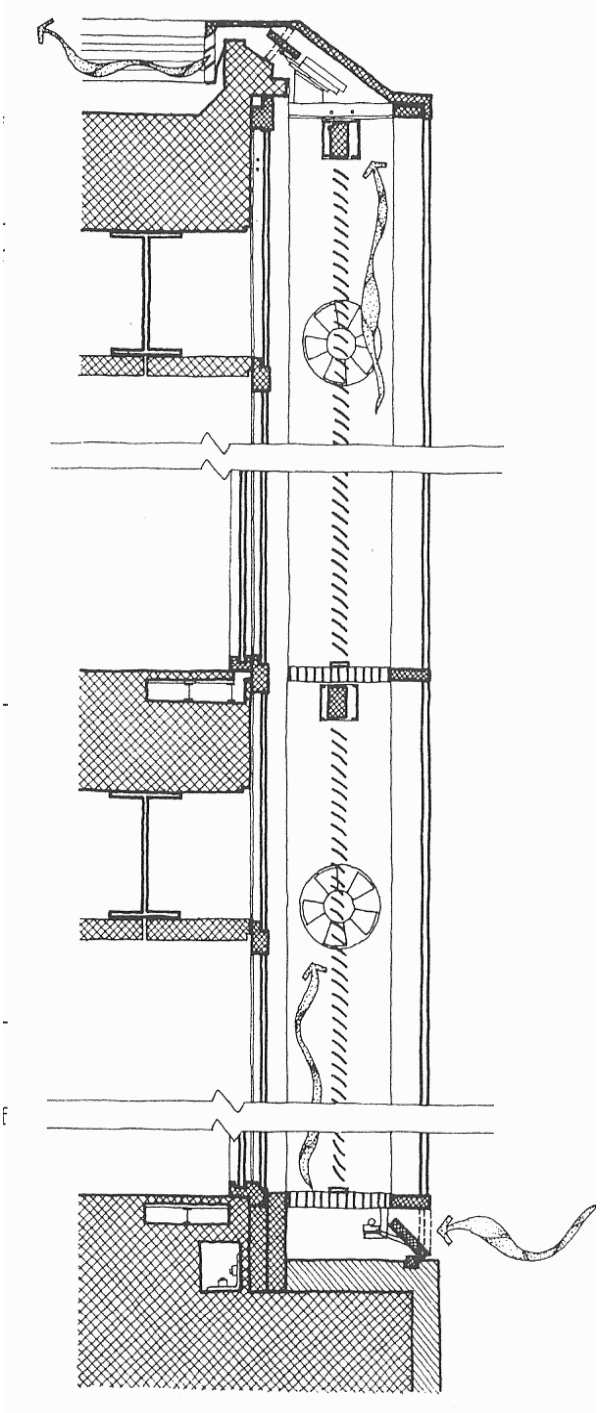

Figure 2.15 According to Brown (2001),"Groz GmbH Head offices, Wurzburg, Germany, Webler + Geisler" (p.271)

2.4 Types of double-skin façades

2.4.1 Box-plot window

The box window is the oldest of double-skin façades. The system simply consists of a framed window that can be opened (inner layer), a cavity divided horizontally and vertically, and an exterior single glass layer with ports into smaller, independent boxes covering the façade of the facility. Many researchers consider the box window as the most reliable double-skin façade type. According to Oesterle and Lieb (2001), "the cavity between the two façade layers is divided horizontally along the construction axes, or on a room-for-room basis. Vertically, the divisions occur either between stories or between individual window elements. Continuous divisions help to avoid the transmission of sounds and smell from bay to bay and from room to room" (p.13). Clearly, this type of double-skin façade is ideal for buildings where sound insulation between adjoining rooms is required.

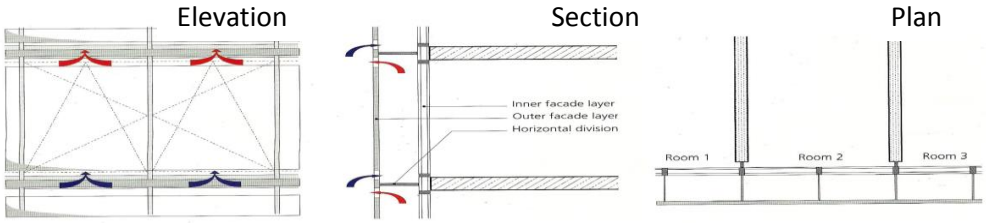

Figure 2.16 According to Oeserle (2001), "Detail drawings of box windows" (p.13)

One example adopting the box double-skin façade is the Print Media Academy designed by Schroder Architeckten and Studio Architekten Bechtloff where each box unit is a single glass pane at the exterior with sealed double glazing on the interior. Enclosed by the two panels is a cavity 46cm wide. The shading system is comprised of aluminum blinds that mechanically control the solar radiation passing into the building. These blinds roll down the inner side of the cavity in response to sun angle. The aluminum reflects the solar heat into the box to warm the air temperature in the buffer space. The lower venting system manages the cavity flow to regulate facility heat loss and gain. Fresh air is available through the inner window port. Furthermore, opening the window allows air exchange between the office and cavity.

Figure 2.17 View of Print Media Academy (http://www.fes.uwaterloo.ca/poject s/terri/ds/PMA.pdf)

2.4.2 Shaft-box system

The shaft-box system is an embellished form of the box window façade. The shaft-box façade employs continuous vertical shafts that rise beyond one floor to link a number of floors. Thus, shaft-box façades require fewer openings on the outside layer. On every building floor, vertical shafts are linked to every box window by openings that allow hot air into the shaft. The hot air is collected and expelled outside through openings at the top of the shaft. Mechanical fans are often used to create suction to draw up this hot air. This system is best for lower-rise constructions.

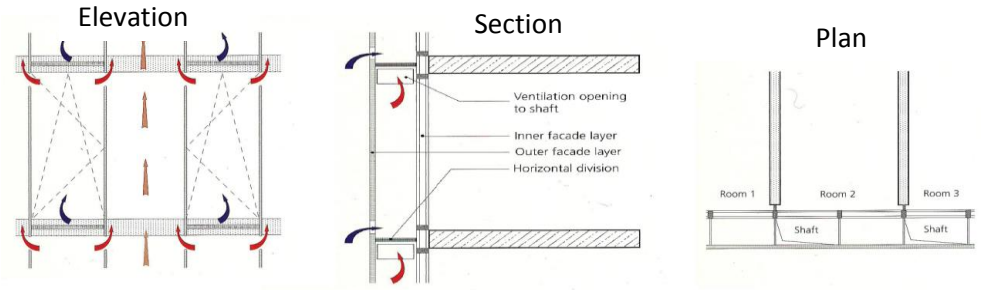

Figure 2.18 According to Oeserle (2001), "Detail drawings of Shaft-box Façades" (p.16)

This system was adopted for the ARAG 2000 tower in Düsseldorf, Germany. This skyscraper was designed by RKW in collaboration with Norman Foster. The inner layer was constructed with conventional, vertical aluminum blinds and low-E glass. Windows are ventilated and able to provide fresh air most of the year. On the other hand, in extreme weather conditions, mechanical ventilation is used to achieve thermal comfort. Each of the box-windows has its own opening for fresh air, but instead of exhaust ports in each window, side bypass vents draw hot air to the system shaft for expulsion to the outside. Thus, the external layer has fewer openings than the typical box window building. According to Oesterle, & Lieb (2001), "Ventilated air is extracted into the exhaust-air shaft via a bypass opening, the size of which is determined according to its position in the shaft. The shaft, in turn, is ventilated via an area of louvers in front of the service story. In order to exploit the collector effect of the façade's intermediate space more efficiently in winter, the air cavity shaft is also designed to be closed if required" (p.17).

Figure 2.19 View of ARAG 2000 Tower (http://www.josef-gartner.de/referenzen/

2.4.3 Corridor system

The corridor system diverts cavity air away from the immediate overhead floor at each level for a diagonal flow. Special care should be taken to prevent sound transmission through the corridor. Horizontal divisions are used along the length of the corridor to address fire and noise concerns. The inlet ports on the external layer for fresh air should lie near the floor, and the exhausted air should leave through an opening near the ceiling.

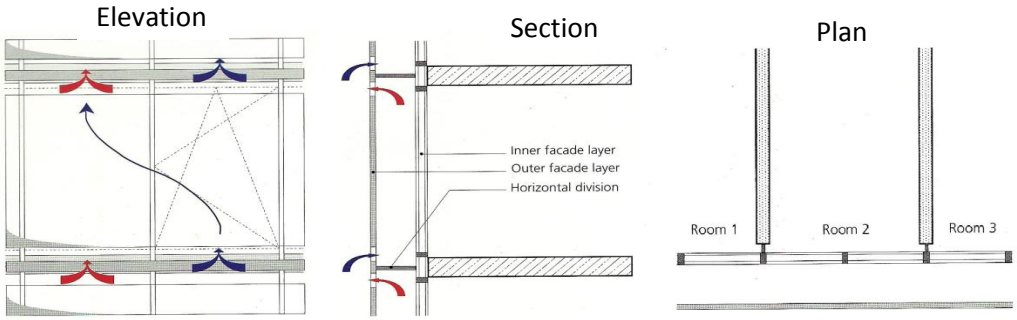

Figure 2.20 As Oeserle described (2001), "Detail drawings of Corridor Façades" (p.20)

Figure 2.21 South face of "City Gate" (LBNL – http://gaia.lbl.gov/hpbf/picture/

A good example of this system is the Dusseldorf City Gate, a building designed by Petzinak and finished in 1998. The façade of the building is a corridor-type, double-skin façade that is closed at each floor level. The building consists of two towers where each is a 16-floor tower with a 56m-high atrium space at the center of the facility. The entire building is covered with a toughened, single-pane glass skin. This exterior layer has ports arrayed near each floor level so that exhausted air from each level will not be able to enter floor space immediately overhead. The cavity, or the middle layer of the building, forms a corridor having two widths (either 90 or 140 cm). This part of the system is naturally ventilated to supply fresh air during off-summer months. According to Oesterle and Lieb (2001), "in drawing up the concept, extensive computer-aided airflow calculations are made to optimize the system and to achieve an even flow of air through the boxes" (p.21). This building is saving a significant amount of energy by supplying air through natural ventilation for up to eight months in the year.

2.4.4 Multistory façades

In the multistory double-skin façade, cavity air rises with very limited connection points. In extreme cases, this intermediate layer can extend from ground to rooftop. Multistory façades show promise for insulating external noise. Ventilation is supplied by large air intake ports near ground level for eventual exhaust at the building cornice. In wintertime, the façade can be closed at top and bottom to maximize solar energy gain. Like corridor façades, special care should be taken for acoustics control.

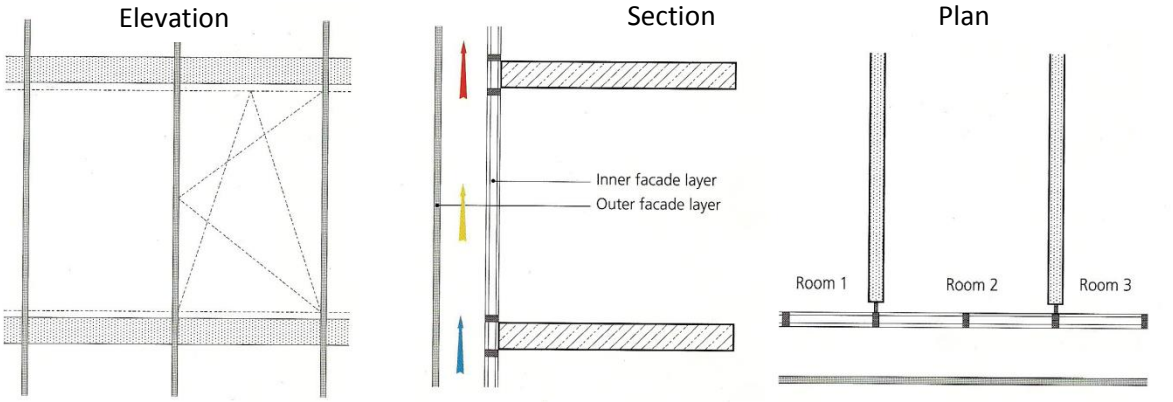

Figure 2.22 As Oeserle mentioned (2001), "Detail drawings of Multistory Façades" (p.23)

The Victoria building (Cologne) is a good example of a multistory double-skin. Air introduced by openings at the bottom level is exhausted at the top of the building using power fans at the top level over 21 meters above the street. Both external and inner layers of this double façade system are sealed. Furthermore, the external skin is laminated with solar-control glazing. Shading devices reside in the middle layer's 80cm-wide corridors. Cavity design includes walkway grills for maintenance access. The inner layer comprises fixed glass with no openings. The main advantage of this double-skin façade system is better thermal performance of the building skin. In wintertime, cavity air temperature can intentionally be heated by controlling the air movement. Vents in the corridor can be closed to help the air inside the cavity capture solar radiation, thus reducing the difference between inside and outside temperatures to curb heat loss.

Figure 2.23 View of Victoria Life Insurance Buildings (LBNL - http://gaia.lbl.gov/

2.5 Advantages of box-plot system

2.5.1 Introduction

Like any façade design, a double-skin façade system's performance is measured by how well it delivers on the architect's specifications. Depending on the building type and design, the double-skin façade can be an optimal solution offering transparency, natural light control, noise reduction, and elevated comfort levels – all while consuming less energy. Glass facades also enhance facility appearance. Double-skin façade systems come in a wide variety where each system performs and reacts differently to the environment. Depending on the location and the building type, the goal is to maximize the advantages of the system.

Along with the different types of double-skin façade systems, there are different operating modes (naturally ventilated, mechanically ventilated). The reasons for selecting the mechanically ventilated box-plot system are explained next.

2.5.2 Box-plot versus other types of double-skin façade systems

In hot weather conditions, the goal of using cavity airflow is to cool the cavity and lower the temperature difference between the inner-layer glass surface and the indoor air space. The box-plot type double-skin façade (*DSF*) meets this aim and is ideal for hot weather conditions when mechanically ventilated.

While box-plot windows are generally one-story high and passive, the box-plot window proposed here is to be mechanically ventilated, resulting in less heat gain inside the cavity. The HVAC return ducts increase airflow to minimize solar heat gain and lower cavity temperature near indoor levels. This means reduced heat transfer through the inner glass and less HVAC energy needed to comfort-cool the air inside the building.

2.5.3 Mechanically ventilated box-plot airflow

Temperature difference reduction between the indoor glass surface and the office area arises when faster cavity airflow extracts more DSF heat. Thus, more office airflow increases the cavity airflow rate that lowers the temperature gap between inner glass surfaces (T_{gi}) and indoor air (T_{in}).

Unlike a passive system, mechanically forced box-plot airflow rates inside the cavity depend on the overall HVAC zone airflow rate. According to Saelens (2008), "For the active flow window, there is a relationship between the overall building airflow rate and the airflow through the cavity" (p.643). Thus, boosting airflow through the *DSF* system cavity demands that HVAC zoning in the building consider the airflow rate needed for *DSF* cavity heat removal. In turn, the office area next to the façade system where mixed air enters the cavity thus sees more airflow than a typical office or windowless interior office space. Though amounts of air expelled from a building vary depending on building requirements, expelled air is roughly the same or more than for a typical office tower, depending on the HVAC zoning and the operation mode.

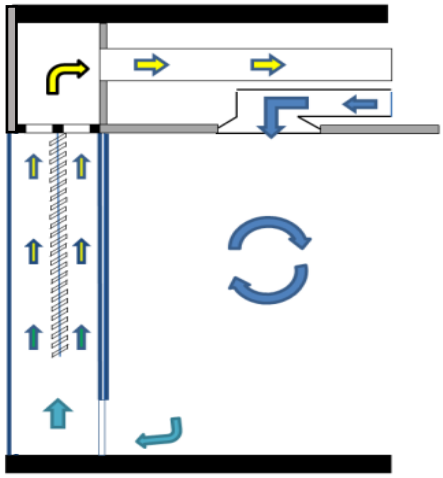

Figure 2.24 Flow diagram for proposed mechanically ventilated box-plot DSF

When installing the double-skin façade system, the building's HVAC heating and cooling must flow through the *DSF* cavity, and the HVAC zoning must consider airflow allocated to the skin cavity. Therefore, HVAC zoning must be segmented. In one operating phase, offices next to the building façade see different airflow rates from its own HVAC zoning than do center zones of the building. In the second phase, office air moves through the cavity before fully exhausting as seen in Figure 2.25.

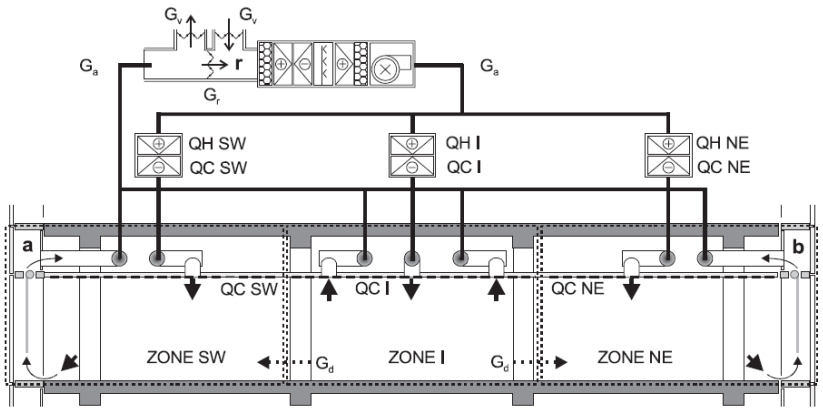

Figure 2.25 According to Saelens et al. (2008), "Schematic representation of office floor for a typical active facade configuration" (p.638).

Office-building service areas with restrooms and elevators have their own HVAC zones with alternate return ducts. Return air from these parts of the building to expel higher concentrations of pollutants is vented at much higher rates than from office areas. Thus, more fresh air from outside is needed to serve these zones. However, return air from the office is not wholly expelled and re-mixes in select proportions at the air exchanger.

An experimental study by Shou-li (2001) evaluated the performance of an active versus passive window system at the RDF in Blacksburg, Virginia. Research results revealed the fraction of heat removal in the cavity to be greater for the active array than for the passive in summertime. As Shou-li (2001) observed, "The mean cavity heat removal rate is 57% for the active system and 32.5% for the passive system. As the flow rate increases, the differences between the two systems become larger" (p.33). Shou-li found the mean fraction of heat removed (Fhr) in the cavity growing with increased airflow, much in line with the square-root of velocity change typical of convection heat transfer (i.e., doubling the flow rate enhances convection by 40%). Here are some of his results:

Table 2.1 According to Shou-li (2001), "The fraction of solar heat removed from the cavity for different cavity air flow rates" (p.31).

	Active System	Passive System	
Cavity air flow rate (ft/min)	Mean A- Fhr	Mean P- Fhr	Difference (A- P)
10-15	-	0.225	-
15-20	-	0.261	-
20-25	-	0.296	-
25-30	0.438	0.363	0.075
30-35	0.504	0.396	0.108
35-40	0.568	0.412	0.156
40-45	0.616	0.410	0.206
45-50	-	0.477	-

The required cavity airflow depended on many factors: ventilation method, operation mode (cooling or heating), type of window, and height and width of the window. Mechanically ventilated window airflow can vary depending on building type and the HVAC zone serving the DSF. Furthermore, the cavity height has a strong influence on airflow demands. Clearly, a multi-story double façade system needs more airflow to exhaust the solar heat gain inside the cavity in summer. In a single-story system, less airflow is needed since the 'cooking' time the air faces in the cavity is much briefer, and cumulative solar radiation heat gain is much smaller.

2.5.4 Actual construction

The ideal construction method has the box-plot DSF prefabricated off-site with plot window units manufactured in a factory for transport to the construction site for installation. Prefabrication allows full assembly, including glass, panels, infill components, and movable parts for delivery to the building site where units are added to create the building façade. Thus, the system forms a skin or a "double curtain wall" surrounding the building to reduce the heat gain into the building.

This approach is, by far, beneficial for other reasons. First of all, factory prefabrication assures greater quality control in terms of cavity airflow performance and system tightness. Inlet and outlet vents are also factory-tested to ensure no leakage or gaps.

Second, DSF system prefabrication reduces assembly time and cost while aiding installation speed. Finally, a system composed of individual units allows easier maintenance and replacement.

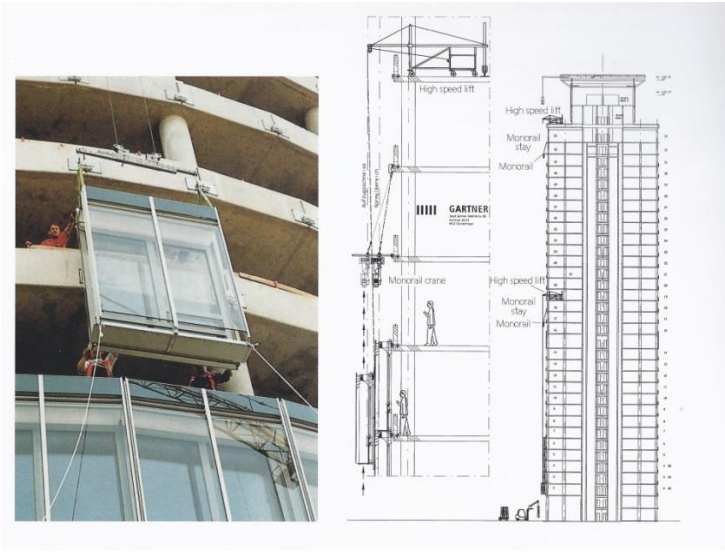

Figure 2.26 Oeserle (2001), "Site picture of prefabricated box-plot and window-lifting process" (p.136).

Prefabrication of double-skin façade systems has advanced to now be much more economical in terms of construction and installation. Prefabricated DSFs are less expensive than site-built DSFs, especially when they are mass-produced. After the units arrive at the building site, cranes can lift units for attachment to the front of the building.

The alternative is to build the DSF system on-site. It is possible to build double-skin systems using an exterior curtain that attaches to an inner layer of existing window systems to form an interstitial cavity. Insertion of cavity-airflow controls in a single-story setup is complex, time-consuming, and labor-intensive. A control system for a front curtain wall or storefront might be more suitable in other double-skin facades for corridor or multistory layouts. However, limiting cavity height is critical to acceptable performance of DSF in hot weather conditions.

On-site construction is better suited for façades with smaller windows. Assembling a system requires much on-site build time that adversely affects construction planning and scheduling. Thus, conventional assembly is advised only when prefabrication is not economically viable for smaller window areas. Structures with in-place curtain walls may attach a second skin to form the double-skin façade system.

In this type of construction, system components (glass, frames, panels and other façade units) arrive on site individually for assembly. This requires longer installation time. Yet, in prefabrication, units arrive just-in-time before the façade undergoes assembly. Of course, many adjustments to

the inner layer of the system will be needed for adding inlet and outlet ports to ventilate cavity air flow.

In conclusion, there are numerous factors that can influence the type of construction used to form a building's DSF. Early study, planning, and coordination among architects, contractors, engineers, and developers can forge decisions toward optimal construction of DSFs. The main design purpose(s) of the system should include choosing the right system, using the best type of construction for the window area, and ensuring optimal airflow to avoid cavity overheating.

2.6 The Mobile Window Thermal Test

MoWiTT is a testing procedure that uses actual weather conditions to study the behavior of different building systems (windows or skylights) in a comparative experimental study. The Mobile Window Thermal Test setup compares net energy passage through configurable windows or skylights exposed to real ambient weather.

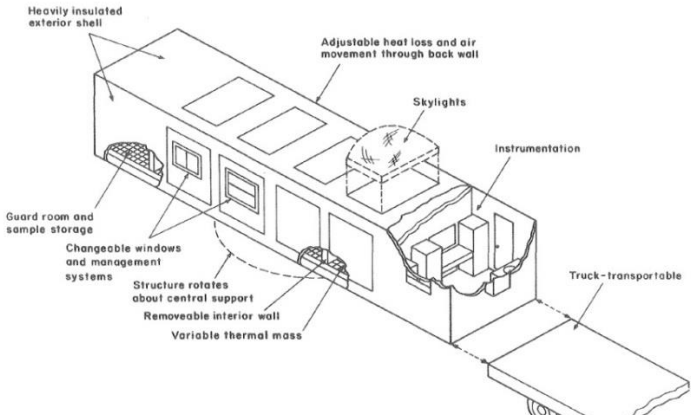

Figure 2.28 According to Klems (2011), "The Mobile Window Thermal Test Facility"

First, the study uses full-scale elements to realize accurate performance. The windows are installed in small, easy-to-move "chambers" (rooms) that can be oriented in different directions to study solar radiation effects on the system. Chambers are well-insulated to eliminate stray heat transfer, and they are usually wrapped in fiberglass or polystyrene foam insulation having high R-value resistance to heat flow. Energy entry to the chamber is the sum of heat flow emitted inward from the hot inner-glass surface plus solar radiation admitted through the window. Both of these variables vary by time, weather conditions, and location.

MoWiTT combines two common methods: field- and controlled-testing. Field testing uses an actual case-study building equipped for test data recording by instruments. Researchers then adjust system variables to see how windows perform in given weather conditions. MoWiTT's drawbacks include frequent building access and travel costs.

The second approach is experimental testing in a controlled setting. MoWiTT uses quasi-controlled test 'rooms' to evaluate a window or skylight system under ambient conditions. This test method allows accurate study of performance where the next step enlists computer models to simulate different scenarios in a controlled environment. Although this method is less expensive than traditional testing, it poses one obvious flaw: it does not assess system performance in real ambient weather conditions. Instead, MoWiTT test chambers are rapidly configured with actual-size windows at various locations where results are then input into a simulation program for validating data comparisons at different venues as required. The MoWiTT procedure essentially compares two or more windows in identical test chambers exposed to the same weather conditions to yield precise solar heat gain coefficients *(SHGC)* and U-factors for each model.

Instruments are installed in each cavity in the same testing chamber at the same site, measuring temperatures, solar radiation, and wind speed. Each chamber is designed to work as a calibrated box with temperature-controlled air inside the chambers. This confines the heat gained or lost to one source – "the window" – and the heat flow can be measured and calculated throughout the experiment.

The Mobile Window Thermal Test process may be summarized as follows:

1) The test uses a full-size window or skylight to study performance.
2) Windows are installed in easy-to-build, well-insulated chambers made of wood or steel.
3) Chamber interior temperature and air flow are controlled to represent real-life conditions inside the building.
4) The study takes place in real ambient weather conditions.
5) External variables like solar radiation, wind, and temperature are recorded for each time increment.
6) Comparative study of one or more systems takes place at the same site for an accurate 'side-by-side' comparison.
7) Logged data can be used to simulate various building functions and interior environments extrapolated to different sites.
8) Chambers can be transported to different locales as needed.

2.7 Performance assessment

In a study performed by Shang Shou-li, two types of double-skin systems were examined in test cells located at the Research and Demonstration Facility (RDF) on Virginia Tech campus. Full-scale models similar to those used in the Commerzbank building were tested. The models for the study were constructed of wood frame, metal, and glass. The first model was a mechanically ventilated (active system) enlisting fans to vent the cavity. The second model used a passive method operated by the stack effect. For both active and passive systems, the window consisted of three layers.

In the active system, a double-layer, outer-skin glass panel enclosed an eight-inch-wide cavity with a single-layer glass panel as the inner pane of the system. The HVAC system was connected to the window's cavity allowing fans to vent hot air in the cavity toward the inside of the building for winter heating purposes. As the wintertime temperatures dropped, warm air was used to heat the room. In summer, this unwanted heat from the cavity is normally exhausted to the outside.

In the passive system, the placement of glass layers is reversed with the double-glass layer *inside* enclosing an eight-inch cavity with an outer single-glass layer. In the experiment, both models were six feet wide and eight feet tall. Interior air temperature was set at 65F° using a standard HVAC setup for the passive system to simulate an occupied condition in an office building. The Shou-li test data were logged from September to October 2000. Shou-li (2000) said, "both systems contain a ceiling heater and fan and a thermostat in each of the test cells. The ceiling heater and fan is a Broan Model 658, a fan-forced heater, which can produce 4436 Btu/h and 70 cubic feet per minute (CFM) of airflow" (p.22). The ceiling heater and fan were centered in the test chamber.

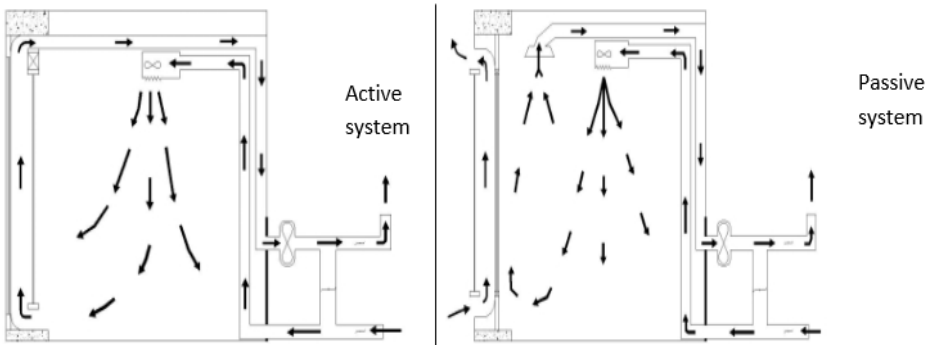

Figure 2.29 According to Shou-li (2000),"The experimental operation modes" (p.22).

After logging data, Shou-li used statistical analyses to compare removals *(H)* of transmitted solar heat gain into the cavity *(q)*. The equation Shou-li used for the study was:

$HRR = H / q$ where:

HRR = fraction of solar gain removed
H = heat removed from the ventilation cavity, Btu/h
q = solar radiation transmitted to cavity, Btu/h

Data were statistically analyzed to calculate the fraction of solar heat removed from the cavity for both systems: active system is (*FHRa*), and passive is (*FHRp*). The results are shown in the following three tables.

Table 2.2 According to Shou-li (2000), "Fraction of heat removed from the cavity" (p.31).

	Mean	Std. Dev.	Std. Error	Minimum	Maximum
FHRa	0.570	0.143	0.007	0.181	0.999
FHRp	0.325	0.099	0.005	0.095	0.785

The mean value of heat rate removed in the system cavity was 75% higher in the active system with a maximum value of 0.999. In the passive system, the mean value of heat removed was less with a maximum value of 0.785. Active system data were more stable *(SDa/mean=1/4 vs. SDp/mean=1/3)* than for the passive data due to a swift, constant airflow driven by fans.

	Active System	Passive System	
Cavity air flow rate (ft/min)	Mean A- Fhr	Mean P- Fhr	Difference (A- P)
10-15	-	0.225	-
15-20	-	0.261	-
20-25	-	0.296	-
25-30	0.438	0.363	0.075
30-35	0.504	0.396	0.108
35-40	0.568	0.412	0.156
40-45	0.616	0.410	0.206
45-50	-	0.477	-

Table 2.3 According to Shou-li (2000), "Fraction of solar heat removed for different cavity air flow rates" (p.31).

The difference between indoor air and indoor glass surface temperature (ΔTga) is an essential measure of thermal comfort. When the ΔTga is high, more heat radiates inward from the glass to disturb occupant comfort.

Table 2.4 According to Shou-li (2000), "The descriptive statistics for the ΔTga" (p.32).

	Mean	Std. Dev.	Std. Error	Minimum	Maximum
A-upper- ΔTga	4.3	2.4	.155	1.0	9.9
A-lower- ΔTga	7.0	3.1	.199	2.1	13.9
P-upper- ΔTga	7.1	2.8	.179	.70	14.4
P-lower- ΔTga	3.2	2.1	.134	0.0	9.9

For the active system, the mean value of the temperature difference in the upper part of the glass surface was 4.3 °F. This value was notably less than for the lower part of the system. The passive system ΔTga tiers were inverted where the lower glass showed less mean ΔTga. The ΔTga between the indoor and glass surface temperatures had a mean value of 3.2 F° and a maximum value of 9.9 F°. The upper part of the passive system had a more significant temperature difference with a mean value of 7.2 and a maximum of 14.4. The active system's lower ΔTga values represents less inward radiant heat disturbing indoor thermal comfort.

In his study examining the solar heat gain mathematical model, Shou-Li (2001) used, "A Protocol to Determine the Performance of South Facing Double Glass." Here, the double-skin system had an external single glass layer with a double-glass panel as the inner layer. Heat transfer through the system was computed recognizing each layer in this system.

Conclusions of the Shou-li research:

1) In the overheated periods, the active system enjoyed a higher heat removal rate 57% versus 32.5% for the passive DSF system. Our research experiment may expect to face much more radiation in summer, thus developing lower heat removal rates in the 30-40% area (0.3-0.4).
2) The difference in temperature between the inner layer glass surface and the indoor air was lower for the mechanically ventilated system.
3) Winds strongly affected passive double-skin system cavity airflow rates.
4) The mechanical equipment in the active system played a large role in system performance. When fans do not work properly, poor thermal performance of the system will result in an overheated cavity.
5) Heat captured by an active system cavity is ample for standard office heating purposes. The average heat gain in the active system was 1991 Btu/h, and a 57% efficiency in heat removal rate recycled nearly 1134 Btu/h for space heating.
6) A building management system should ideally both control fans and shading devices in any active system.
7) The level of energy savings provided by the double-skin system differs with location depending on energy costs and weather conditions.

In a different study by Dirk Saelens, two "as-built" examples of buildings using double-skin façade systems were evaluated. For Saelens' two single-story buildings, both mechanically and naturally ventilated systems were tested. The first building was the DVV headquarters in Brussels, Belgium where the double-skin system was adopted to achieve energy efficiency as well as acoustic insulation. The building was equipped with a window featuring downward ventilation. Measurements were taken every three minutes with mean values calculated every fifteen minutes. Thermocouples were placed on both sides of the glass at three heights, cavity temperature was recorded, and supply duct temperature was logged at the cavity inlet. Analyzing the system performance, Saelens found leakage in the cavity that stemmed from poor design of the interior glass pane. Lack of an air-tight cavity, poor duct insulation, and the choice of downward airflow were identified as the major shortcomings in the system design.

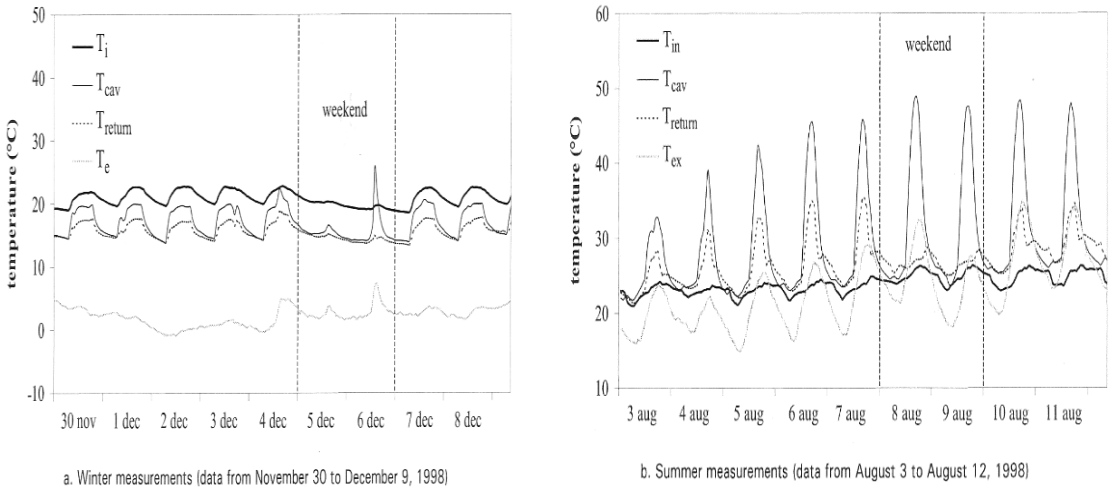

Figure 2.30 According to Saelens (2002), "Overview of the winter and summer measurements showing interior temperature, average cavity temperature, return air temperature, and the exterior temperature" (p.31).

Saelens found that during winter, the outdoor temperature neared 2ºC while the average temperature of the building was 20.8ºC. Here, cavity temperature was only 2º to 3ºC lower than the interior during the daytime. The small difference in indoor and cavity air temperatures reduced heat loss through the inner glass layer. During nighttime, the cavity was 5ºC lower than the indoor temperature. For summer, the average outdoor temperature was 35ºC, and cavity heat increased markedly as a result of solar heat gain. Removing summer heat from the cavity was crucial for maintaining comfort inside the facility. Though exposed to direct sunlight, the window's cavity temperature was lower than the outer glass surface temperature by virtue of the cavity airflow.

According to Saelens (2002), "Improperly installed insulation of the inlet region causes a temperature drop between the light fixtures and the upper inlet of the cavity during winter conditions" (p.35). In winter, air movement inside the cavity did not favor a cavity temperature increase. Air movement inside the cavity may have reversed direction. Thus, both inlets and outlets for any test system must be insulated and tightly sealed.

Despite the 'leaky' U-value of the inner glass panel, the system should have been tight enough to isolate cavity air from the building air. Wintertime cavity air was warmer than outdoor temperature and closer to that indoors. As a result, less heat was lost from the inside of the building

through the inner layer. In both cases, the poorly insulated inlet region hindered the thermal performance of the double-skin system.

Table 2.5 According to Saelens (2002), "Overview of the measurements" (p.40).

	period	shading	average	st.dev.	min	max
air-change rate (1/h)	1.	up	8.7	2.3	3.3	16.9
	2.	down	7.0	2.1	2.9	22.4
	3.	up	7.7	1.6	2.5	12.9
cavity temperature (°C)	1.	up	18.1	2.8	13.2	26.4
	2.	down	22.4	3.5	16.2	41.6
	3.	up	5.5	1.3	2.6	9.7
temperature difference between the cavity and the exterior (K)	1.	up	4.4	2.0	1.3	12.7
	2.	down	4.1	2.1	-0.6	18.3
	3.	up	2.4	1.0	-0.2	4.2
absolute pressure difference between the inlet and outlet grid (Pa)	1.	up	0.78	0.57	|-0.93|	3.30
	2.	down	0.82	0.47	|-1.18|	4.05
	3.	up	0.40	0.38	|-2.74|	2.96

In a different project, Saelens studied the Postcheque building in Brussels. During building renovation, the designer chose to add a second layer approximately 130 cm inside the original exterior façade. The new inner layer comprised an insulated glass panel in a wood frame and an enclosed cavity ventilated with external air. Venetian blinds were located in the cavity 10 cm from the interior layer. The measurement array resided on the fourth floor facing south. Cavity temperature, humidity, and the static pressure difference between the inlet and outlet were measured. Inner room temperature and heat losses were monitored. The average air exchange rate with the shading device up was 8.7 air changes per hour. Air exchange in the cavity dropped to 7.0 air changes per hour with the shading device down. Air changes in winter were often less than in summer. Airflow in the passive cavity hinged on cavity temperature since hotter air is less dense for a more buoyant flow. Wind posed a stronger influence on the system's winter performance. Saelens' Postcheque case study clearly involved a complex airflow. In summer, the airflow was mainly influenced by thermal buoyancy to remove heat in the cavity. In wintertime, wind dominated passive system air flow.

In a third study performed in Hong Kong by Matthias Haas, a double-skin system was evaluated for performance in hot, humid climate conditions. The study assessed overall energy consumption for various double-skin systems in the building. For muggy weather conditions seen in Hong Kong, mechanical ventilation and air conditioning are needed. Haas (2003) remarked in his Ventilated Façade Design for Hot and Humid Climate, "52% of the total energy in Hong Kong is used by buildings. Office and commercial buildings use 37% of this total energy" (p.1). In summertime, natural ventilation can reduce cooling energy requirements.

One of the main goals in the Haas research was to show that double-skin facades must take into consideration climate factors to determine the appropriate system. According to Haas (2006), "A new approach for double-skin facades has to take the climate factors into account to find out if a Double-skin façade can help to reduce the energy consumption in buildings in a hot and humid climate" (p.2). European case studies of double-skin facades face mean temperature and humidity levels very different from the climate seen in Hong Kong. Since building facades can save a great deal of energy for comfort control inside the building, Haas began by studying the climate in Hong Kong.

Figure 2.25 presents findings by Lam and Li for the day-lighting and solar-heating loads upon office-dominated structures. Data show the building facade (wall + glass + solar) making up over 35% of peak cooling loads. Furthermore, electrical light usage can be reduced by prudent design of the building façade and the amount of daylight it provides.

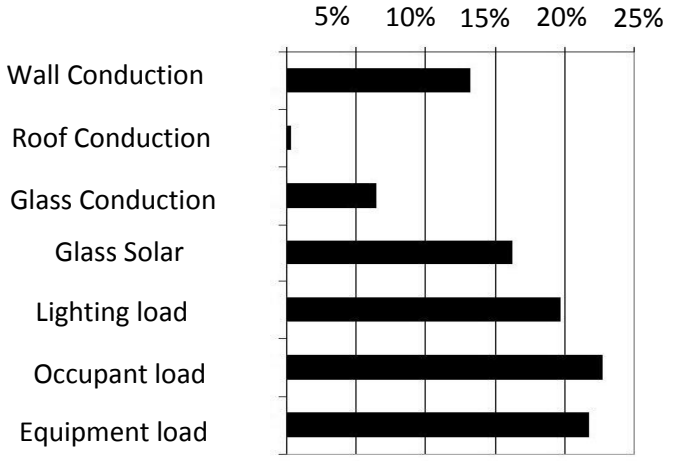

Figure 2.31 Peak cooling load (Li et al. 2003)

In his research, Haas collected data for six buildings using a questionnaire to survey newer buildings with double-skins employing one of two airflow control strategies. Three buildings used external air curtains (EAC), and the other three used internal air curtains (IAC). System control featured one of two approaches: (1) controlling the amount of solar radiation on the façade through automated shading and (2) controlling airflow through an open interior layer. Both systems included climate indicators.

Table 2.6 Haas (2006), "List of buildings in Hong Kong with Double-skin facades included in the study" (p.3).

Building	year of completion	number of storeys		GFA	type of DSF
		total	with DSF	in m^2	
1	2000	10	10	13912	EAC
2	2001	19	16	33800	IAC
3	2002	8	8	10400	EAC
4	2002	6	5	32500	EAC
5	2003	29	14	12200	IAC
6	2004	8	2	81800	IAC

Natural and nighttime ventilation can remove heat from inside a building to enhance thermal comfort. According to Haas and Amato (2006), "In Hong Kong, thermal comfort improvements by natural ventilation during the three hottest months (June, July, August) are 10%" (p.4). Therefore, the design of existing buildings with double-skin facades makes possible openings to the outside to increase cavity airflow at certain times. Faster cavity airflow reduces solar heat gain and, in turn, energy needed for cooling.

The model used by Haas and Amato enlisted both thermal and airflow simulation regimes. A model created for this study compared three different systems according to the analysis of existing double-skin facades in Hong Kong. The base-case model office was 6.6m wide by 8m deep, and a single-glazed curtain wall with a 44% window-to-wall ratio facing south was used (8 am to 8 pm). Three types of glass were tested. The first curtain wall had single, clear glazing with internal shading. The second curtain wall had reflective glazing without shading. The third curtain wall featured solar-control glass without shading.

Table 2.7 According to Haas (2006), "List of glass used in base-case simulation"

Description	clear	reflective	solar control
U-Value	5.46	5.73	5.73
g-value	0.774	0.527	0.482
T-sol	0.72	0.463	0.322
Rf-sol	0.07	0.304	0.103
T-vis	0.87	0.322	0.403

The design of the second model proposed a double-skin façade with a 600 mm cavity. A single 6mm clear pane was installed as an exterior layer with two openings at both top and bottom of the one-story model where cavity air ventilated naturally via the stack effect. Another single clear pane 6mm thick comprised the inner layer. A venetian blind for solar control was installed in the 600 mm cavity for the first scenario (DSF1-1).

For the second scenario, a regulator assisted the cavity exhaust (DSF1-2). According to Haas & Amato (2006), "A regulator indicates the times of the year when the enthalpy of the air in the window gap exceeded the enthalpy of the outside air. The regulator will then exhaust the air which is expected to result in energy savings" (p.5). The third model had a second layer of glass on the inside of the window creating the double-skin system. Both layers were single clear panes of 6mm. Venetian blinds were installed and controlled automatically. The inner layer had inlets at the bottom of the room and a ventilation slot on top of the window. Air from the room vented through the cavity back to the HVAC system. According to Haas & Amato (2006), "the cavity of the double-skin system is connected to the interior air handling unit, allowing air from the room to be forced through the gap and back to the air handling unit. The purpose of this design was to improve the thermal microclimate in the space next to the window" (p.5).

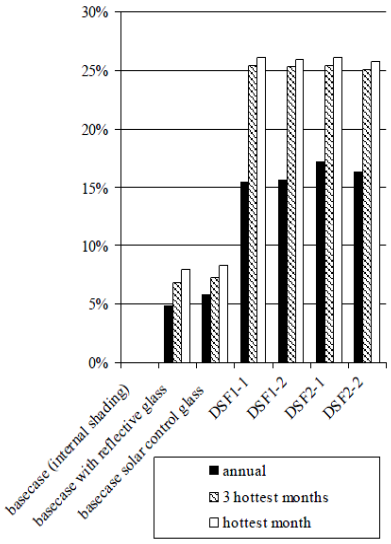

Figure 2.32 Haas (2006),"Results of Double-skin facades study in Hong Kong"

Simulations using DOE-2 estimated energy savings up to 17% for the external air curtain wall system. For the hottest three months of the year, energy savings were estimated to be 25%. Airflow around the building did not affect DSF performance or the results.

In research done by Bartak, Dunovska & Hensen Design (BDHD, 2002), computer modeling and simulations were designed to advise recommendations via a design support platform for double-skin systems. Computer simulations are currently among the most powerful tools for predicting performance of a building under varying energy-use scenarios. Accurate, advanced software can create a good building simulation. Computer models can be quite precise and much cheaper than a field performance study. Two critical elements are needed to create an advanced model. First, a designer should have the savvy to understand how the actual system works and its complexity. Second is the ability to enter system data into the software.

In the BDHD study, the ESP-r advanced building simulation environment was used to develop a simulation model for the building performance. The methodology of the study enlisted this powerful tool using the four main steps. According to Bartak, Dunovska, & Hensen (2002), "these four steps are: 1) analyzing the problem and re-expressing the building design in a manner suitable for simulation; i.e., at suitable levels of detail and complexity, 2) calibrating the model against measured data or relying on the experience, intuition and professional judgment of the simulator, 3) performing simulations against relevant hourly in and outside boundary conditions, and 4) investigating and recording of results." Double-skin performance depends on the airflow rate exhausting heat gain from inside the cavity. Thus, fans were used to hasten the cavity airflow. Temperature differences between the outdoor air, the cavity and the indoor air all affect heat transfer into the building. Also, wind speed and direction may influence airflow rates inside the cavity due to pressure differences.

The model design was an eight-floor (zone) office building, 7.5m wide and 5m deep. Seven floors (zones) covered with double-skin facades were linked via an airflow network of inlet-outlet ports. Shading devices were closed with no exchange of air between the offices and system cavities. The external layer of the double-skin system was a single clear pane 6mm thick, while the interior layer comprised double-glazed windows with shading devices in the cavity.

Four simulations were performed to compare the level of savings offered. The first model was a base scenario with a conventional window system during a hot summer day. The second scenario was the building on a hot summer day with a double-skin system installed. The third model was similar to model two, but without wind effects. The final model was the building with double-skin facades assuming the exhaust outlet closed. Comparing the first model with the second showed how much influence the double-skin system would have on energy performance. Model three revealed wind effects on the performance of the double-skin system. Scenario four simulated the impact of malfunction by having the outlet closed in this unlikely event of failure to maintain the system.

Table 2.8 According Bartak, Dunovska, & Hensen (2001), "Maximum sensible cooling loads for the offices adjacent to the double-skin facade during an extreme summer day for modes 1 and 2"

Floor level	Maximum sensible cooling load		Additional maximum sensible cooling load due to double-skin façade	
	Case A kW	Case B kW	W	W/m^2 floor
8th	2.41	3.29	880	23
7th	2.40	3.24	840	22
6th	2.40	3.20	800	21
5th	2.39	3.14	750	20
4th	2.37	3.08	710	19
3rd	2.31	2.95	640	17
2nd	2.16	2.67	510	14

Comparing double-skin façade (A) with conventional Case B reveals the energy saved.

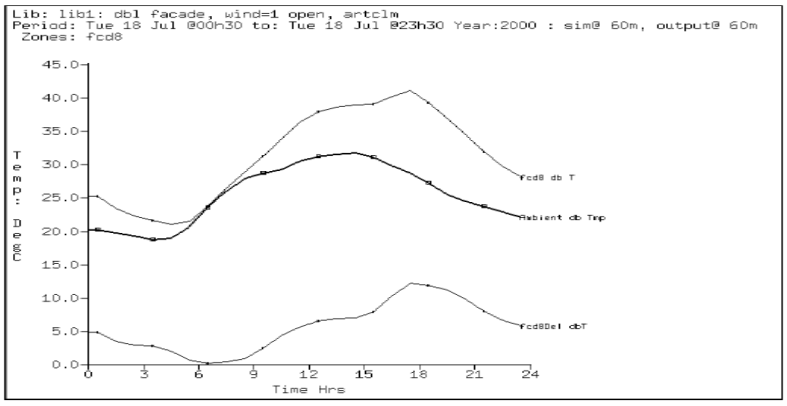

Figure 2.33 According to Bartak, Dunovska, & Hensen (2001), "Second model inlet and outlet air temperatures of the double-skin facade during an extreme summer day"

The third model lacking wind showed no significant change versus the second model, indicating the stack effect as dominant in cavity airflow. The cavity in the fourth model with a closed outlet rose more than 50°F higher than the ambient temperature in the middle afternoon on a hot summer day! In the simulation of the second model, airflow inside the cavity increased due to its higher temperature. However, the simulation showed early morning temperatures inside the cavity to be lower than for ambient air, and the cool dense air inside the cavity sank downward.

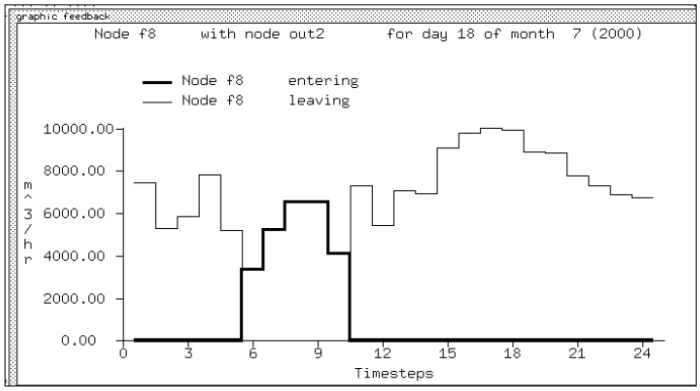

Figure 2.34 According to Bartak, Dunovska, & Hensen (2001), "Airflow rate through the double-skin facade during an extreme summer day"

The simulations indicated the temperature inside the double-skin façade cavity to be greater than the outdoor temperature most of the time, thus cushioning winter heat loss. In summer, higher temperatures inside the cavity increased the rate of the airflow while allowing more heat indoors. Minimizing heat admission means cutting air residence time in the cavity ($T_{cavity} \approx T_{OA}$) while reducing solar gain. Furthermore, an extra layer of the double-skin façade reduced solar radiation transmitted through the office windows when using the cavity shading devices. Shading devices can lower energy needed for cooling to counter solar radiation. However, the double-skin system may actually trap heat gains in summer if the system is not designed properly. Cavity airflow is essential! Successful heat removal must minimize cavity air residence time to reduce inward solar gains.

Simulation applies when the model is well designed. To do so, it is vital to choose the appropriate model in terms of detail and level of complexity. Simulation can then be used to compare design options and system

technologies to predict potential savings. Results from building simulation software apply when model data are validated and sensors calibrated.

In their paper titled "Defining the performance of the double-skin façade with the use of simulation model," Stec and Paassen studied double-skin façade performance via computer modeling. They began their research by creating an airflow model. Cavity airflow is driven by two main forces: (1) stack effect, caused by temperature difference between the cavity and the outside, and (2) wind, an exogenous factor affecting the airflow. The stack effect can be easily measured in a controlled environment. Validation of wind pressure data impact on the system can be complex with changing wind speed and direction. In order to compute the total force driving air inside the cavity, both stack and wind pressure effects need to be calculated:

$$\Delta P_{tot} = \Delta P_{stack} + \Delta P_{wind} \quad (2.1)$$

The total pressure cavity drop is measured by the difference between the inlet opening in the lower part of the system and the outlet opening at the upper part of the double-skin façade. To calculate the amount of air flow for the facade, the next equation relates wind and cavity pressures:

$$q_{in} = C_{tot}\sqrt{\Delta P_{tot}} \text{ where} \quad (2.2)$$

q_{in} = amount of air entering the cavity through the inlet.
C_{tot} = wind total pressure
ΔP_{tot}= total pressure difference between inlet and outlet of the cavity.

There are values of resistance coefficients that need to be used in order to calculate the double-skin system performance through Equation 2.7. According to Kouch (2001) and Recknagel et al. (1994), a selected number of values were taken into consideration for this research.

Table 2.9 According to Kouch (2001), Recknagel et al. (1994) "The Values of the resistance coefficients"

Coefficient	Value
ξ_{inlet}	2,01
ξ_{valve_max}	0,78
ξ_{valve_min}	100
ξ_{cavity_max}	1,60
ξ_{cavity_min}	1,90
ξ_{outlet}	1,45

To calculate the outlet airflow of the cavity, the difference of the flow inside the cavity and the ventilation through the window must be known. The following equation is used:

$$q_{out} = q_{in} - q_{vent} \text{ where} \quad (2.3)$$

q_{out} = the amount of outlet airflow.
q_{in} = the amount of air entering the cavity through the inlet.
q_{vent} = the amount of ventilation flow through the window

The amount of ventilation flow through the window is calculated based on the Passen and Groninger equation

$$q_{vent} = A_{eff}\sqrt{\frac{2}{10^{-3.333y+2.198}}}\sqrt{\Delta P_{window}} \text{ where} \quad (2.4)$$

A_{eff} = Effective area of the operative opening of the window.
ΔP_{window} = Pressure difference in the cavity between room and cavity.

$$A_{eff} = \sqrt{\frac{1}{\frac{1}{(h_w * b_w)^2} + \frac{1}{(2h_w * b_w * \sin(0.5\varphi) + h_w^2 * \sin(\varphi))^2}}} \text{ where} \quad (2.5)$$

h_w = Height of the window.
b_w = width of the window.
φ = Opening angle of the window.

Laboratory tests quantifying the stack effect were conducted in a facility that protected the model from air movement to isolate the stack effect as the sole driving force in the cavity. Stec and Paassen (2003) remarked, "The test facility is situated inside the laboratory. It consists of a cavity formed by a front surface of the glass and a well-insulated back wall. During the measurement, it was protected from the air movement inside the laboratory." (p124). To calculate pressure difference in the model, the following equation was used:

$$\Delta p_{stack} = \left[\frac{\theta_c - \theta_o}{273 + \frac{\theta_c + \theta_o}{2}}\right] * g * h * \rho \quad \text{where} \qquad (2.6)$$

Δp_{stack} = Pressure difference caused by stack effect.
θ_c = Temperature in the cavity.
θ_o = Temperature outside the model.
g = 9.81 (acceleration due to gravity).
h = Height of the wall.
ρ = Air density at cavity inlet temperature.

Airflow in the cavity was calculated using Bernoulli's equation:

$$\Delta p_{stack} = \sum_1^n \xi_{i,v,c,o} * \frac{1}{2} * \rho * v^2 \quad \text{where} \qquad (2.7)$$

Δp_{stack} = Pressure difference caused by stack effect.
$\xi_{i,v,c,o}$ = Resistance of inlet, valve, cavity and outlet (Table 2.9).
θ_o = Temperature outside the model.
v = Velocity of the air in the duct.
ρ = Air density for a temperature of the air that enters the

Airflow has a major influence on the system performance, and cavity airflow is caused by two main drivers: the temperature and pressure differences between the inlet and outlet. Both differences need to be calculated in order to study airflow rate inside the cavity. In this experiment, the system was used for cooling purposes: to exhaust heat from the cavity to the outside and to minimize heat gain through the inner layer of the system. Naturally ventilated systems are driven by the stack effect's temperature difference between the air inside the cavity and air

outside. The bigger the temperature difference, the faster cavity air rises. The second driving force is the pressure difference between the inlet and outlet openings of the system. The pressure difference in naturally ventilated systems can also be influenced by wind. Recall the total pressure force in the system is:

$$\Delta P_{tot} = \Delta P_{stack} + \Delta p_{wind} \text{ where} \quad (2.1)$$

P_{stack}= pressure created by stack effect.
p_{wind} = pressure created by wind effect.

In summary, natural ventilation is a complex, dynamic fluid interaction of changing air properties, radiation and wind conditions beyond the control of building users. Better and simpler are mechanically ventilated systems with fans located near the upper outlet that create suction drawing cavity airflow at faster known rates to reduce heat transfer through the inner layer. This is precisely what the system needs to do for A/C energy reduction in hot weather conditions. Airflow needed to remove a specific amount of heat in the cavity can be calculated using this consolidated equation (ASHREA, 1985):

$$Q = H \,/\, c_\rho \, \rho \, (t_i - t_0) \text{ where} \quad (2.8)$$

$\boldsymbol{Q}$ = Air flow required to remove heat, cfm
$\boldsymbol{H}$ = Heat to be removed, Btu/min
$\boldsymbol{c_\rho}$ = Specific heat of air, Btu/lb_m °F
$\boldsymbol{\rho}$ = Air Density, lb_m / ft^3
$\boldsymbol{t_i}$ = Air inlet temperature, °F
$\boldsymbol{t_0}$ = Air outlet temperature, °F

In a study of a new type of double-skin façade configuration for the hot, humid climate, Wong, Prasad, & Behania (2008) used CFD (computational fluid dynamics) simulations to investigate the thermal performance of the double-skin system. In this research, CFD was used to analyze different thermal comfort parameters with several double-skin facades to improve indoor thermal comfort in hot, humid climate using natural ventilation strategies for high-rise buildings. Parameters related to the building design were analyzed, e.g., air velocity and humidity, using CFD.

Ventilation within the cavity space is an essential aspect in double-skin system performance that determines efficiency, the operation of thermal controls, and adjustments to the sun shading device installed in the cavity. The ventilation mode can also vary according to building requirements. The ventilation mode can be selected as naturally driven, mechanically forced or both. In any case, experiments have shown significant energy savings to be possible exploiting the ventilation of cavity air using the double-skin facade system.

Airpak is a CFD software with object-based modeling and libraries using automatic unstructured meshing to enable complex model-building. Airpak enlists the FLUENT CFD solver engine for instant thermal and fluid-flow calculations. Wong, Prasad & Behania (WPB, 2008) noted, "Airpak is an easy-to-use design tool for the design and analysis of ventilation systems which are required to provide acceptable thermal comfort and indoor air quality solutions. It is virtual prototyping software that allows for accurate modeling of airflow, heat transfer, contaminant transport and thermal comfort" (p.2). The most powerful element of this program is that it produces colorful and easy-to-read animations that effectively analyze results. The post-processing feature also yields fast and comprehensive results for the ventilation problems at hand.

WPB research examined natural ventilation performance for an 18-floor office building in hot, humid climate exploiting the double-skin facade. Airpak modeled complex energy transfer through each component of the multilayer facade while optimizing glass opening size, cavity space width, and ventilation rate through the office area. Office volume model dimensions formed a 3.5m cube with a 2.6m-high false ceiling.

The double-skin system used in the building simulation was simple with a single 6mm glass pane for the external layer. The inner layer comprised double-glazed 6mm panes enclosing a 12mm gap. Both inner and external layers had windows that could be opened for natural ventilation. For the thermal comfort study, internal heat loads from two people using two computers and four ceiling lights were simulated undergoing fixed weather conditions. Wong, Prasad, & Behania (2008) remarked that "simulated wind speeds of 1.5 m/s and 3.0 m/s are used to model expected ground level wind velocities with an ambient temperature of 30˚C and relative humidity of 70%. The external temperature at the rear wall is set to 23 ˚C to simulate an internal air-conditioning space like an internal corridor" (p.3).

For better computational efficiency, the 18-floor model building was segmented into three stages of six floors each. Stage one of the model consisted of a ground floor without a double-skin and five stories of office space with the double-skin. The DSF adopted in the model is a ventilated-shaft design, and simulations were carried out oriented north, south, east and west. The first group of simulations modeled the DSF system.

The researchers set these boundary conditions for all three stages of modeling in order to compare results:

1- Wind speed was 0.5m/s to a maximum of 3 m/s.
2- Wind direction was perpendicular to the double-skin system.
3- External temperature was 26 ˚C to 30 ˚C.
4- External Humidity was 70% to 100%.
5- Window opening size for inner layer of double-skin system was 300mm.
6- Air gap size varied from 300mm up to 1200mm.
7- Vent ports were 300mm x 600mm.
8- Simulation was performed twice daily (10 am and 2 pm).

Six scenarios were simulated the different times and conditions tabulated:

Table 2.10 According to Wong, Prasad & Behania (2008), "Different boundary conditions for stage one" (p.4).

Simulation	Orientation	Date	Time	Air Temp. (^{0}C)	Wind Vel. (m/s)	Air RH (%)	Air Gap Size (mm)
S1-1	South	15 Jan	2pm	28	1.5	80	300
S1-2	South	15 Jan	2pm	28	1.5	80	600
S1-3	South	15 Jan	2pm	28	1.5	80	900
S1-4	South	15 Jan	2pm	26	1.5	80	300
S1-5	South	15 Jan	10am	26	1.5	80	300
S1-6	South	15 Jan	10am	28	1.5	80	300

Results for different boundary conditions are presented next in Table 2.11. Indoor operative temperature (OT) is lower and acceptable for thermal comfort using the better-insulated 300mm air gap (SI-4-6). Also, the south-looking facade benefitted most, followed by the eastern facade during the morning period in January. Northern and western facades did not offer acceptable indoor thermal comfort for office use. Simulations were run with various ambient temperatures, external velocities, orientations of the double-skin facade, periods of time during the day, etc. to determine the appropriate window periods for acceptable indoor office usage. These ample data aid the study of DSF performance in various climates.

Table 2.11 Wong, Prasad, & Behania (2008), "Simulation results (shaded are acceptable thermal comfort conditions" (p.4).

Simulation	Floor Level	Air Temp. (^{0}C)	Air Vel. (m/s)	Radiant Temp. (^{0}C)	Air RH (%)	PMV	OT (^{0}C)
S1-1	1	28.5	0.04	29.93	70.49	1.99	29.22
	3	29.08	0.01	29.52	77.3	1.8	29.30
	5	29.47	0.01	29.64	75.59	1.85	29.56
S1-2	1	29.95	0.02	32.96	70.69	2.41	31.46
	3	30.67	0.04	31.50	76.60	1.97	31.09
	5	30.72	0.03	31.19	75.42	2.13	30.96
S1-3	1	29.99	0.03	32.48	70.61	2.38	30.59
	3	30.47	0.06	32.25	77.40	2.04	31.36
	5	30.43	0.04	31.98	76.25	1.9	31.20
S1-4	1	27.49	0.04	28.98	70.54	1.8	28.24
	3	28.15	0.05	29.45	76.39	1.66	28.80
	5	27.40	0.03	28.67	75.44	1.6	28.04
S1-5	1	27.38	0.02	28.74	70.22	1.97	28.06
	3	28.07	0.04	29.59	76.13	1.62	28.83
	5	27.61	0.03	28.81	74.85	1.59	28.21
S1-6	1	28.41	0.03	29.73	70.17	1.92	29.07
	3	29	0.01	29.38	77.04	1.78	29.19
	5	29.26	0.01	29.5	75	1.84	29.38

The efficiency of natural cooling strategies in an office building with and without a double-skin facade during a sunny summer day was examined in the study conducted by Gratia, & Herde (2004). The research featured natural ventilation possibilities in relation to double-skin orientation versus wind speed and direction. Simulations enlisting TAS software studied a multi-story, double-skin facade building proposal according to Subtask A of Task 27 (performance of solar facade components) as part of the International Energy Agency solar heating and cooling program.

The double-skin facade is used for buildings in areas where open-window ventilation is impossible with high, upper-floor wind velocities and lower-floor traffic noise. These DSFs provide daylight, outdoor uniformity, and appealing aesthetics. Simulation of cooling loads for the building without double-skin, with a south double-skin and with a north double-skin was implemented to compare system performance.

The simulation was carried out with the help of TAS to consider various options and designs of the double-skin. The program performs a thermal investigation of buildings using a 3D modeler, a thermal/energy analysis module, a systems/controls simulator and a 2D-CFD package. TAS is a powerful design tool for optimizing a building's environment, energy and comfort performance. The building examined was a facility consisting of office spaces aligned on two facades and a central corridor separating the two office clusters with end-hallway staircases.

The building housed 150 offices distributed over five floors and arrayed in two orientations. Internal walls between office modules and corridor had upper windows to link airflow between northern and southern zones. Four windows in each office (two above and below) allowed natural day and night ventilation.

Building envelope data: Roof U = 0.3 W/sq.m-K, Ground Floor U = 0.379, Opaque part of facade U = 0.373 W/sq.m-K, Low-e double glazing U = 1.8, and direct solar transmission coefficient of 0.708.

Double-skin data: Clear single glass, U-value = 5.33 W/sq.m-K, SF = 0.76, width of air cavity = 1.2 m, H (double-skin facade) = building height + 1m.

When DSF is oriented south and wind direction is from the north, only the top vent of the double-skin is opened with the following results:

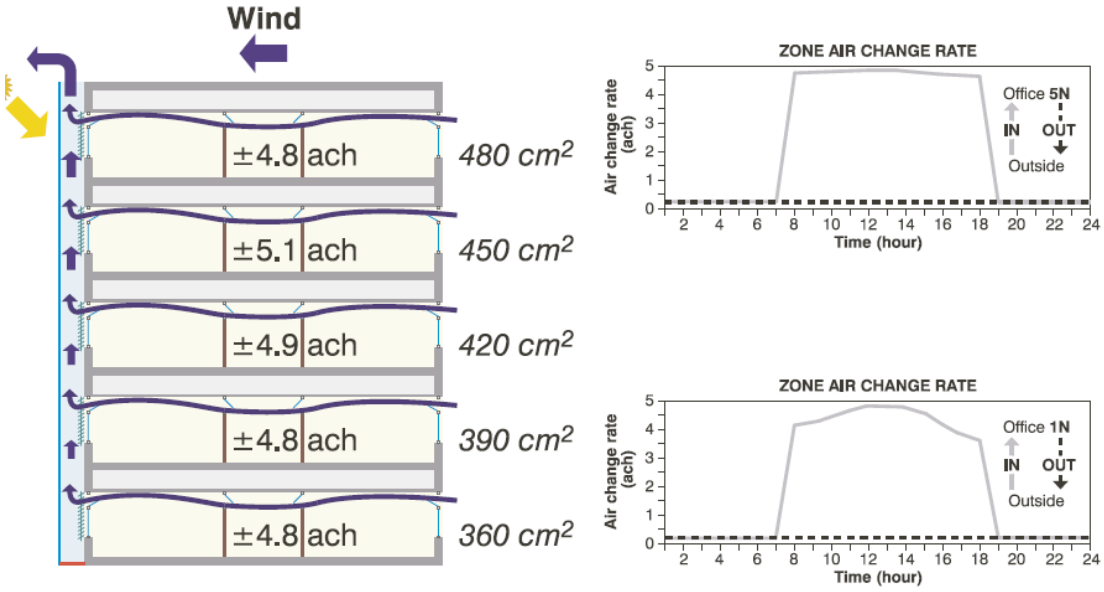

Figure 2.35 According to Gratia & Herde (2004), "Office air change rate (ach) for a North oriented wind when only the top window of the Southern double-skin is opened and when day ventilation is operated" (p.142).

Figure 2.35 presents zone air change rates and aperture areas in each office for various floors. Graphs represent air change rates during the day for *north* offices at the fifth and ground floors that feed the southern DSF. To obtain a ventilation rate of 4 "ach", openings for the upper floors must enlarge for decreasing stack effect at upper building levels and for a smaller wind pressure coefficient at the top floor. At the ground floor, the zone air change rate curves with radiation and the temperature profile in the double-skin. At higher floors, however, airflow is constant since the stack effect is negligible where the DSF temperature peaked at 35 deg. C.

When wind is from the south with just the top vent of the double-skin open, very different results are obtained. For lower floors where the temperature in the double-skin is lower for minor stack effect, airflow reverses direction!

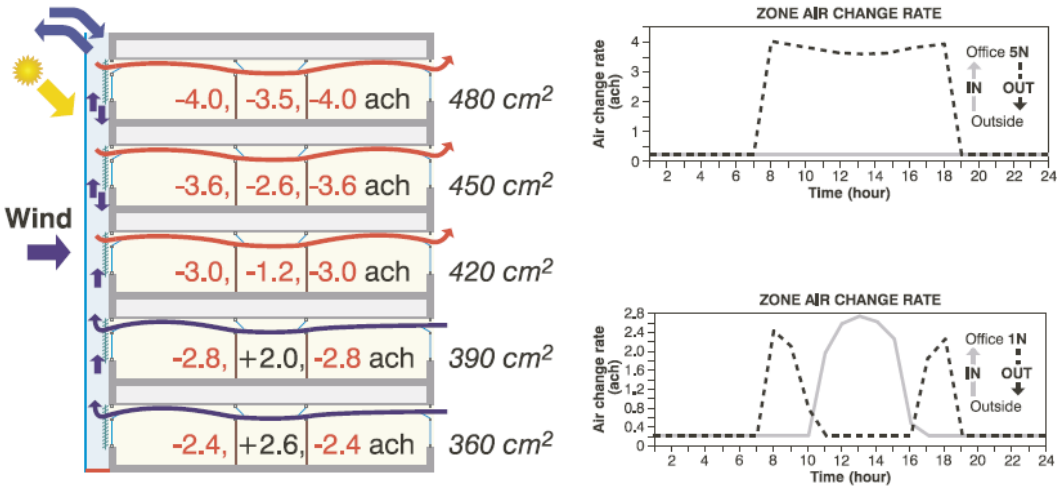

Figure 2.36 According to Gratia & Herde (2004), "Office air change rate for a South oriented wind when only the top window of the Southern double-skin is opened and when day ventilation is opened" (p.143).

Figure 2.36 shows the daily (morning, midday, afternoon) zone air change rate for each office on most floors to be negative with *inward* airflow! However, from 11 a.m. to 4 p.m, air flowed *out* of lower offices to the DSF. Cavity temperature exceeded 30C with only one opening at the DSF top. Figure 2.37 shows the cavity air temperature rise over outdoor air (20C).

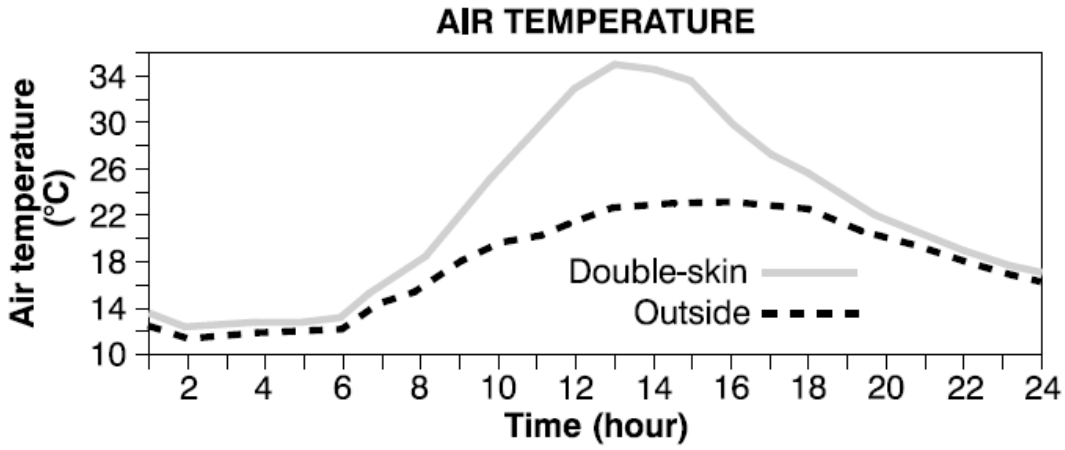

Figure 2.37 According to Gratia & Herde (2004), "Temperature evolution in the South double-skin with only the top window opened when day ventilation is operated" (p.143).

Natural night ventilation modes operated as follows in all the cases for the double-skin oriented north or south:

Evening air movements are mainly driven by the wind since there is no rise in cavity temperature from solar radiation. If the double-skin facade is oriented south and the wind direction is from the north, only the top vent of the double-skin is opened. Here, airflow through the building is in the desired direction at a more or less constant rate since the temperature variation in the double-skin during the night is small. The temperature of double-skin remains high during the night due to ventilation from office air.

If the double-skin facade is oriented north and the wind direction is from the north, then the air movement is reversed with the double-skin directly ventilated by outside air: cavity and outdoor temperatures are the same. Still, ventilation is more effective if air flows from offices to the double-skin.

Cooling consumption comparisons for a sunny summer day considered the following configurations.

Building without a double-skin:

1. No shading device, no increased ventilation: 1033 kwh/d cooling load.

2. Southern façade, external shading device, no increased ventilation: daily cooling load of 685 kwh.

3. Southern façade, external shading device, increased natural day ventilation: 549 kwh daily cooling load.

4. Single-sided natural ventilation: 474kwh/day, Cross-natural ventilation: 608 kwh/day.

Building with a double-skin facing south:

1. No shading device, no increased ventilation and closed double-skin: daily cooling load of 1147 kwh.

2. With shading device, no increased ventilation and closed double-skin: drops to 911kwh daily.

3. With shading device and increased natural night ventilation (where air flow direction has no importance) – one double-skin vent open: 721 kwh, both double-skin top and down vents open: 665 kwh daily cooling load.

This study offered a clear view of various configurations of the double-skin. It revealed how improper operation of the double-skin could lead to catastrophic results, such as the injection of hot cavity air into the building during summer when it should be cooled. Given the diverse typologies of the double-skin system, the operation mode must react properly to the climate conditions as well as the building interior environment. The aim of the research was to find which conditions permitted natural ventilation and how the DSF may favorably ventilate office buildings.

2.8 Conclusion

Prior research conducted by Shou-li compared two systems in a controlled experimental setup to yield findings that apply to this dissertation's research. Shou-li compared the performance of naturally versus mechanically ventilated systems. In the study, full-scale models were constructed of wood, metal, and 6'x 8' glass windows. The first model was a mechanically ventilated system using fans to vent the cavity. The second was passive operating by the stack effect. The active system offered higher heat removal rate in overheated periods per Shou-li (2000): the "mechanically ventilated system had a 57% heat removal rate compared to 32.5% for the passive system" (p.12). Shou-Li's research also found the average temperature difference between the indoor glass surface and indoor air to be lower in the mechanically ventilated system.

These conclusions inspired the design of a new system that mechanically vents air from the system cavity. In hot weather conditions, higher airflow rates inside the double-skin system are crucial to minimizing the heat that is transferred into the building interior. The new system uses fans that do not require electricity to operate, enhancing energy savings. This system will be detailed in Chapter 3.

The Saelens case studies evaluated "as-built" buildings. The first was the DVV headquarters in Brussels, Belgium. In winter, the system provided heat to the building to cut heating costs. In summer, the cavity heat from solar heat gain was removed by cavity airflow while the temperature was cooled a bit lower that of the outer glass surface. However, findings did not conclusively indicate a reduction in system energy needs for cooling. In a different case study, the Postcheque building in Brussels that used the natural ventilation method was studied. Saelens found that air exchange rates inside the cavity slowed when the shading device was closed. Venetian blinds were shut in hot weather to minimize solar admission.

In summary, literature review findings may be presented by:

A. Performance.
B. Variables.
C. Research Method Summary.

2.8.1 Performance

The performance of the double-skin façade can be evaluated by a number of factors. System traits and issues as found in the literature were:

1. Sound-insulating properties: the external layers of forced ventilated façades have better sound-insulating properties when compared to the naturally ventilated system. In general, fewer ports in the external layer mean better sound insulation. Using the right system is a decision that should be made after studying location and weather conditions.

2. Level of cooling or heating energy reduction: how did the system perform as to warming the cavity near the indoor air temperature in winter and reducing the amount of cooling needed to maintain comfort inside the building in summer?

3. Daylight utilization and control: shading devices located inside the cavity can reduce heat gain caused by solar radiation. Yet, it is crucial to remove cavity heat in summer and recycle it in winter. Sun angle and building orientation also factor in toward optimal shading benefits.

4. Night-time ventilation: night ventilation can lower energy needed to maintain comfort inside buildings. Under certain conditions, natural ventilation removes heat stored in furniture and fixtures inside buildings. Ports in the external layer promote fresh cavity airflow (without risking security) for natural ventilation of the building via inner layer openings.

5. Natural ventilation: fresh air introduced into the building can lower the risk of "sick-building" syndrome that results from a lack of fresh air.

6. It is unclear how the double-skin façade system will perform in hot weather conditions. Most studies focused on how the double-skin façade system functions in winter months for heating purposes. Presently, there is no clear evidence of how the double-skin façade system will perform in hot, arid weather conditions.

2.8.2 Variables

From the literature, there are a number of variables that influence the performance of the double-skin façade system. We can categorize these variables in two forms: indigenous and exogenous.

2.8.2.1 Indigenous variables are internal system factors that can affect the system performance, such as those listed next.

Cavity height: cavity height can influence the amount of temperature increase inside the cavity. A one-story window will have less temperature increase than a multi-story system. In cold weather conditions, a multi-story system well warms the cavity closer to the inside temperature to thus cut heating costs. On the other hand, a single-story system best limits cavity temperature overheating in hot weather conditions.

Cavity width: the width can vary from a few inches up to several feet. Cavity width can accommodate or hinder shading device capacity, maintenance and cleaning concerns, and airflow rate inside the cavity.

Openings: the size of ventilation ports and the distance between them can affect the quantity of fresh air introduced and heated air removed. Furthermore, these openings can be useful during night ventilation modes.

External (natural) versus internal (forced) airflow: the external, naturally ventilated system is driven by the stack effect. Air inside the cavity increases in temperature and rises through vents. A naturally ventilated system usually has a single external glass layer, a cavity, and a double glass inner layer. An internal, forced-air layout differs with an external double-glass layer, a cavity, and a single inner glass pane. This system is good for sound insulation, but with no windows, delivery of fresh air inside the building requires a mechanically mixed flow.

Glass type and properties: technologies like low-E glass can help reduce summer heat transfer through the inner layer. The external layer is usually a single, clear glass layer to capture winter radiation warmth in the cavity.

Shading devices: the material used, the dimension and location inside the cavity can greatly affect the performance of the double-skin system.

2.8.2.2 Exogenous variables are external factors that can further affect system performance, regardless of the design specifications.

Building type: the function and the behavior of the building can significantly impact building performance. An office will have different requirements than a residential facility. The interaction between the inner zones and the envelope will affect performance.

Climate: hourly wind speed and direction, sun angle, temperature and other environmental factors can impact performance. Climate variables, too, can influence the required long-term features of the system.

Orientation of the building: the direction of system exposure plays a role.

Ventilation: each type of double-skin system vents cavity air differently.

2.8.3 Research method summary

Prior DSF studies have used three research methodologies that offered valuable knowledge and insight shaping the line of proposed research:

1. Experimental research (Shou-Li)
2. On-site monitoring and case studies (Saelens).
3. Simulations and statistical studies (DOE-2, Airpak, TAS, CFD).

2.9 Proposed double-skin façade system for hot, arid weather conditions

To take full advantage of the double-skin façade system in hot weather conditions, a few factors need to be considered when building the system to reduce energy consumption. Adopting the system in locations with high solar radiation needs to consider that the double-skin façade air cavity can rise in temperature, impairing the performance of the system. To avoid air cavity overheating, the following are recommendations to consider when using the double-skin façade system in hot, arid climate:

1) The box-window and corridor type of double-skin façade systems are the best choices for hot weather conditions. Both systems are just one-story high to limit cavity overheating from longer air-residence times. Compressed heights maintain a lower summer temperature difference between the cavity and indoor air. Better sound insulation is also a plus.

2) The box-window proposed is to be mechanically ventilated, resulting in greater heat removal inside the cavity. The HVAC return ducts will increase airflow to minimize solar heat gain and keep the cavity closer to the indoor temperature. Less heat transfers through the inner glass. Unlike the passive system, mechanically forced box-plot airflow inside the cavity is fed by the overall HVAC zone airflow which will increase heat removal rates inside the system cavity.

3) Shading device inside the cavity is recommended. Not only will the shading device help control light transmission, but it will help capture admitted solar radiation. The shading device should be constructed of low specific heat material (wood) coated with a reflective tint (white). The shading device should reside in the middle of the cavity, allowing airflow around it to aid heat removal. Furthermore, the lower two feet of the cavity should be free of venation blinds to foster air inlet mixing for a better distribution of air to avoid hot pockets in the cavity.

4) The DSF cavity should be mechanically ventilated. Increased airflow in the cavity will remove more heat to prevent dramatic cavity temperature rises. Naturally ventilated DSFs rely on cavity heating to expel hotter, less dense air rising through the outlet. Hot cavities must be strictly avoided when cooling any facility in hot weather conditions.

5) The DSF cavity should be wide enough to house a central shading device that allows ample airflow to avoid hot pockets in the cavity. Hot pockets enhance conductive heat admission. Spacing of 1'-2' is advised to promote airflow and hinder radiation from the outer glass.

6) The box-window double-skin façade system should enlist low-e glazing to better reflect sunrays that will curtail solar radiation admission.

The proposed double-skin façade system has great potential to reduce energy consumption. Nevertheless, the right specifications are crucial! The system cavity must be designed for consistent flow allowing air to remove captured heat while preventing huge cavity air temperature rises. It is normal for cavity to warm, but the lower the difference in temperature between the cavity and office, the better the system below will perform.

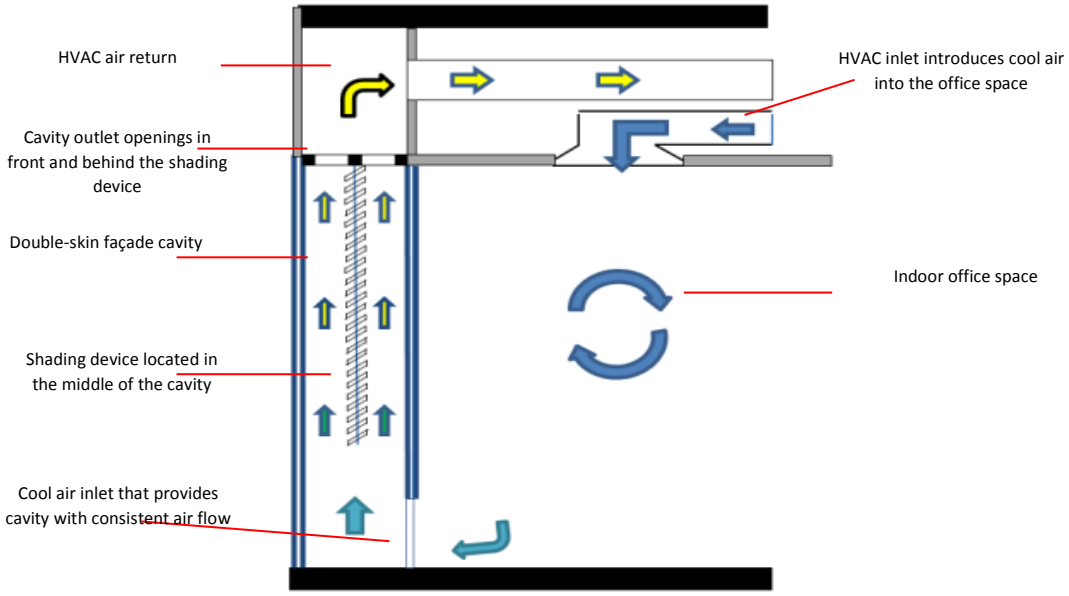

Figure 2.38 Proposed window system for hot weather conditions.

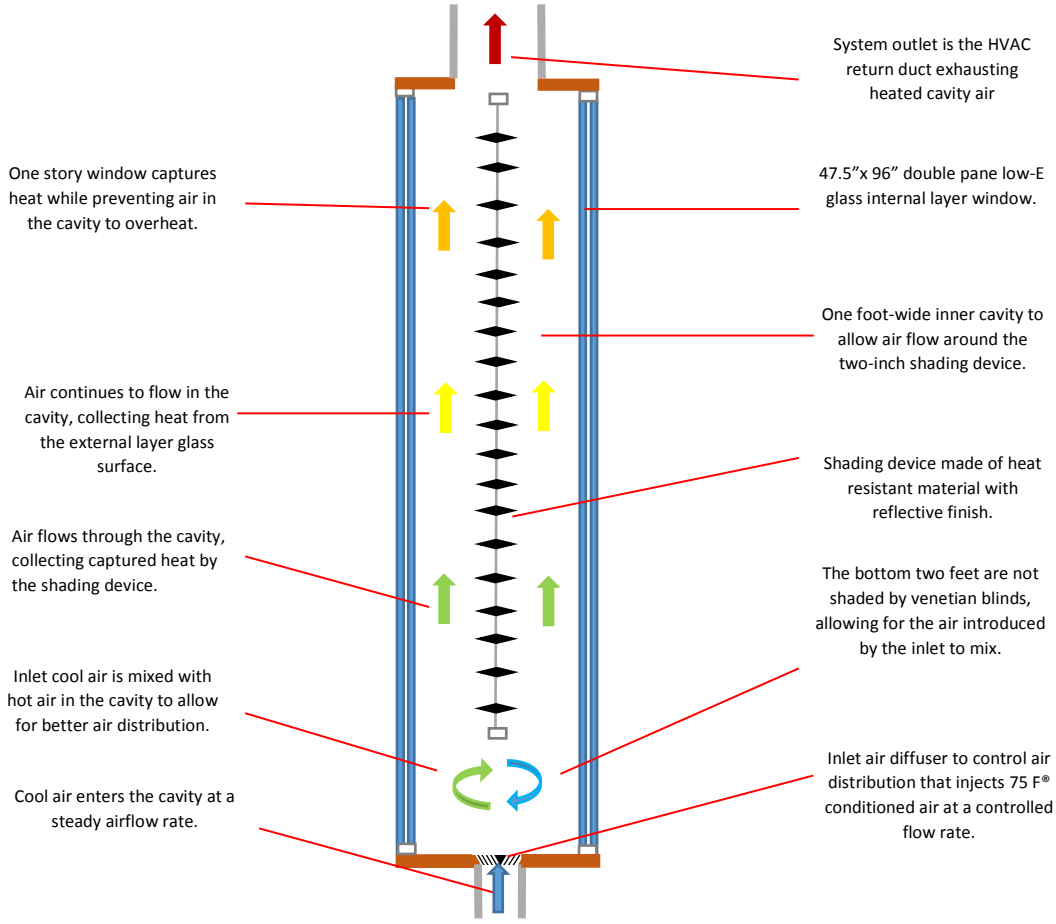

Figure 2.39 Proposed window system for hot weather conditions.

Chapter 3

3. Methodology

3.1 Introduction

This chapter describes the research methodology toward studying the performance of a double-skin façade system. The research goal is to assess the performance a double-skin façade system in comparison with windows typically found in mixed-use / office buildings located amid hot, arid climates. This chapter presents possible test methods, and the selected methodology will be described and justified. The methodology attempts to meet the following research objectives:

1. Assess the thermal and light performance of the double-skin façade (DSF) system when compared to a single layer, low-E window.
2. Collect on-site test data for hot weather conditions.
3. Statistically compare DSF thermal and light performance with the reference window.
4. Simulate a representative building in the desired climate conditions using the on-site data results.
5. Summarize energy-related findings.

3.2 Qualitative approach overview

Qualitative methods of research attempt to study different phenomena in their natural settings without intervention. In other words, qualitative approaches try to understand various systems or occurrences as they are. Authors Groat and Wang describe the qualitative research method as a multi-method enlisting interpretive and naturalistic approaches to attain research goals (Denzil & Lincoln, as quoted in Groat & Wang, 2002 p.176).

This can take the form of learning from case studies, from prior relevant literature, or through interviews. The goal is to collect data or opinions about a certain aspect for assessment. Qualitative research is mostly summarizing lessons learned from studying a certain system or phenomenon where the researcher himself will make sense of these lessons (Miles & Huberman, 1994).

Since there is relatively little use of standardized measures such as surveys and questionnaires, the researcher is "essentially the main measurement device in the study" (p.7).

In qualitative research approaches, researchers base their work on facts, observations, interviews, and literature. Common qualitative research method types include the following.

Holistic. "The goal of qualitative research is to gain a holistic (systematic, encompassing, integrated) overview of the context under study" (Miles and Huberman, 1995, p.6).

Prolonged Contact. **"**Qualitative research is conducted through intense and/or prolonged contact with a 'Field' or life situation. Hence, the emphasis in many studies is on fieldwork" (Miles and Huberman, 1994, p.6).

Open-ended. Qualitative research tends to be more open-ended in both theoretical conception and research design than other research strategies (e.g. experimental or correlational) because it typically eschews the notion of a knowable, objective reality (Creswell, 1994, p.44).

Analysis through words. Since an emphasis on descriptive numerical measures and inferential statistics is typically eschewed, the principal mode of analysis is through words, whether represented through visual or narrative devices (Miles and Huberman, 1994, p.7).

Personal information writing stance. In contrast to the typical journal format of experimental or correlational studies, the writing style of qualitative work is typically offered in a personal, informal writing style that lessens the distance between the writer and the reader (Groat & Wang, 2002, p.179)**.**

3.3 Quantitative method overview

The quantitative method of research is completely different from the qualitative approach. While the qualitative approach is more subjective, quantitative research methods use numerical data to understand a certain system or phenomenon.

The quantitative methodology answers certain questions by collecting numerical data to compare the performance of two or more subjects using statistics and visual charts. According to Creswell (2003), "Quantitative research involves the collection of data so that the information can be quantified and subjected to statistical treatment in order to support or refute alternate knowledge claims" (p.153). Quantitative research therefore does not depend on the researcher since the data collected quantitatively measure reality or a certain set of facts. The data collected uncover a relationship through statistical studies useful for making suggestions and recommendations based on those numbers. The findings from this kind of statistical analysis can be explanatory, affirmative, or predictive.

The questions that a quantitative study attempts to address could be broad or specific, depending on the goals and answers that are sought. Generally, the goal of quantitative research methods is to quantify the results of incident samples of data or opinions for advising definitive paths of action. "Quantitative researchers seek explanations and predictions that can be applied to other persons and places. The intent is to establish, confirm, or validate relationships and to develop generalizations that contribute to theory" (Leedy and Ormrod (2001), p.102). While it seems that a quantitative approach is forthright in recording data of a certain system or phenomenon, quantitative research findings can be elusive. Groat & Wang (2002) note, "Although the notion of measurement may seem straightforward, it can involve complex decisions" (p. 209).

It is crucial to identify the salient variables and ask the right questions. Three typical phases of quantitative studies include the research design, measurement procedure and testing, and the statistical evaluation. Quantitative research starts with a statement usually presented as a problem that the research study will solve. This statement also defines the purpose of the study.

In this research, the question concerns what, if any, reduction in energy consumption will result from the double-skin façade system as compared to the commonly used commercial window. The recipe for a quantitative study usually contains the following ingredients:

1. Selecting a problem (statement) that defines the purpose of the study.
2. Reviewing literature that enhances the knowledge of the researcher.
3. Discussing all of the questions that the study will attempt to answer.
4. Creating a hypothesis.
5. Identifying the variables that will most affect the performance of the system or phenomenon.
6. Planning and justifying a proper test procedure for executing the study.
7. Experimenting.
8. On-site monitoring.
9. Collecting data.
10. Analyzing data.
11. Modeling and simulating.
12. DSF statistical calculations for each individual window using Riyadh weather data.
13. Summarizing lessons learned.

A few forms of the quantitative method include: descriptive, correlational, cause-compared, and experimental. The experimental and numerical simulation approaches were used in this research. More details about the experimental, statistical and simulation phases come later in this chapter.

3.3.1 Flowchart of the research process

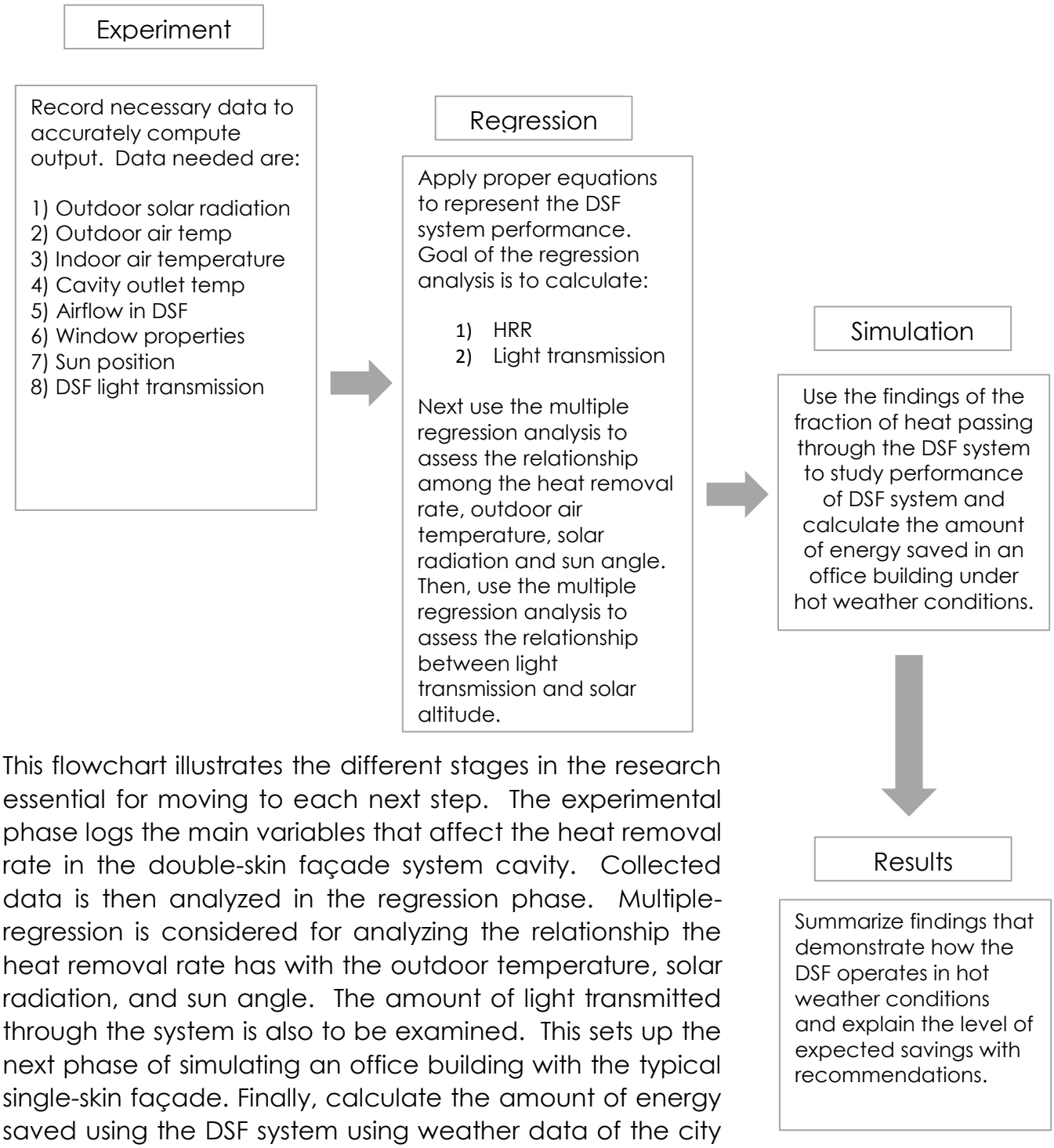

This flowchart illustrates the different stages in the research essential for moving to each next step. The experimental phase logs the main variables that affect the heat removal rate in the double-skin façade system cavity. Collected data is then analyzed in the regression phase. Multiple-regression is considered for analyzing the relationship the heat removal rate has with the outdoor temperature, solar radiation, and sun angle. The amount of light transmitted through the system is also to be examined. This sets up the next phase of simulating an office building with the typical single-skin façade. Finally, calculate the amount of energy saved using the DSF system using weather data of the city of Riyadh, Saudi Arabia.

3.3.2 Experimental approach

Experimental research is data-driven. This research approach can be applied to compare the performance and behavior of two or more systems using an array of controlled or uncontrolled variables. Usually, an experiment is designed to answer a problem statement by providing data collected over a certain period of time. Using this method allows the researcher to gain hands-on experience regarding the system via access to instruments, data logger, and system at any time.

In an experimental study, the researcher studies the performance of a system and measures the outcome. We can categorize experimental approaches as pre-experimental, true-experimental or quasi-experimental (Leedy & Ormrod). The pre-experimental approach uses an independent variable that stays fixed. A true-experimental method is more controlled, taking place in a manipulated environment to examine a certain number of facts or variables. The researcher selects those variables for study to see how they affect system performance. Thus, true-experimental data tend to be more accurate. In the quasi-experimental method, control is very limited, making the validity less certain.

Using a true/quasi-experimental approach in this study will permit control of specific factors to study the emergence of uncontrolled variables and their effects on double-skin façade system performance when compared to a typical window system. More details about the observed variables will be explained later in this chapter. Both independent and dependent variables will be studied regarding system performance.

Hands-on experience with the double-skin façade increases knowledge and understanding of the system. This experimental approach deepens a researcher's sense of inputs shaping system performance. Groat & Wang (2004) state, "Strengths of experimental research are potential for establishing causality, the potential for generalizing results to other settings and phenomenon, and the ability to control all aspects of experimental design enabling attribution of causality" (p.270).

In addition, studying the system through an experimental setup will allow unlimited access to the instrumentation, data logger, and test chambers comprising the proposed double-skin system. Ease of access is crucial to ensure that all sensors and systems are functioning properly. Siting the test

setup in Blacksburg, Virginia offered the advantage of being familiar with regional weather to frame needed changes to the shading-device angle to achieve the best results. Moreover, the test cells in the RDF (Research and Development Facility) ideally face south for convenient sun angle and variable control. Thus, an experimental approach was chosen to explore system performance. Experimental studies help predict and simulate phenomena for validating the results from the recorded data.

3.3.3 Simulation approach

In recent decades, computer simulation has gained much popularity. Simulations rely on software programs to predict system performance and to support data analyses in ways that were not feasible until recently. Simulations helps to understand and assess data rapidly and accurately. Computer simulations provide flexibility and advantages that traditional research methods lack. Using simulation allows one to create a scenario or describe an event for controlling its development over time. This eases the study of system behavior and variables in less time versus experimental methods, making it easy to analyze and to present using visual graphics. Indeed, simulation offers convenient 'what if?' explorations of a specified phenomenon or system in ways not possible in the past.

To simulate the building, certain variables needed selection based on the characteristics suitable for simulation. For this study, the following elements were identified:

1. Building description: to simulate office/mixed use, mid-size tower.
2. Climate: hot arid conditions.

System performance was to be evaluated for a mid-size office building under various energy loads. The eQUEST simulation program was enlisted for this part of the study. The rationale for using computer simulation were:

1. Performance of a whole-building analysis.
2. Interactive load analysis.
3. Time efficiency.
4. Cost efficiency.

3.3.4 eQUEST energy simulation program

The eQUEST building simulation tool used in this study was comprehensive enough for accurate, and fast. Furthermore, eQUEST performs detailed analyses of 'green' building technologies quickly without detailed working blueprints.

This program is user-friendly, and prior studies have confirmed its reliability. eQUEST also features a handy building-creation 'wizard' that graphically displays model simulation results. eQUEST offers two levels of schematic building designs, simulation graphics, and data generation based on model parameter inputs.

The first step specifies the building design, architectural details, and its geometry using a step-by-step procedure to input the model's structure, ventilation, heating, air conditioning, and more. The second phase features a design-development 'wizard' offering further detailed design and building system options for an accurate, customized facility analysis. Since the design-development (DD) option simulates buildings with a more complicated building shell, the multiple-shell component function was ideal for representing the double-skin façade system in the program. Since eQUEST does not yet offer the double-skin system as a preset option, our cutting-edge study used the DD function to simulate an office building in the city if Riyadh, Saudi Arabia with different energy loads.

This program also allows the setup of various HVAC zones in the same building for different HVAC systems. The design-development wizard also allows input of building schedule information to model how the building façade will perform hour by hour. Furthermore, the building occupancy and equipment layout inside the building can be adjusted. The DD wizard even offers average building-load defaults to expedite the process.

Program simulation concludes by generating easy-to-read graphics useful for comparison analysis. The graphics explain energy usage and suggest solutions to curtail energy demands for optimal savings. The expected simulation results were to offer thermal and light performance assessments of the double-skin system versus the specified single-skin system reference.

3.3.5 On-site monitoring disadvantages

A quantitative approach poses challenges for this study. The number of buildings in the United States or Saudi Arabia adopting these double-skin façade systems is very limited. Also, costs for traveling and living near an observable site makes a case study expensive and time-consuming.

Limited access to case-study buildings was a possibility. However, double-skin façade systems require full access to the building site. Furthermore, the instruments used to collect the research data would have remained installed for the double-skin system over a few months, leaving the sensors and data logger in an unsecured location – increasing the chance of theft or damage.

In order to examine the performance of a double-skin facade system versus a typical window, a DSF system facing south would have been required at or near the same site, a rarely attainable configuration. Accessing a second facility in the immediate area would have doubled the instrument count for a side-by-side comparison.

The low chance of accessing adjacent buildings oriented south meant facing a distance factor between the two, thus losing the 'side-by-side' data quality that would have averted wind, sun, and temperature offsets.

3.4 Research Limitations Description

Every research proposal has challenges that can be difficult to overcome. While the goal of this study is to evaluate the double-skin façade system performance in hot weather conditions, the study included limitations caused by factors that were addressed to get the best possible outcome.

1. Research scope was confined to a thermal and light performance of the double-skin system compared with a typical commercial window and did not examine specific building and maintenance costs.
2. The study was limited to experimental and simulation data and did not evaluate actual performance of buildings using the double-skin system. This avoided several field-test factors like transportation costs, lodging, equipment constraints, and ongoing access to building(s) for securing and maintaining the test setup(s).

3. The experiment was performed at the RDF facility at Blacksburg, VA. The research was defined to study the thermal and light performance of the double-skin system for evaluation in hot, arid climate conditions. Since Blacksburg is far from hot and arid all year, the experiment was conducted during the summer to best approximate hot, arid climate.
4. Test chamber dimensions were 3' deep, 4' wide and 8' tall with the double-skin cavity being 1' deep. The window size was 47 ½" by 96". The size of the double-skin cavity allowed sufficient air-flow and heat-gain control. Inner test chamber (office space) dimensions were compressed to conserve space at the RDF and its resources.
5. Simulation was done in a program lacking double-skin property inputs. Thus, calculations were made to study the heat removal rate and light transmission for each individual DSF box-plot window to study the significance of the total heat removal rate of all windows facing south in our office building.

3.5 Variables

In order to test and compare the double-skin system with the common SSF window system, the influence of several variables was acknowledged. Variables are factors that must be measured to determine the amount of total heat transfer through the double-glass skin system. Chosen variables were to be measured for statistic regression into performance equations to complete the study. The two key variables of interest were the thermal performance and light performance for both DSF and SSF systems.

3.5.1 Thermal performance

The aim of this study is to assess the performance of a double-skin façade system compared to the single, double-pane, low-E window system (SSF). Since solar radiation played a large role in the performance comparison, this study targeted the thermal and light performance for both systems.

Summertime heat sources into any building are solar and atmospheric. Solar energy acts in one of three ways: reflects off the outside glass surface, 'cooks' the window, or passes through the window to the inside. Atmospheric heat works its way inside whether it's sunny or not, driven by simply the air temperature difference between outdoors and indoors. Resistance to this heat flow depends on the material properties of the glass and the surface air motions and glass temperatures on the window.

The window itself has three traits: absorption for heating, a cooling inner-cavity air flow, and an inward energy emission by the window from whatever heat remains after the air-flow cooling. Thus, the heat entering the structure features three components: a solar 'pass-through', an atmospheric 'dT', and a window heating minus cooling 'inward emission'. Ideally, if the outside glass surfaces 'mirrored away' all of the sunshine, no solar heat would enter the facility. Next best, if the window absorbed or 'caught' all the un-reflected energy, then the cooling inner-cavity air flow could exhaust any inward emission potential from the window along with some of the atmospheric input, too. Worst case, the glass would simply transmit all of the solar radiation and atmospheric 'dT' indoors.

3.5.1.1 Total heat passing through the system

The thermal performance of both double-skin and single-skin systems were studied to assess the performance differences and advantages of each. The main source of heat entered the building through the window glazing. Thus, solar radiation and heat removal rate needed to be quantified for both window systems.

The ASHRAE Handbook of Fundamentals depicts the total heat passing through a single pane of glass as shown in this following figure.

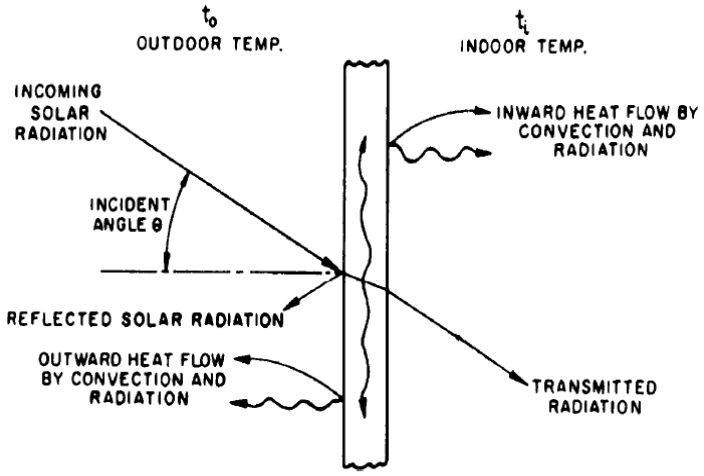

Figure 3.1 **ASHRAE Handbook of Fundamentals** "Instantaneous heat balance for sunlit glazing material" (5-14).

Heat admission through the glass includes transmitted solar radiation, heat flow by convection, and radiant heat flow.

From the ASHRAE Handbook of Fundamentals, the following equations were used to identify the variables needed for the study:

$$Q_a = SHGC\ E_t + U\ (t_0 - t_i) \quad (3.1)$$

$SHGC$ = fraction of incident solar radiation transmitted indoors.

This equation was to be used in this study to calculate the solar heat gain transmitted through the double-skin system cavity. Variables affecting this calculation will be detailed later in this chapter.

3.5.1.2 Double-envelope heat removal rate

Double-skin façade system performance differs from typical single-layer window performance. As mentioned in the literature review, the double-skin façade system contains multiple layers of exterior glass, inner glass, and an interior ventilation cavity with a shading device. In this research, a mechanically ventilated double-skin façade system was to be tested to compare its performance versus a typical single-layer window.

The mechanically ventilated system has great potential to lower energy for cooling in hot climate conditions since it cuts cavity-air residence time. To understand the system's performance, the ventilation airflow rate (Q) that removed cavity heat gain needed to be measured. According to the ASHRAE Handbook of Fundamentals, the heat removal equation is:

$$H = Q\ C_p\ p(t_0 - t_i) \quad (3.2)$$

H = Heat removed, Btu/min.
Q = air flow rate that removes cavity heat, cfm.
C_p = specific heat of air, Btu/lbm-F.
p = Air density, lb_m/cu.ft
t_0 = Cavity outlet temperature, F^0.
t_i = Cavity inlet temperature, F^0

Thermal performance of the DSF system relies mainly on the amount of heat removed by cavity airflow that common windows for commercial buildings lack. Furthermore, comfort levels inside the building are affected by the amount of heat passing through the inner glass surface. Thus, DSF cavity airflow capturing and removing heat is vital to this study.

Many factors affect the amount of heat passing through the exterior glass into the double-skin façade cavity. Some of these are environmental and cannot be controlled. Other variables, such as DSF cavity airflow rate and dimensions, can be selected. Such factors include:

a) Solar radiation intensity: the level of solar radiation has huge impact on the amount of heat gain inside the cavity. Experimental data show solar radiation responsible for over 80% of the amount of heat gain in the cavity. For a highly radiant location like Riyadh, Saudi Arabia, solar flux can far exceed 1000 W/m². More details appear in Chapter 4.

b) Incident sun angle: sun angle also plays a major role on the amount of solar heat gain through the DSF's solar heat gain coefficient (SHGC). SHGC represents the fraction of total solar radiation passing through the DSF external layer into the cavity. SHGC is dynamic and ranges from 0 to 1 depending on the incident sun angle. To apply the SHGC, the Window program developed by Lawrence Berkley labs was used. Incident sun angle affects window light transmission since a larger sun angle reflects more light off the window's outer surface. The following is a comparison between the SHGC data for the same window type that is used in the experimental phase (described in chapter 2 section 9) and between the incident angle:

Table 3.1 Different incident sun angle optical value using the Window 7.6 program for ¼ inch double pane low-e e2 window.

Angle	0	10	20	30	40	50	60	70	80	90	Hemis
Vtc	0.639	0.642	0.633	0.622	0.605	0.574	0.503	0.368	0.173	0.000	0.534
Rf	0.249	0.243	0.240	0.243	0.253	0.273	0.313	0.403	0.599	0.999	0.297
Rb	0.198	0.192	0.191	0.194	0.206	0.231	0.286	0.412	0.652	1.000	0.266
Tsol	0.372	0.374	0.368	0.360	0.349	0.330	0.288	0.210	0.097	0.000	0.308
Rf	0.379	0.374	0.373	0.375	0.383	0.397	0.426	0.495	0.656	0.999	0.414
Rb	0.294	0.290	0.288	0.287	0.290	0.301	0.332	0.414	0.595	1.000	0.327
Abs1	0.194	0.197	0.204	0.209	0.211	0.215	0.230	0.246	0.212	0.001	0.214
Abs2	0.055	0.055	0.056	0.056	0.057	0.058	0.056	0.049	0.035	0.000	0.054
SHGCc	0.431	0.433	0.428	0.422	0.412	0.393	0.352	0.269	0.142	0.000	0.368

c) Temperature difference: the outdoor air temperature influences the amount of heat gained inside the cavity of the double-skin façade. Temperature differences between the system cavity and the outdoor air can drive heat transfer through the fenestration. Still, the influence of temperature difference was subordinate to the level of heat gained from solar radiation. More details will be provided in Chapter 4.

d) Airflow inside the cavity: airflow rate was controlled by mechanical fans that exhausted the captured heat gain. Controlling the air flow mechanically did affect the difference between the cavity inlet air temperature (Tin) and the cavity outlet air temperature (Tout). Reducing the cavity temperatures meant less heat passing through the inner glass layer to the indoor space. Equation 3.6 can be rewritten as:

$$H\,(Btu/hr) \;\; = Q\;1.08\;(t_0 - t_i) \tag{3.3}$$

Q = The Air flow rate in *CFM*.

his calculated heat removal was then to be divided by the total heat load of radiation plus conduction expressed next in Equation 3.8:

$$q_A = \;\; F\;E_t + U(\,t_0 - t_i) \tag{3.4}$$

q_A = Total heat transmitted through glass, Btu/hr-ft^2.
F = The fraction of incident solar radiation transmitted.
E_t = Total solar radiation, Btu/hr-ft^2.
U = U-value, Btu/hr-ft^2-F.
t_0 = Outdoor temperature, F^0.
t_i = DSF cavity air temperature, F^0.

Here, the total heat transmitted through the glass is the heat gained by solar radiation ($F\;E_t$) and heat gained from conduction ($U(\,t_0 - t_i)$). A main focus in this research is to study the amount of solar radiation transmitted through the outer glass surface. Heat gain via solar radiation often dominates temperature-driven conduction. Thus, Eq. 3.8 may be simplified to:

$$q_A = F\, E_t \quad (3.5)$$

F = The fraction of incident solar radiation transmitted.
E_t = Total solar radiation, Btu/hr-ft^2.

This simplified equation is justified based on assumptions described in details later in chapter 4 section 2.

Heat removal rate was to be studied over the duration of the experiment every 15 minutes. Calculating sun angle every 15 minutes allowed the sun position to change enough to note the effect on HRR. To use Eq. 3.9, the relationship between the sun location and F (SHGC) needed quantifying. The changing angle of incidence affected the amount of both heat and light passing through each window system. The incident sun angle will be addressed using equations for sun altitude and azimuth described later.

The amount of solar radiation removed from the double-skin cavity can be calculated using the following equation:

$$HRR = H/q_A \quad (3.10)$$

$HRR =$ Fraction of transmitted solar radiation removed.
H = The heat removed from the system cavity, Btu/hr.
q_A = solar radiation transmitted in the cavity, Btu/hr.

In order to accurately estimate the performance of the system in terms of heat and light, some variables were controlled and others monitored. Airflow rates for the test chamber and cavity were fixed. Also, the indoor air temperature was limited to a narrow range using HVAC in the test cell.

Non-controlled variables that were measured included light illumination inside the chamber, glass surface temperature, outdoor ambient air temperature, solar radiation and incident angle. These variables are depicted below:

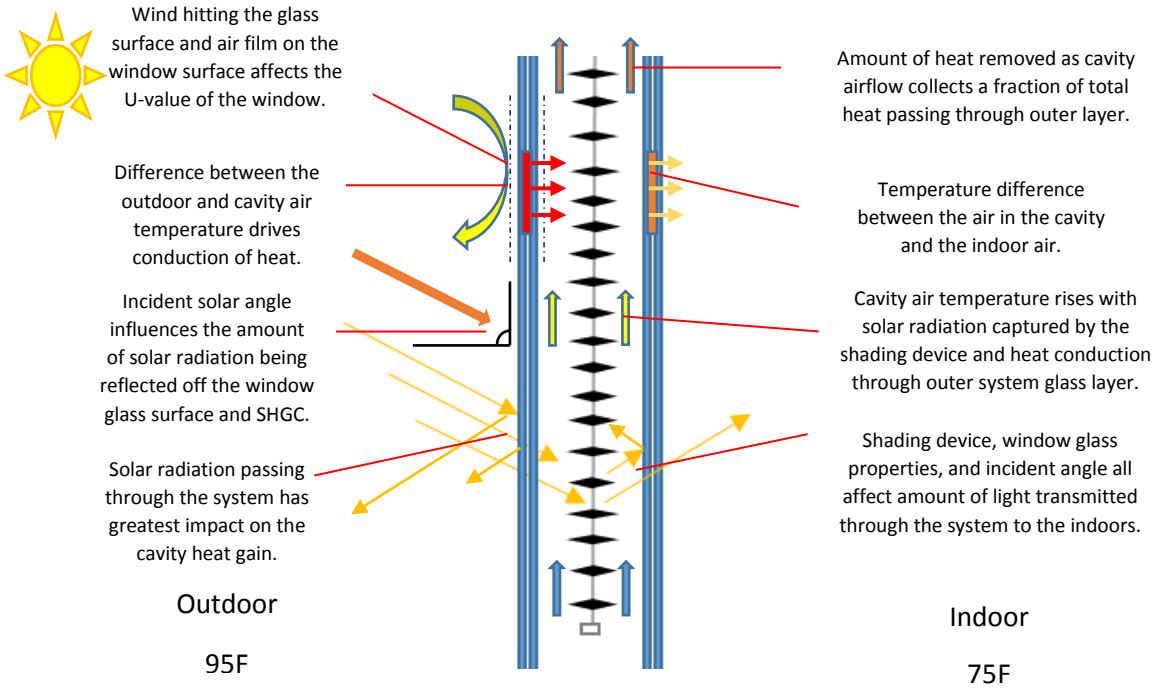

Figure 3.2 Total heat gain and light transmission diagram

3.6 Environmental Factors

In order to study the performance of the double-skin façade system and compare it to the single layer system using the set of equations 3.1 to 3.6, a number of variables need to be calculated or measured. The following section describes each of these variables.

3.6.1 Data measurement

To measure variables, environmental factors were considered to develop a test protocol. Both designed and environmental factors described earlier affected system performance. The following table details these variable and environmental factor interactions.

Table 3.2 Data measurements

Heat-Light Factor	Environmental Factor	Variables	Method of Determination
SHGC	Sun angle	Sun altitude Sun azimuth	Berkeley Lab's Window program
Et	Solar radiation	Window solar radiation Rooftop solar radiation	Pyranometry
Outdoor light	Illumination	Klux out	Photometer mounted on the DSF outer layer
Indoor light	Illumination	Klux in	Photometers mounted at two different heights inside chamber
Toa	Air temperature	Air temperature	Thermocouple
Q	Air flow rate	Cavity airflow rate and chamber air flow rate	Air velocity transducers
t_i, t_o	Cavity air temperatures	Cavity inlet air temperature Cavity outlet air temperature	Thermocouples
t_{ig}, t_{og}	Glass surface temperatures	Inner layer glass surface temperature	Thermocouples

3.6.2 Exogenous variables

Exogenous variables are those not influenced by others in the experiment. Exogenous variables impose factors affecting system performance while acting outside the system itself. Several independent environmental factors affected the performance of our double-skin facade. This section describes these factors and their effects in the study along with processes used to measure these factors.

3.6.2.1 Sun (Solar radiation)

The solar heat gain coefficient SHGC was tabulated based on sun angle and incident solar radiation (Et) using Berkeley Lab's Window program. Solar altitude and azimuth both play large roles in system performance. Depending on the sun angle, some amount of solar radiation (Et) passes through the glass surface. The ASHRAE standard defines an incident angle as zero when perpendicular to the surface. The smaller the angle, the more solar radiation that passes through. For this experiment, angle increments were calculated every 15 minutes from sunrise to sunset using Equations 3.11 through 3.13.

3.6.2.2 Incident solar radiation (*Et*)

Incident solar radiation forms rays impinging the external glass pane of the window. Transmission through glass varies by angle of incidence. When light striking the glass window is perpendicular at angle zero, more of it passes through the glass surface. For non-zero angles, some light reflects off the surface for lower light transmission. Therefore, this key variable was expected to have large effect and was included in the dataset for measuring system performance. A number of equations were useful for incorporating angle of incidence, and a description of the variables and equations used is discussed next.

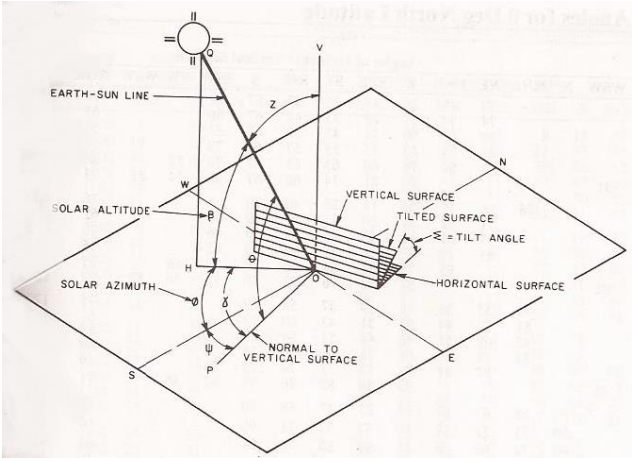

Figure 3.3 ASHRAE Handbook of Fundamentals, "Angle of incidence."

3.6.2.3 Apparent solar time

Apparent solar time relates to true sun position. According to the ASHRAE Handbook of Fundamentals (2013), "The earth's orbital velocity also varies through the year, and so apparent solar time, as determined by a sundial, varies slightly from the meantime kept by a clock running by a uniform rate "(p.27). To calculate apparent solar time (AST), Eq. 3.11 was used:

$$AST = LST + ET + 4 * (LSM - LON) \quad (3.11)$$

LST = Local standard time in minutes, military format. Depends on the time of the day data are recorded.
ET = Equation of time found in third column of Table 3.2.
4 = Minutes required for one degree rotation of the earth (15 degrees hourly).
LSM = Local standard meridian as referenced at Greenwich in the UK.
LON = Local longitude in degrees depending on the time zone for location, i.e., 60 degrees for AST, 75 degrees EST, 90 degrees CST, 105 degree PST, etc.

Table 3.3 ASHRAE Handbook of Fundamentals (1985), "Extraterrestrial solar radiation intensity and related data for 21 days of each year" (p.27).

	I_0 Btu/h * ft^2	Equation of time,min.	Declination, deg.	A	B	C
				Btu/h * ft^2	Dimensionless Ratios	
Jan	448.9	-11.2	-20.0	383.3	0.142	0.058
Feb	445.0	-13.9	-10.8	378.4	0.114	0.060
Mar	438.4	-7.5	0.0	369.5	0.156	0.071
Apr	431.0	1.1	11.6	353.8	0.180	0.097
May	424.5	3.3	20.0	344.0	0.196	0.121
June	421.4	-1.4	23.45	339.1	0.205	0.134
July	421.0	-6.2	20.6	338.1	0.207	0.136
Aug	425.8	-2.4	12.3	335.0	0.201	0.122
Sep	432.3	7.5	0.0	359.0	0.177	0.092
Oct	739.2	15.4	-10.5	371.5	0.160	0.073
Nov	446.3	13.8	-19.8	380.4	0.149	0.063
Dec	449.3	1.6	-23.45	384.3	0.142	0.057

3.6.2.4 Solar altitude

Solar altitude captures the sun's height in terms of angle β as referenced from the surface of the earth or from the horizontal surface of an object:

$$\sin\beta = \cos L \cos\delta \cos H + \sin L \sin\delta \quad (3.12)$$

L = Latitude of the location in degrees.
δ = Declination of the sun in degrees.
H = Hour angle calculated multiplying 0.25 (15 degrees hourly) by time difference between noon and local time (in minutes).

3.6.2.5 Solar azimuth

Solar azimuth is the horizontal position of the sun in terms of angle ∅ as referenced from true south:

$$\cos \emptyset = (\sin \beta \sin L - \sin \delta) / (\cos \beta \cos L) \quad (3.13)$$

β = Solar altitude from previous equation in degrees.
L = Latitude of the location in degrees.
δ = Declination of the sun in degrees.

3.6.2.6 DSF cavity temperature difference (Δ T)

The temperature difference between the cavity inlet and outlet played a vital role computing heat removal rate, a main finding in this experiment. Thermocouples were installed inside the double-skin façade system near the cavity's inlet and outlet to record this key air temperature difference. More details about the physical setup are presented later in this chapter.

3.6.2.7 U-value (U)

This variable expresses the amount of heat transfer owing to conduction. U-values can be found considering the glass and gas-gap conductivities of the window system. Indoor and outdoor convective surface films may amass to add further resistance to heat transfer through the glass surface. Wind speed lessens air film resistance to raise the U-value to a maximum. While sensing wind speed may give more precise U-values, this study used the maximum U permitted by the gas gap insulating the double panes. This simplified the analysis in a conservative way. The difference between outside ambient and indoor air temperatures was expected to exert minor impact on heat passing through the window compared to solar radiation. Thus, conductive heat transfer was believed to play a modest role in DSF performance for hot, arid climates. Further details appear in Chapter 4.

3.6.3 Endogenous variables

Endogenous variables are dependent factors within a regression model. Such factors under the sway of other variables needed to be computed. Next listed are the endogenous variables in our experiment:

3.6.3.1 Air flow rate (CFM)

Heat removed from the double-skin façade system cavity Q (Btu/hr-sq.ft) was calculated knowing the flow rate of the air through the cavity and the temperature difference between the cavity inlet and outlet as follows:

$$Q = 1.08 * CFM * (T_{out} - T_{in}) \quad (3.14)$$

CFM = Air flow rate cu.ft/min.
1.08 = Constant reflecting air properties and unit conversion.
T_{out} = Air temperature, outlet °F.
T_{in} = Air temperature, inlet °F.

Airflow rates were held steady for both the test chamber and DSF cavity to properly reflect real-world office ventilation. The double-skin façade's inlet and outlet ducts were sized and placed for accurate air flow sensing to quantify the heat removal of incoming solar radiation and conduction.

3.6.3.2 DSF cavity air temperatures $(T_{out} - T_{in})$

Double-skin façade cavity air temperatures may rise from solar radiation transmitted through the outer layer system glass and by air temperature differences between outdoors and the cavity. To compute the heat removal rate HRR, the cavity inlet and exit air temperatures were needed. Temperatures were taken at proper locations. The lower inlet end of the cavity was expected to be cooler than the upper exit of the system.

3.6.3.3 Window glass surface temperatures (Δ T)

In addition, temperatures for the outer glass pane of the DSF system and its inner surface were measured at the top and bottom.

3.6.3.4 Light transmission

Light passing through the building skin can affect comfort levels inside the building and determine the amount of artificial lighting costs required. Light transmission can thus play a significant role in energy consumption. Outside light levels were monitored using a photometer mounted on the outer glass pane. Indoor lighting was measured for two different heights: at desk level for sitting and at average human-eye level for standing.

3.7 Research methodology plan

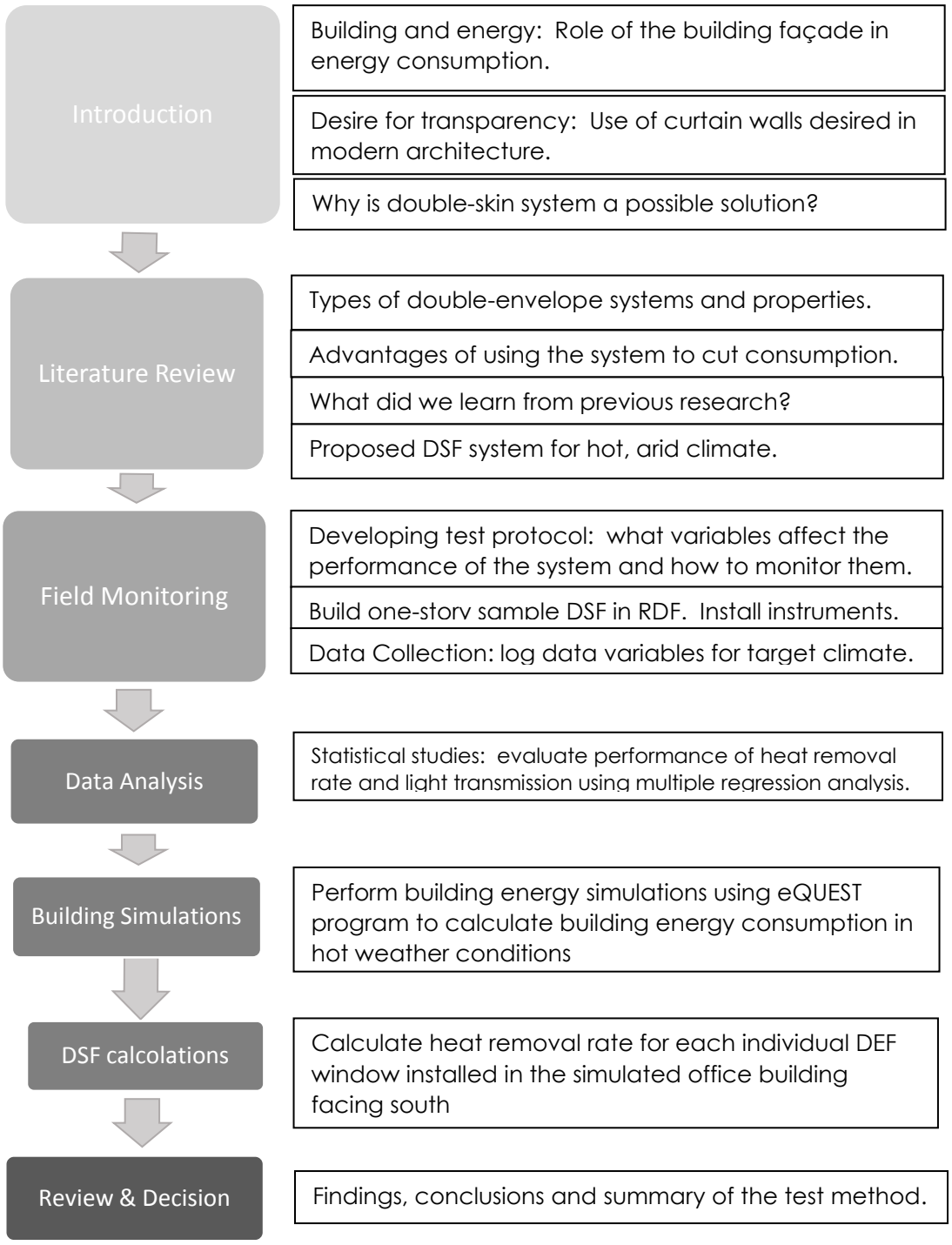

3.8 Experimental setup

Studying the performance of a double-skin façade system in hot summer months is the research purpose. Variables affecting system performance were logged using instruments discussed later in the chapter. A series of tests were performed to assess the performance of the double-skin facade system through hot summer months.

3.8.1 Structure

The test setup comprised one full-scale model exposed to outdoor weather conditions. A full-scale box was built at the Research and Demonstration Facility (RDF) site in Blacksburg, VA. The model was one story high with a window installed facing south. The box was sized 8 feet tall by 4 feet wide to house a full window. The inner test chamber was 3 feet deep, enough to simulate indoor office spacing without affecting air flow. The box served as a full-scale test window to gather data for an accurate heat transfer protocol.

Figure 3.4 Box under construction

A full-scale, one-story high window supported the examination of indoor lighting at various heights. The full-scale window dimensions also allowed noting how much heat passed through the system as temperature rose in the chamber. This simulated as-built condition where air was introduced into a room, heated with solar radiation, and contacted the window glass surface area while flowing to the outlet. Air residing in the cavity space captured heat from solar radiation admitted the system. It was vital to relate the heat gain to the airflow inside the double-skin cavity with the inner 'office' space to approximate system behavior. Lastly, the size of glass area affected window performance. Sensor configurations will be detailed later in this chapter.

3.8.2 Insulation

Figure 3.5 Photo of insulation-wrapped box

It was crucial to eliminate all leaks of light or heat into the test chamber for proper data collection. Thus, insulation was installed to reduce heat transfer through the box walls. R40 insulation was applied to all sides and the top of the box. Four 2" insulation foam sheets R10 each were glued together and applied to the top, back, and sides. The box bottom had R10 insulation. After gluing the insulation on the box, roofing felt was added to protect the insulation and chamber from moisture.

High-gloss white roof paint was applied to the felt to cut solar absorbance and to reflect solar radiation and heat. Heat collected inside the cavity determined the efficiency of the system. Thus, several layers of insulation were installed to wrap the exterior surfaces. The inner surface was coated with white mold-resistant commercial paint. Silicon was applied in all corners and cracks to seal the box completely. Special insulation foam and silicon were applied around the windows to seal any gaps.

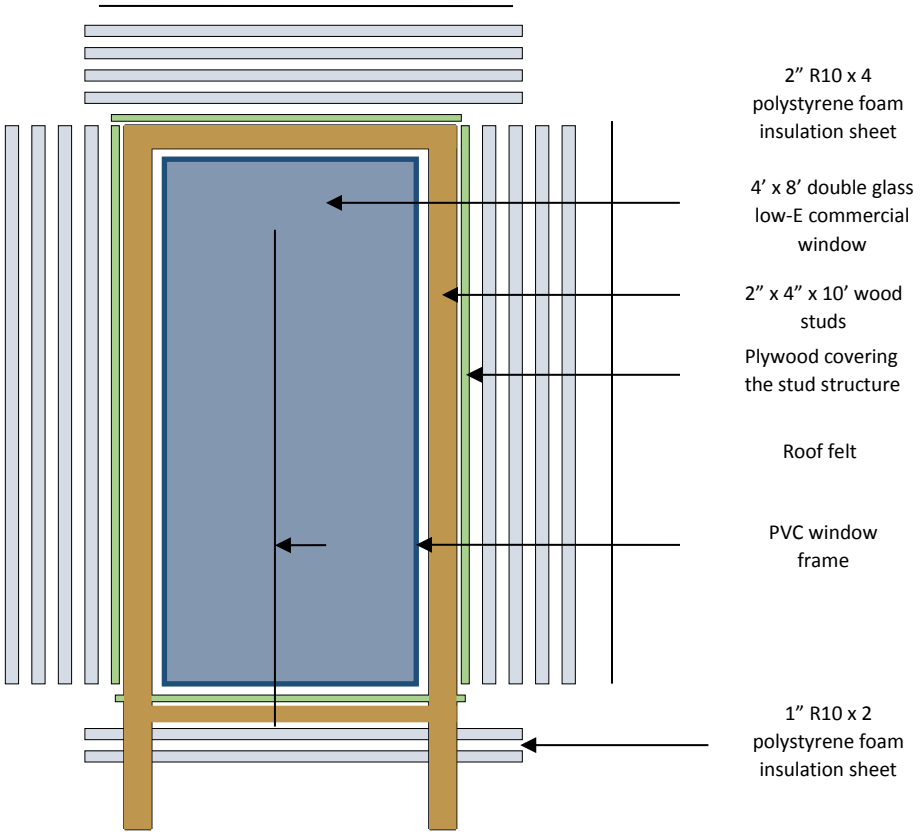

Figure 3.6 Diagram of insulated installation

3.8.3 Window

The same window was installed for both layers of the double-skin façade. Double-glass windows are widely used in commercial buildings, having great ability to cut energy costs in the summer's hot climate conditions. One of the favorable traits of this window is its heat reflection. The low-E window offers today's lowest solar heat gain coefficient (SHGC), and this technology enjoys increasing industry-wide use. Identical low-E double-glazing was installed as the inner layer of the double-skin model box with the frame size of 47.5" x 96". An interstitial cavity served as the location of a shading device. The description of the window is as follows:

Exact size = 47 ½" W x 96" H Rough opening = 48" W x 96" ½ H 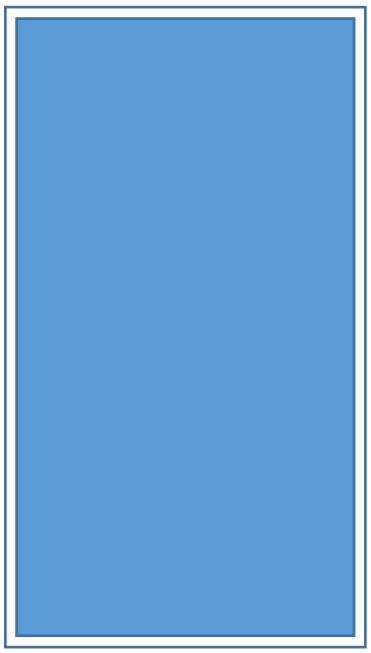	Manufacturer: Ply Gem Windows Product: Window Type: Picture Material: Vinyl Division: Millwork Product line: New Construction Frame to Match: Casement/ Awning Frame: 2-5/16" Standard profile (2700 Series) Fin Type: Nail Fin Configuration: Picture Window Performance Rating: Standard DP performance Exterior Color: White Opening Type: Exact Exact Width: 47 ½" Exact Height: 96" Rough Opining Width: 48" Rough Opening Height: 96 ½" Glass Type: Dual Glazed Tempered Glass: Yes Low E Glass: Low E Tint: No Glass Option: Clear Gas Filled: Argon Grid Type: None Wall Depth: So Extension Jamp Series: 2700

Figure 3.7 Window property specifications

3.9 Experiment model

In order to study the double-skin façade system appropriately, a proper test setup was designed. The full-scale model built at the RDF test facility faced south. The goal of this setup was to:

1) Quantify the solar heat gain through the DSF window system.
2) Study the light transmission through both layers and shading device.
3) Record the temperature difference between outdoor and indoor air.

The data collected from this experiment underwent statistical multiple regression analyses to study the relationship among variables affecting the double-skin façade system performance. Data were analyzed using statistical procedures that included regression scores and scatter plots.

3.9.1 Mechanically ventilated double-skin model

The active system proposed for this study offered a layout comprising an external layer of double-pane glazing, a one-foot deep cavity with solar shade control, and double inner-layer panes of glass. Fans located at the top of the system vented hot air from the cavity, curtailing heat emission from the cavity's inner layer into the structure. Air entering the cavity was air-conditioned and set to 75 degrees for a typical office temperature. Furthermore, cavity air was mechanically driven by a fan at the bottom of the window. A double-glass panel window was installed as an external layer of the system. The inner glass piece contained a double-layer glass panel to frame the cavity and insulate the inner chamber. A shading device located in the center of the cavity was installed to control light transmission into the office area. The shading device aided cavity heat removal while allowing light through the double-skin façade. A diagram of the experimental setup is shown next:

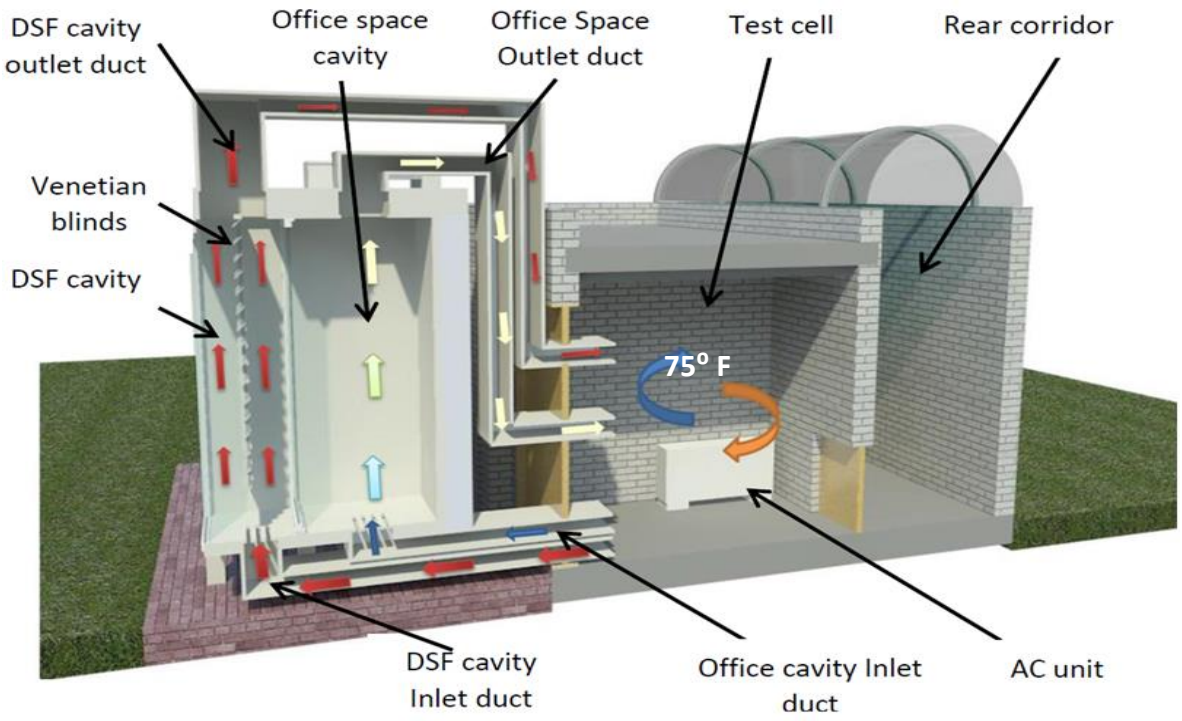

Figure 3.8 Vertical section of the mechanically ventilated model

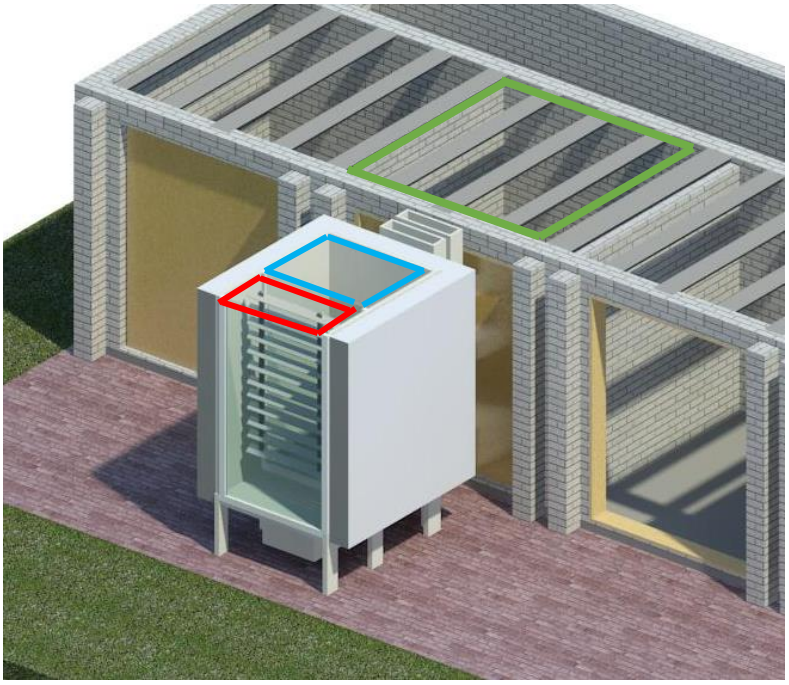

Inner cavity (office space) with two photometers to study light transmission & thermocouples (3) to study the amount of heat gain and removal by the DSF. Dimensions were 3' x 4' x 8' tall.

DSF system cavity included three thermocouples to study system heat removal rate. Cavity included a shading device to control direct sun light. Dimensions were 1' x 4' x 8' tall.

RDF test cell that included an air conditioning unit set for 75 degrees, two electric fans for controlling air flow into both cavities at different speeds, and the data logger unit used to record the measurements.

Figure 3.9 Horizontal section of the mechanically ventilated model

3.10 Recording instruments

Instruments for collecting and logging data enlisted eight thermocouples at different locations in the test setup. Three photometers (one located outside the test chamber and two located in the office space chamber) were used to study the fraction of light transmission passing through the double-skin façade system. One window pyranometer and one rooftop pyranometer were used to measure solar radiation. Finally, two airflow transducers were placed inside the air ducts. All sensors were connected to a data logger that recorded every 15 minutes. The placement of the instruments are depicted in schematic drawings later in this chapter.

3.10.1 Thermocouples

To sense temperature, type-T copper-constantan thermocouples were placed in both chambers and in the double-skin façade system cavity. The thermocouples measured temperature at different sites in the double-skin cavity and office area to aid computing of heat removal rate (HRR).

3.10.2 Photometer

Light illumination inside the test chamber was measured using three Li-Cor LI-210 silicon photometric sensors. The office housed two photometric sensors at two different heights. The first sensor was vertically installed at desktop-level with the second at eye-level. The third photometer was mounted on the outer pane facing south to measure outdoor light for direct use in the light transmission calculation. The average reading from both indoor sensors was divided by the outdoor reading to calculate light transmission as follows:

$$\mathfrak{T} = \frac{(Photo_{in\,1} + Photo_{in\,2})}{2} / Photo_{out} \quad (3.15)$$

$\mathfrak{T}$ = transmitted light as a dimensionless fraction of incident light
Photo = photometer sensor in Klux units

The photometric sensors were designed to measure light level in Klux units. The Li-Cor sensors below have been chosen to gauge the light passing through both layers and shading device in the double-skin façade system.

Figure 3.10 Web Photo of the Li-Cor LI-210 (http://www.ni.com/cms/images/devzone/tut/idnrdnds23870.jpg).

3.10.3 Pyranometer

Solar radiation was measured using two Li-Cor LI200X Silicon Pyranometers. One was vertically mounted to sense incoming window radiation with the other mounted horizontally to measure rooftop solar radiation.

3.10.4 Air velocity transducer

To measure airflow velocities, two TSI Model 8475 transducers were mounted: one at the DSF cavity duct inlet and the second at the office chamber duct inlet.

Figure 3.11 Web Photo of the TSI 8475-03 Air Velocity Transducer (http://wwwmitchellinstrument.com/air-velocity-transducer-tsi-8475-03-air-flow.html).

3.10.5 Data logger module

Data were logged using the Campbell Scientific CR-300 Micro. Logger capacity of 28 inputs used a program called PC200W to link the logger with the computer. The data logger recorded measurements every 15 minutes – ample time for sun motion of a few degrees to gradually alter the input variables. Data were stored in 4MB memory.

Figure 3.12 Web Photo of the CR-3000 micro logger (http://www.campbellsci.com/cr3000).

The data logger was placed at the RDF within a few feet of all sensor sites. To protect the data logger from weather damage, the CR-3000 resided within a sealed case from Campbell Scientific. This protective case had a small opening through the bottom to input wiring from the instruments. Even though the CR-3000 can be powered by a rechargeable battery, it was advised to power with AC to avert data loss. The logger had a small screen to monitor recorded data without a computer hookup, allowing a data check every few days without disturbing the equipment wiring setup.

3.10.6 HVAC system

The test cell enlisted an air-conditioning unit and fan for ventilation using thermostat control. The test cell was cooled by air-conditioning delivered through HVAC 6" aluminum piping. The temperature was fixed at 75 Fº. Two fans drove air-conditioned flow through both cavity and chamber ducts at two corresponding speeds. More set-up details appear next.

3.11 Instrument installation

3.11.1 Thermocouple setup

Since heat transfer through the enclosed system is the most important performance factor for the double-skin facade, the experimental setup used thermocouples to log temperature at different sites in the test cell. The goal was to gather enough data to calculate total heat flow passing through the system. Eight thermocouples were installed in these spots:

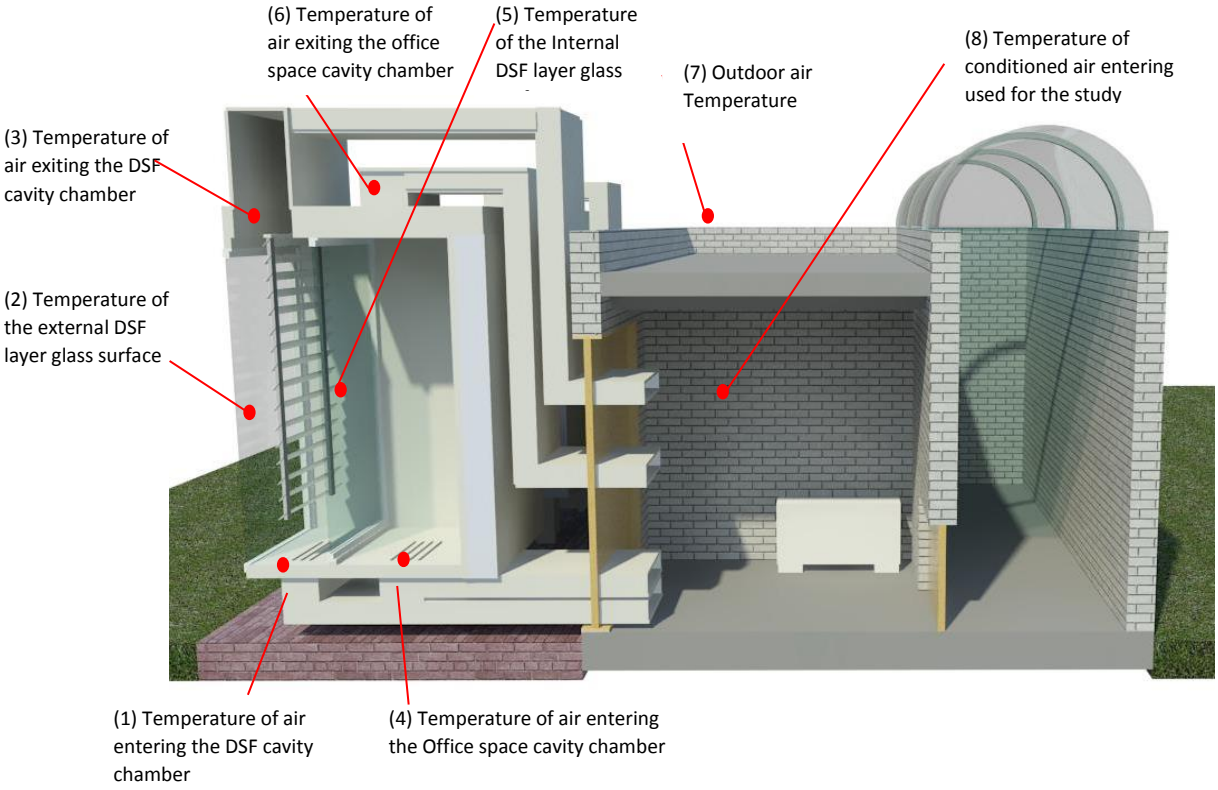

Figure 3.13 Double-skin system TC setup

As the above diagram shows, three sensors were situated in each section: three in the DSF cavity and another three in the (office space) chamber. The inlet thermocouple recorded air temperature entering the cavity, and the cavity outlet thermocouple was used to calculate the amount of heat removed from incoming solar radiation and conduction driven by the outdoor-indoor air temperature difference. Thermocouples on the exterior and interior glass surfaces monitored glass temperatures.

3.11.2 Photometer setup

Light transmission reveals how the system's shading device affected the quantity of the light passing through the double-skin façade. The amount of light transmitted through the DSF determines the cost of artificial lighting in the building. Light transmission was calculated using data recorded every 15 minutes dividing the average indoor photometer readings by the outdoor photometer measurement. Indoor photometers were installed at two different heights: desk-level and eye-level to capture workspace illumination effects toward light quality and energy savings. The outdoor photometer was installed facing south to measure the level of light entry into the DSF. These three photometers occupied three lines in the data logger. Li-Cor photometer specifications included a 0.15% per degree C temperature sensitivity that may have incurred some non-DSF variance into the model. Here are diagrams of photometry orientation:

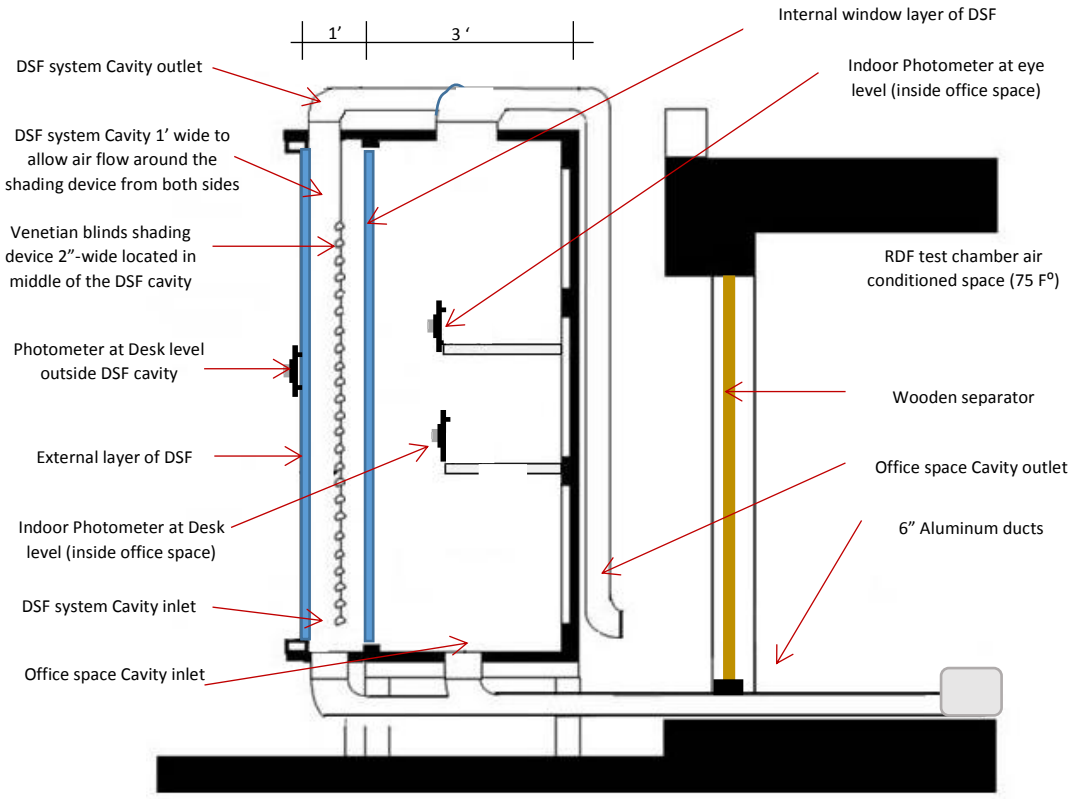

Figure 3.14 Detailed diagram of photometer locations in the test chamber to determine the amount of light transmitted through the DSF system.

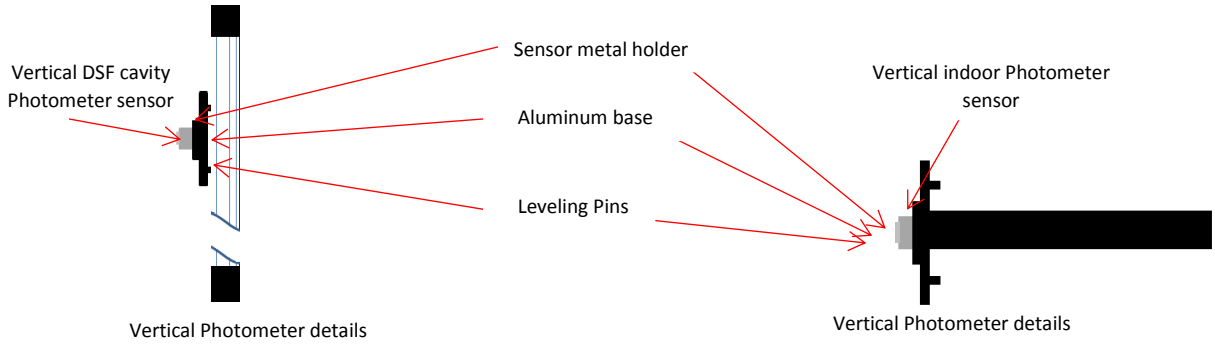

Figure 3.15 Detailed drawing of photometer mounting in test chambers

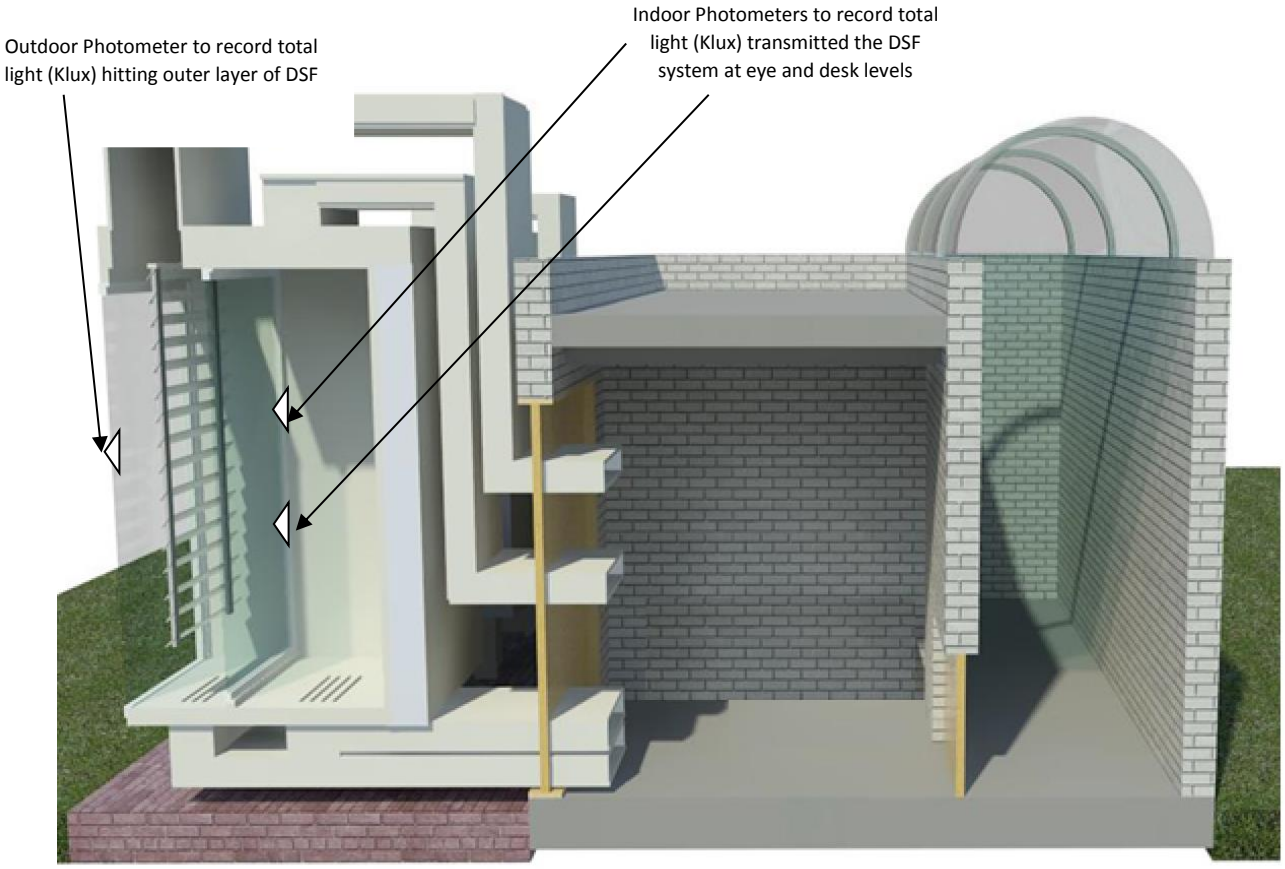

Figure 3.16 Photometer locations to determine the amount of light transmitted through the DSF system.

3.11.3 Air velocity transducer setup

Airflow entering both test spaces (office area and double-skin façade cavity) was fan-controlled. Airflow was a critical factor for approximating the performance of the DSF for two reasons. First, measuring this variable enabled the computation of heat removal rate. Thus, one air velocity transducer was installed in the inlet duct of the double-skin façade cavity. Second, office airflow had to be realistic, and its air velocity transducer was installed in the inlet duct to the office space. Readings every fifteen minutes were logged to ensure constant airflow rates. The cavity air duct vented conditioned air of 75º F at a steady 160 cfm. The office-area air duct moved the same conditioned air of 75º F at 40 cfm.

One-fourth the cavity flowrate reflected a typical office depth of 12' – four times larger than the 3'-deep test chamber. For a real-world building, the same office ventilation airflow should move through the DSF cavity. The DSF cavity duct simulated the return air for a 4'x 12' office space. Both ducts were made of 6" diameter aluminum.

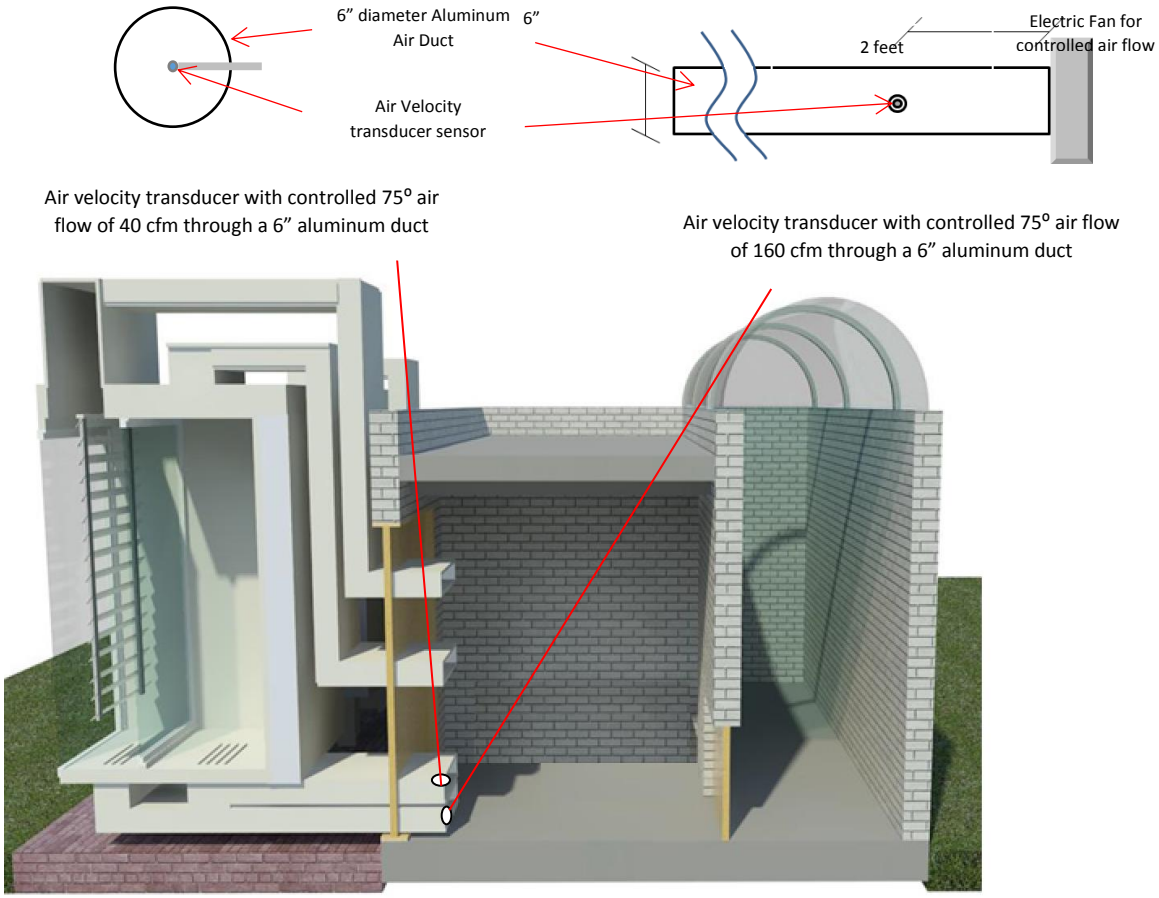

Figure 3.17 Air velocity transducer location for inlets to both DSF cavity and office area

3.11.4 Pyranometer setup

One pyranometer was installed on the external pane of the double-skin façade surface facing south to measure the incident window radiation – data used in the solar heat gain calculation. The rooftop pyranometer also measured solar radiation to confirm sunny versus cloudy days.

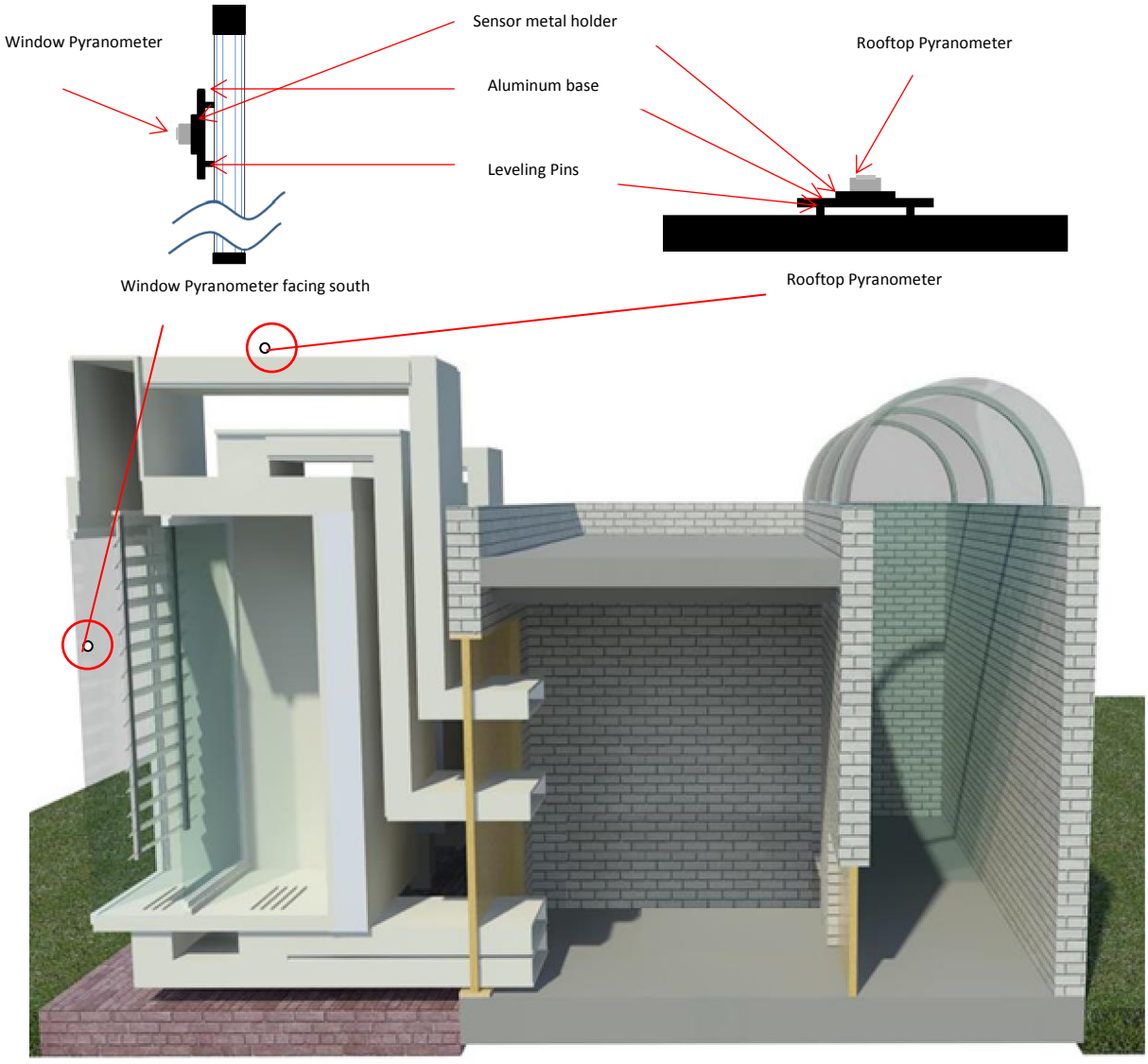

Figure 3.18 Pyranometer locations

3.11.5 Shading Device

A 2"-wide shading device resided in the one-foot cavity depth to control light transmission and aid heat absorption. Venetian blinds were installed in the middle of the cavity with 10" spacing (5" clearance front and back) to allow air flow. The device shaded the upper 6' of the total 8' window. For good air distribution, the lower cavity inlet had two feet unhindered by a shading device to develop smooth airflow across the front and back of the shading device. The slat angle was set at 20 degree to reflect sunlight deeper into the inner office space for improved light distribution while avoiding glare. The wooden shading device featured white slat surfaces to stabilize light rays deeper into the office area for better lighting. The shading device also aided heat interception for eventual cavity removal.

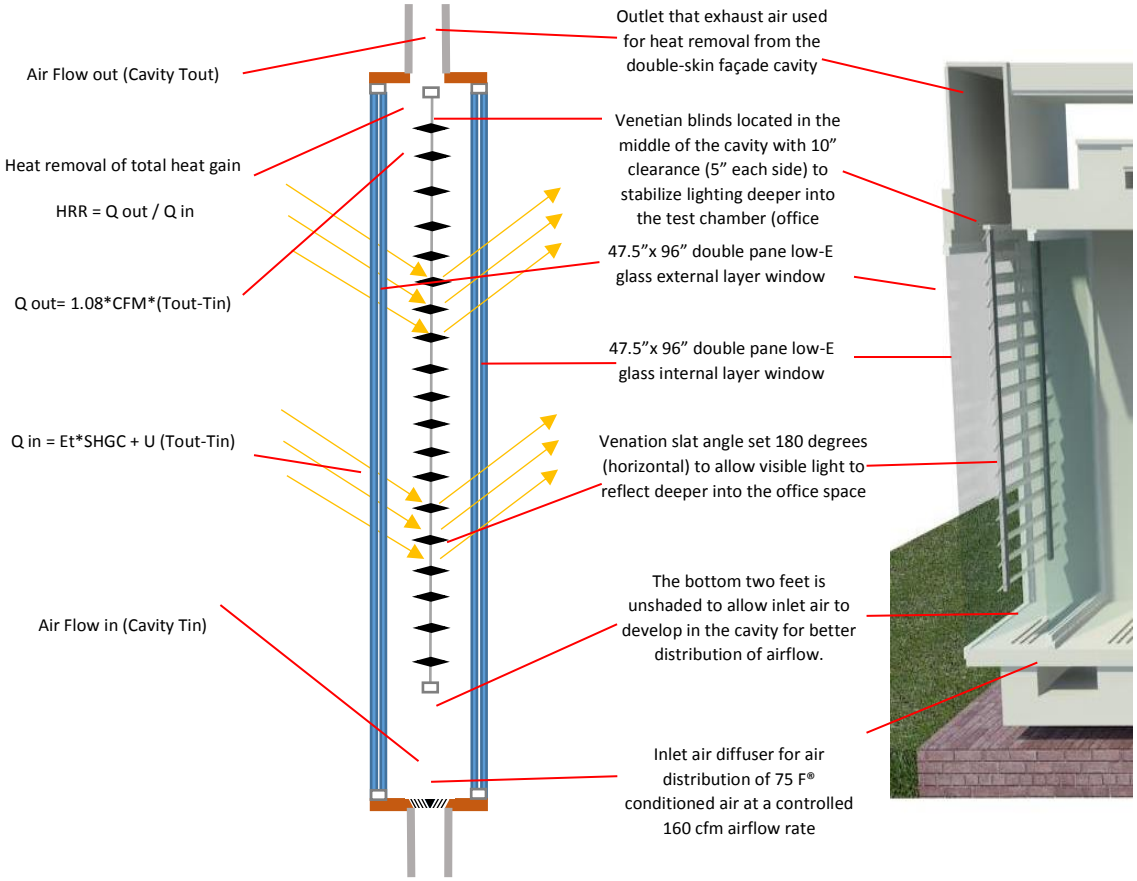

Figure 3.19 Shading device setup in DSF system cavity

3.12 Conclusion

Improving the indoor environment is a design goal in today's architecture. Toward this aim, the use of glass and curtain walls is common in offices. Clear glass that increases transparency is desired in high / mid-rise towers. The external building skin largely shapes the energy consumption for any given building since façades safely control lighting and glare, noise, heat gain, and energy usage. The double-skin façade might be the answer. Double-skin façade systems have great potential to foster transparency with less heat gain.

This part of the research examined the relationship among the variables influencing system performance of the double-skin façade. Test sensors were deployed to log data influencing the amount of heat gained in the double-skin façade system cavity. The goal has been to calculate the heat removal rate the DSF system offers during the hot summer months.

The setup was crafted to capture exogenous and endogenous variable data affecting DSF system performance. Test data underwent multiple regression analyses to find the relationship among the variables driving the DSF heat removal rate. Illumination data for the DSF also underwent regression analysis to see how much light transmitted through the system. The amount of "free" lighting influences building energy consumption of artificial lighting needed for office comfort.

A full-scale model (test chamber) was built at the RDF facing south since structures north of the equator gain solar heat from the south façade most of the day. Data chosen for the regression analysis were collected during hot summer months. Sun angle, solar radiation, and outdoor temperature along with the light transmission were recorded every 15 minutes from sunrise to sunset. The reason for logging every 15 minutes was to allow the sun angle to change every few degrees for a smooth acquisition of data. Regression analyses next aided the prediction of DSF system performance extrapolated to hot climate conditions. More details regarding the regression analyses are discussed next in Chapter 4.

Chapter 4

4. 1 Regression analysis

This chapter describes the method and results for ordinary least-squares (OLS) linear regression of light and thermal performance for a double-skin façade (DSF) in Blacksburg VA. The entire approach reinforces the main goal of being able to extrapolate DSF performance for use in an eQUEST simulation of building utility costs in hot, arid climate. Ideal windows would block all heat and transmit all visible daylight to save A/C and lighting expenses. In reality, attempts to intercept heat may also block some light, and DSF costs more to install and run than single skin façade (SSF). Eventually, the simulation aims to quantify the gain in A/C savings. When such savings clearly exceed the added costs of DSF installation and maintenance plus increases in electrical use due to DSF's lower visible light transmission, then DSF offers value. Light transmission through a SSF typically runs in the 0.3 to 0.7 range, and this could drop into the 0.1 to 0.5 range for the DSF.

As an introduction, OLS regression seeks to find a line slope and intercept that minimizes the departure of model prediction from measured output. Departure error equals model output minus the actual value. Each error is then squared so that overshoots do not cancel shortfalls. The best-fit OLS regression slope and intercept minimizes the sum of these squared errors.

OLS regression that favors extrapolation must fulfill basic requirements of a linear relationship of the output to significant, independent input variables demonstrating random, balanced errors from an expected value of zero. While some inputs analytically suggest linear effects on the output, other variables, such as angles, pose obvious nonlinear trigonometric relations. Nonlinearity may be treated through variable transformation or piecewise linearization to qualify for regression.

Significant variables pose a low probability; say 5%, of posing as "mirage" linear inputs. There is a chance that a regression model is simply a fluke. Testing can quantify odds ruling this out. Large sample sizes can boost the probability of variable significance that would otherwise require exclusion. Not all variables are independent. One may surmise sun angle, radiation and outdoor air temperature to be strongly correlated. High correlation ($R > 0.90$, $Rsq > 0.80$) between inputs flags a potential for multicollinearity.

Lastly, when departures of a model from actual are plotted, these residual errors may be visually inspected for balance and randomness. Any sign of imbalance, skewing, lopsidedness or clustering serves as an alert against linear extrapolation. Models may be transformed or recast as worst-case proxies to avoid overstating DSF performance in an eQUEST simulation.

Residual errors may often reflect sensor variance in the experimental data. Effort was made to use data from hot, sunny days to avoid measurements on the low end of sensor range where "scatter" can dominate. A 2% error at full scale may easily yield 20% error in the lower end of sensor readouts. Sunny summer day data points, though limited in number, also seem more appropriate for extrapolating to hot-climate DSF performance in eQUEST.

This basic line of reasoning will be developed in this chapter:

- Since sun angle highly correlates with radiation, it becomes difficult to assign distinct slope coefficients accurately with both variables in the same set. Regression attempts may use just one, but not both.
- Toa-based convection may amplify independently enough in a hot climate for Toa to pair significantly with radiation in the variable set.
- Since radiation and Toa analytically are direct factors in heat load, this variable pair is favored over sun angle for model extrapolation.
- Since visible light is just a fraction of solar radiation, the sun angle is favored over radiation in the light transmission (LT) variable set.
- Nonlinear light transmission is best modeled conservatively so that model over-prediction will not overstate DSF cost savings in eQUEST.

4.2 Measured data analysis

Within this research, the experimental setup is developed to characterize the effects of using the double skin façade (DSF) system. Principal results emerged from two analyses and applied to the experimental procedure:

A. Calculating the fractional heat removal rate of the double skin façade system in terms of selected independent variables.
B. Obtaining the fraction of incident light transmitted through the DSF system based on chosen independent variables.

Final slates of independent variables will be disclosed later in this chapter. To analyze the data within the research, a statistical approach was

performed using mean values and regression analysis scores to determine the validity of the experiment. Research limitations required using data gathered during the summer months when conditions were sunny and warmest with outdoor air temperatures ranging between 65 degrees and 92 degrees Fahrenheit. The heat removal rate via the DSF cavity was next calculated for subsequent statistical analysis.

The thermal and optical properties of the window used in the Blacksburg experiment were obtained from two sources: the Ply Gem supplier out of Rocky Mount VA and Berkeley Labs, with its test data tabulated below:

Angle	0	10	20	30	40	50	60	70	80	90	Hemis
Vtc	0.639	0.642	0.633	0.622	0.605	0.574	0.503	0.368	0.173	0.000	0.534
Rf	0.249	0.243	0.240	0.243	0.253	0.273	0.313	0.403	0.599	0.999	0.297
Rb	0.198	0.192	0.191	0.194	0.206	0.231	0.286	0.412	0.652	1.000	0.266
Tsol	0.372	0.374	0.368	0.360	0.349	0.330	0.288	0.210	0.097	0.000	0.308
Rf	0.379	0.374	0.373	0.375	0.383	0.397	0.426	0.495	0.656	0.999	0.414
Rb	0.294	0.290	0.288	0.287	0.290	0.301	0.332	0.414	0.595	1.000	0.327
Abs1	0.194	0.197	0.204	0.209	0.211	0.215	0.230	0.246	0.212	0.001	0.214
Abs2	0.055	0.055	0.056	0.056	0.057	0.058	0.056	0.049	0.035	0.000	0.054
SHGCc	0.431	0.433	0.428	0.422	0.412	0.393	0.352	0.269	0.142	0.000	0.368

The top-line Vtc tabulates the angle-dependent visible-light transmission coefficient with an average value of 0.534 over the hemispherical arc. The bottom-line tabulates SHGC versus angle for an average of 0.368 over the whole arc. A nominal U-value of 1.67 W/sq.m-K (0.29 Btu/hr-sq.ft-F) was listed along with a test U-value of 2.5 W/sq.m-K (0.43 Btu/hr-sq.ft-F) in the face of a 5.5 m/s (18 ft/s) wind.

Ply Gem's data for a 4'x 8' double-glazed, low-e, Ar-gas window listed as:

U-value	= 0.28 Btu/hr-sq.ft-F	for the conduction-convection load.
SHGC	= 0.29	for radiant heat load component.
VLT	= 0.54	for portion of visible light transmitted.

No angle orientation or wind speed was disclosed. Nominal heat factors may be viewed as "average" over a yearly cycle, and VLT may represent average light transmission in agreement with Berkeley's. Ply Gem's SHGC of 0.29 lies below Berkeley Lab's summer-tested average value of 0.368.

4.2.1 DSF thermal properties, heat load, and heat removal

DSF heat transfer involves tracking two phenomena: solar radiation (Et) and a combined convection-conduction mechanism. Radiant heat acts through an angle-dependent solar heat gain coefficient (SHGC) applied to a pyranometer Et measurement scaled by a window area of 32 sq.ft. Berkeley Labs provided these SHGC data for our DSF (Double Low-e, Uc of 1.668 W/sq.m-K, SHGCc of 0.292) in 10-degree angle increments:

Angle	0	10	20	30	40	50	60	70	80	90
SHGC	0.431	0.433	0.428	0.422	0.412	0.393	0.352	0.269	0.142	0.000

Notably, high-angle radiation will largely reflect to reduce the solar heat load on the DSF for greater fractions of heat removal in nonlinear fashion. Near Blacksburg's solar noon of 75 degrees altitude, the radiant heat load = SHGC interpolated at angle 75 * 300 Btu/hr-sq.ft * 32 sq.ft ~ 2000 Btu/hr.

Surface convection and double-pane conduction through an air gap is driven by a difference in outdoor and indoor air temperatures (Toa – Tin) scaled by 32 sq.ft window area and a surface wind-dependent U-value. Berkeley Lab's U-value of 2.5 W/sq.m-K (0.44 Btu/hr-sq.ft-F) was tested with a 5.5 m/s wind (18 ft/s) on one surface. Berkeley lists gas-gap conductivity of 0.031 W/m-K through a 12.7 mm thickness to yield nearly 2.5 W/sq.m-K. For well-insulated windows, the gas-gap conductivity governs the U-value. Forced convection on even both surfaces cannot eliminate the gas-gap thermal resistance that caps the U-value. To be conservative, our model will use this maximum U-value of 2.5 W/sq.m-K (0.44 Btu/hr-sq.ft-F).

Conductive heat load for a solar-noon Toa = 90F and Tin = 75F figures as: U of 0.44 Btu/hr-sq.ft-F * 15F * 32 sq.ft ~ 210 Btu/hr, over 10% of Et portion.

Heat removed per minute is cavity flow of 160 cfm scaled by constant air properties of density and specific heat (0.018 Btu/cu.ft-F) applied to the DSF cavity's outlet-inlet temperature difference (Tout– Tin).

DSF heat removal during the cool morning hours involves another notable factor: a.m. conduction *out* from the DSF. Here, Toa < Tin directs heat *outward* through the façade, and this component must be added to any cavity heat vented at its exit. It is thus expected that a greater fraction of reduced morning radiation will be removed during low solar angles, with much of the heat driven across the window pane than out the cavity exit.

Table 4.1 Excel spread sheet calculations sample

Time Recorded	Altitude	Window Solar radiation Btu/hr-sq.ft 2Et * 0.3171	Window Solar radiation W/sq.m PYRANOMETER WINDOW need max 1KW 2x	Cavity Air Flow cfm @ Vel 2 ft/m	Toa Outside Air Temp °F	T office = T cav in Temp Cavity (IN) °F	T cav out Temp Cavity (OUT) °F	Heat Cavity Removed Btu/hr Hc (Btu/hr)= Q 1.08 (t0-ti)	Solar Btu/hr Qs = SHG Et A	Convection through Glass Btu/hr Ar-gap Umax = 2.5 W/sq.m-K Qc = UA (to-ti	Total Heat Removed Hc (minus Qc < 0)	Fraction heat removal rate Btu/hr basis HRR= H/Qs	SHGC vs ALT	Altitude Sun Angle	\Toa-Tin\	Et-120 squared	Et	Alt-27 squared	Toa-Ti squared	Et-120 squared	Fraction heat removal rate HRR= H/Qs
SUNRISE 7/1/2015 6:00:00 AM																					
7/1/2015 6:15	0.9	49.787384	78.52	160	65.1	75.1	75.2	17.3	678.0743716	-136.1708224	153.4508	0.226303823	0.43	0.91	10	4928.407	49.79738	680.6881	10	4928.407293	0.226304
7/1/2015 6:30	3.55	63.42	100	160	65.3	75.1	75.3	54.6	863.5668629	-133.4474059	168.0074	0.194550547	0.429999	3.55	9.8	3201.296	63.42	548.9025	9.8	3201.2964	0.194551
7/1/2015 6:45	6.29	73.9153758	116.549	160	65.6	75.2	75.5	91.8	1006.457257	-130.7239895	182.564	0.18139269	0.42999	6.24	9.6	2123.793	73.91538	430.9776	9.6	2123.792588	0.181393
7/1/2015 7:00	8.99	78.3256026	123.503	160	65.3	75.3	75.7	69.1	1066.425075	-136.1708224	205.2908	0.192503747	0.429956	8.99	10	1736.755	78.3256	324.3601	10	1736.755399	0.192504
7/1/2015 7:15	11.77	83.2901202	131.331	160	65.4	75.4	75.7	51.8	1133.794665	-136.1708224	188.0108	0.165824402	0.429871	11.77	10	1347.615	83.29012	231.9529	10	1347.615275	0.165824
7/1/2015 7:30	14.59	98.243922	154.91	160	65.5	75.5	75.8	51.8	1336.810233	-136.1708224	188.0108	0.14064137	0.429696	14.59	10	473.3269	98.24392	154.0081	10	473.3269299	0.140641
7/1/2015 7:45	17.44	121.186741	191.086	160	65.7	75.4	75.9	86.4	1647.780877	-132.0856977	218.4857	0.132593903	0.42938	17.44	9.7	1.408355	121.1867	91.3936	9.7	1.408354676	0.132594
7/1/2015 8:00	20.32	148.419289	234.026	160	66.7	75.4	75.9	86.4	2015.607372	-118.4686155	204.8686	0.101641132	0.428858	20.32	8.7	807.656	148.4193	44.6224	8.7	807.6559986	0.101641
7/1/2015 8:15	23.23	135.680748	213.94	160	67.8	75.7	76	51.8	1839.136658	-107.5749497	159.4149	0.08667923	0.428049	23.23	7.9	245.8859	135.6807	14.2129	7.9	245.8858578	0.086679
7/1/2015 8:30	26.19	151.947978	239.59	160	67.6	75.6	76.2	103.7	2053.926841	-106.2132415	209.8932	0.102191197	0.426862	26.16	7.8	1020.673	151.948	0.7056	7.8	1020.673298	0.102191
7/1/2015 8:45	29	153.996444	242.82	160	69.9	75.4	76.2	138.2	2073.488919	-74.88395232	213.134	0.102790013	0.425196	29.1	5.5	1155.758	153.9964	4.41	5.5	1155.758205	0.10279
7/1/2015 9:00	32.03	182.231028	287.34	160	70.2	75.4	76.2	138.2	2440.4818	-70.80882765	209.0488	0.085658835	0.422913	32.07	5.2	3872.701	182.231	25.7049	5.2	3872.700846	0.085659
7/1/2015 9:15	35.04	184.99614	291.7	160	70.2	75.8	76.2	69.1	2459.861503	-76.25566054	145.3757	0.059099124	0.4199	35.04	5.6	4224.498	184.9961	64.6416	5.6	4224.498215	0.059099
7/1/2015 9:30	38.03	190.868832	300.96	160	70.9	75.36	76.3	162.4	2514.379679	-62.09389501	224.5259	0.089296735	0.416	38.02	4.56	5022.391	190.8688	121.4404	4.56	5022.391349	0.089297
7/1/2015 9:45	41	193.68468	305.4	160	71.8	75.4	76.7	224.6	2521.219506	-51.74491251	276.3849	0.109623502	0.411067	41	3.8	5429.432	193.6847	196	3.8	5429.432067	0.109624
7/1/2015 10:00	43.96	197.04594	310.7	160	72.1	75.2	77.1	328.3	2526.556208	-42.21295494	370.533	0.146655338	0.404911	43.99	3.1	5936.077	197.0459	288.6601	3.1	5936.07687	0.146655
7/1/2015 10:15	46.87	187.856382	296.21	160	72.8	75.1	77.3	380.2	2363.985053	-31.31928915	411.4793	0.174061714	0.39739	46.97	2.3	4604.489	187.8564	398.8009	2.3	4604.488578	0.174062
7/1/2015 10:30	49.81	196.614684	310.02	160	73.5	75.1	77.4	397.4	2417.974315	-21.78733158	419.2273	0.173779564	0.388359	49.93	1.6	5869.81	196.6147	525.7849	1.6	5869.809804	0.17538
7/1/2015 10:45	52.88	197.020572	310.66	160	74.1	75.1	78	501.1	2355.908921	-13.61708224	514.7371	0.218487685	0.377611	52.88	1	5932.169	197.0206	669.7744	1	5932.168511	0.218488
7/1/2015 11:00	55.79	205.220778	323.59	160	74.7	75.1	78.38	566.8	2372.606073	-5.446852896	572.2308	0.241182403	0.365092	55.79	0.4	7262.581	205.2208	828.8641	0.4	7262.581003	0.241182
7/1/2015 11:15	58.69	215.177718	339.29	160.4	75.4	75.3	78.43	542.2	2389.444779	1.361708224	542.2162	0.226792157	0.350669	58.66	0.1	9058.798	215.1777	1002.356	0.1	9058.798004	0.226792
7/1/2015 11:30	61.48	217.187815	342.4595	160.5	75.6	75	78.8	658.7	2299.037412	8.170249344	658.692	0.285493157	0.334278	61.48	0.6	9445.471	217.1878	1188.87	0.6	9445.471365	0.285493
7/1/2015 11:45	64.21	285.39	450	160.5	76	75	79	693.4	2856.796971	13.61708224	693.36	0.241554001	0.31611	64.21	1	27353.85	285.39	1384.584	1	27353.8521	0.241554
7/1/2015 12:00	66.83	295.50549	465.95	160.4	77.7	75	79.4	762.2	2773.170593	36.76612205	762.2208	0.271259063	0.296353	66.83	2.7	30802.18	295.5055	1586.429	2.7	30802.17702	0.271259
7/1/2015 12:15	69.28	304.682364	480.42	160.3	77.9	75	79.7	813.7	2659.548046	39.4895385	813.6828	0.30147146	0.27565	69.28	2.9	34107.58	304.6824	1787.598	2.9	34107.57557	0.301471
7/1/2015 12:30	71.5	317.150736	500.08	160.2	78.8	75.2	79.9	813.2	2559.935955	49.02149606	813.1752	0.31168588	0.254895	71.5	3.6	38868.41	317.1507	1980.25	3.6	38868.41271	0.311686
7/1/2015 12:45	73.39	327.393066	516.23	160.3	79.1	75.2	80.3	882.9	2442.913486	53.10662073	882.9324	0.353736093	0.235633	73.39	3.9	43011.88	327.3931	2152.032	3.9	43011.88382	0.353736
7/1/2015 13:00	74.83	328.5156	518	160	79.3	75.1	80.5	933.1	2287.861289	57.19174541	933.12	0.397909877	0.219923	74.83	4.2	43478.76	328.5156	2287.709	4.2	43478.75544	0.39791
7/1/2015 13:15	75.68	329.08638	518.9	160	79.3	75	80.9	1019.5	2190.65838	58.55345363	1019.52	0.453278782	0.210214	75.68	4.3	43717.11	329.0864	2369.742	4.3	43717.1143	0.453279
7/1/2015 13:30	75.83	329.784	520	160	79.5	74.9	81.2	1088.6	2177.051051	62.6385783	1088.64	0.486067349	0.208467	75.83	4.6	44009.33	329.784	2384.369	4.6	44009.32666	0.486067
7/1/2015 13:45	75.26	325.3446	513	160	79.9	74.9	79.5	794.9	2215.599142	68.0854112	794.88	0.348069088	0.215053	75.26	5	42166.4	325.3446	2329.028	5	42166.40475	0.348069
7/1/2015 14:00	74.04	320.486628	505.34	160	80.1	74.9	79.5	794.9	2320.562792	70.80882765	794.88	0.332395013	0.228655	74.04	5.2	40194.89	320.4866	2212.762	5.2	40194.88801	0.332395
7/1/2015 14:15	72.31	310.758	490	160	80.1	74.8	79.5	812.2	2428.91487	72.17053587	812.16	0.324723018	0.246824	72.31	5.3	36388.61	310.758	2052.996	5.3	36388.61456	0.324723
7/1/2015 14:30	70.21	298.7082	471	160	80.2	74.7	79.5	829.4	2527.411872	74.89395232	829.44	0.318732715	0.267194	70.21	5.5	31936.62	298.7082	1867.104	5.5	31936.62075	0.318733
7/1/2015 14:45	67.84	289.683534	456.77	160	80.4	74.8	79.5	812.2	2642.723962	76.25566054	812.16	0.298700289	0.288088	67.84	5.6	28792.9	289.6835	1667.906	5.6	28792.90171	0.2987
7/1/2015 15:00	65.28	268.564674	423.47	160	80.4	74.9	79.2	743.0	2622.178988	74.89395232	743.04	0.275498667	0.308327	65.28	5.5	22071.46	268.5647	1465.358	5.5	22071.46236	0.275499
7/1/2015 15:15	62.59	253.68	400	159.8	80.4	74.9	79.1	724.9	2628.270026	74.89395232	724.8528	0.26814977	0.327176	62.59	5.5	17870.34	253.68	1266.648	5.5	17870.3424	0.26815
7/1/2015 15:30	59.81	253.667316	399.98	159	80.4	74.9	78.5	618.2	2765.392513	74.89395232	618.192	0.217651285	0.344263	59.81	5.5	17866.95	253.6673	1076.496	5.5	17866.95137	0.217651
7/1/2015 15:45	56.99	248.6064	392	160	80.3	75	78.1	535.7	2829.96501	72.17053587	535.68	0.184581317	0.359473	56.96	5.3	16539.61	248.6064	897.6016	5.3	16539.60612	0.184581
7/1/2015 16:00	54.09	226.973838	357.89	160	80.4	75	78.9	673.9	2679.632842	73.53224409	673.92	0.244780091	0.372818	54.05	5.4	11443.4	226.9738	731.7025	5.4	11443.40202	0.24478
7/1/2015 16:15	51.12	200.4072	316	160	79.2	75	78.69	637.6	2438.50663	57.19174541	637.632	0.255492413	0.384245	51.12	4.2	6465.318	200.4072	581.7744	4.2	6465.317812	0.255492
7/1/2015 16:30	48.19	196.79226	310.3	160	78.8	75	78.2	553.0	2455.043577	51.74491251	552.96	0.220585024	0.393957	48.16	3.8	5897.051	196.7923	447.7456	3.8	5897.051196	0.220585
7/1/2015 16:45	45.19	191.743394	302.339	160	77.8	75	78.16	546.0	2441.250775	35.40441382	546.048	0.220478007	0.402059	45.19	2.6	5147.115	191.7434	330.8761	2.6	5147.114554	0.220478
7/1/2015 17:00	42	186.594958	294.221	160	76.9	75.1	78	501.1	2415.248415	20.42562336	501.12	0.205741816	0.408752	42.2	1.5	4434.888	186.595	231.04	1.5	4434.888458	0.205742
7/1/2015 17:15	39.11	179.207162	282.572	160	75.7	75.1	77.7	449.3	2350.241413	8.170249344	449.28	0.190501093	0.414147	39.22	0.6	3505.488	179.2072	149.3284	0.6	3505.488079	0.190501
7/1/2015 17:30	36.24	174.953583	275.865	160	74.2	75.2	77.8	449.3	2318.259156	-13.61708224	462.8971	0.199674433	0.418443	36.24	1	3019.896	174.9536	85.3776	1	3019.896285	0.199674
7/1/2015 17:45	33.39	170.671465	269.113	160	74	75.3	77.85	440.6	2279.663862	-17.70220691	458.3422	0.201056925	0.421801	33.26	1.3	2567.597	170.6715	39.1876	1.3	2567.597325	0.201057
7/1/2015 18:00	30.59	151.961296	239.611	160	73.8	75.4	77.79	413.0	2042.06648	-21.78733158	434.7793	0.212911448	0.42436	30.29	1.6	1021.524	151.9613	10.8241	1.6	1021.524455	0.212911
7/1/2015 18:15	27.81	151.70064	239.2	160	73.7	75.5	77.53	350.8	2047.70049	-24.51074803	375.2947	0.183276192	0.426262	27.33	1.8	1004.931	151.7006	0.1089	1.8	1004.930576	0.183276
7/1/2015 18:30	24.9	148.789662	234.61	160	73.5	75.4	77.27	323.1	2014.829769	-25.87245626	349.0085	0.173219823	0.427625	24.4	1.9	828.8446	148.7897	6.76	1.9	828.8446381	0.17322
7/1/2015 18:45	21.88	133.355137	210.273	160	73.1	75.4	77.06	286.8	1809.829289	-31.31928915	318.1673	0.175799613	0.428574	21.48	2.3	178.3597	133.3551	30.4704	2.3	178.3596736	0.1758
7/1/2015 19:00	18.78	104.85736	165.338	160	71	75.7	77.62	331.8	1425.150701	-36.76612205	368.5421	0.258598703	0.4292	18.59	2.7	229.2996	104.8574	70.7281	2.7	229.2995583	0.258599
7/1/2015 19:15	15.73	89.8686768	141.704	160	72.8	75.6	76.97	236.7	1222.547433	-38.12783027	274.8638	0.224828766	0.429591	15.72	2.8	907.8966	89.86868	127.2384	2.8	907.8966378	0.224829
7/1/2015 19:30	12.86	85.8491172	135.366	160	72.4	75.4	76.28	152.1	1168.475979	-40.85124672	192.9152	0.165099882	0.429815	12.89	3	1166.283	85.84912	199.0921	3	1166.282796	0.1651
7/1/2015 19:45	10.08	63.4783464	100.092	160	72	75.1	75.74	110.6	864.2238893	-42.21295494	152.905	0.176811769	0.429931	10.09	3.1	3194.697	63.47835	285.9481	3.1	3194.697326	0.176812
7/1/2015 20:00	7.33	53.3412936	84.108	160	71.6	75.1	75.26	27.6	726.297944	-47.65978784	75.30779	0.103687183	0.429981	7.33	3.5	4443.383	53.34129	386.9089	3.5	4443.383139	0.103687

Heat removal rate (HRR) is the heat removed as a fraction of heat load, all scaled in Btu/hr units. Although outdoor air temperature itself appears analytically as a linear element, the change in direction of conduction poses physical nonlinearity, as do radiation Et and non-constant SHGC (more information will be presented later in this chapter). Linear transformation of variables seemed inevitable. Summer solar-noon radiation and Toa were expected to log 1kW/sq.m and 90F, respectively. July 2015 test data confirmed the proper sensor scaling factors for these.

4.2.2 DSF optical properties and light transmission

Light transmission simply averages the indoor photometer reading divided by that from outdoors: LT = photo in / photo out. Since outdoor light must pass through *two* double-paned window frames to hit the indoor sensor, DSF LT may reasonably log as the *square* of Berkeley Lab's Vtc data for a horizontal LT readout of 0.4 falling to 0.2 when nearing 60 degrees or so.
This expected range was confirmed experimentally. Solar-noon lighting was expected to measure 25 Klux facing south on a bright day, with dawn-dusk values of 400 lux. Outdoor photometry validated these values:

Table 4.2 Excel spread sheet sun altitude and photometers readings in Klux

	Transmission Outer skin	**Transmission Inner skin**	**Fraction of light Transmitted Through both layers uncompensated for sensor temperature**
Altitude	OUTSIDE PHOTOMETER expected 0.4 - 25 Klux	PHOTOMETER OFFICE KLUX	PHOTO (IN) / PHOTO (OUT)
6.24	0.49886	0.211	0.422964359
8.99	0.75686	0.317	0.418835716
11.77	1.16686	0.471	0.403647396
14.59	2.08686	0.882	0.422644547
17.44	3.39086	1.422	0.41936264
20.32	5.12286	2.137	0.417149795
23.23	6.54086	2.718	0.415541687
26.16	7.97286	3.123	0.391703855
29.1	6.65436	2.998	0.450531681

32.07	6.84436	3.072	0.448836706
35.04	8.95636	3.912	0.436784587
38.02	9.83036	3.988	0.405681989
41	10.49836	4.182	0.398347932
43.99	10.74236	3.547	0.364080161
46.97	10.97836	3.92	0.357066083
49.93	12.498	4.226	0.272680346
52.88	13.77092	3.738	0.21034364
55.79	14.39892	2.707	0.218325467
58.66	15.69892	2.508	0.214378763
61.48	16.25092	3.391	0.208665109
64.21	19.01092	3.951	0.207827922
66.83	18.25092	3.851	0.211003062
69.28	20.39092	4.178	0.20489512
71.5	19.17092	3.917	0.204319876
73.39	18.73092	3.834	0.204688291
74.83	18.09092	5.016	0.192250791
75.68	18.31092	3.677	0.200809135
75.83	15.37692	2.503	0.220006821
75.26	13.18092	2.696	0.204538075
74.04	12.91092	4.23	0.212446236

Solar position or radiation might serve in LT's independent variable set. However, since visible light forms only part of the Et spectrum, and with the trigonometry involved, linearity was far from assured using either input. More details about nonlinear issues will be presented later in this chapter.

4.3 Introduction to regression analysis

Regression analysis is a statistical approach that reveals the relationship between an independent input variable and its dependent output. Regression models offer predictive merit when functional relationships among independent and dependent variables are well-comprehended. As Ott, L., & Longnecker, M. (2010) note, "The basic idea of regression analysis is to obtain a model for the functional relationship between a response variable (often referred to as the dependent variable) and one or more explanatory variables (often referred to as the independent variables)" (p.572).

Linear regression analysis may superpose predictable results by applying a "regression coefficient" for each causative input to quantify the degree of change that variable (x) has on output (y) for each unit of change in (x). Such coefficients serve as "slope" or sensitivity factors in data predictions. Slope coefficients along with an intercept (or offset) are computed to minimize the departure of actual data (sum of the square of the errors) from the regressed line equation.

For single-variable regression, a modeled line takes the form of:

$Y = b_0 + b_1 X + error$ where (4.1)

Y = predicted output
X = independent input variable
b_0 = intercept or offset for no input, X=0
b_1 = slope coefficient applied to the input
$error$ = predicted Y – actual Y = Y-y.

Slope b_1 and intercept b_0 are then selected to minimize the sum of the squared individual errors (Y-y)*(Y-y) at each data point. Standard error SE for the model is the square root of the average of this sum for the number of data points. Standard errors may then be expressed as a percentage of the mean (Y). The lower the SE per mean Y, the better the model fits. Nearly two-thirds of actual outputs generally lie within +/- one standard error of the model prediction.

The individual errors, called residuals, can be plotted for each input and visually inspected. When residuals appear random, balanced, and symmetrical about the zero-error line across the range of inputs, the linear regression offers fair prospects for extrapolation. Kinks, skews, clusters or imbalances in the residual plot suggest possible over-understatement from the regression, perhaps owing to nonlinear effects curving away from the straight-line model. Sensor error, too, may widen the residual distortion at the lower end of inputs. Next, a probability check, called t-test testing, should rule out the chance (< 5%) for a coincidental line when none exists. Finally, a second dataset can be enlisted to validate the regressed model. Favorable standard errors should arise in comparison with the original SE.

While a single input variable may explain some or much of an output, using more inputs may more fully model the output in multiple regression, provided these inputs offer separate, distinct, independent effects.

4.4 Multiple Regression

Since many phenomena are multi-variate, multiple regression analysis can embody more than one independent variable to yield predictive data. Sensitivities of a dependent variable (target output) arising from two or more causative independent variables can aid researchers in recognizing how extensively the dependent variable changes under the influences of two or more inputs – a requirement for predicting valid future outcomes. For multiple regression, a modeled line now takes an expanded form:

$$Y = b_0 + b_1 X_1 + b_2 X_2 + b_3 X_3 + b_i X_i + error \quad \text{where} \qquad (4.2)$$

Y = predicted output
X_1 to X_i = independent input variables
b_0 = intercept or offset for no inputs, all Xi = 0
b_1 to b_i = partial slope coefficients applied to each input
$error$ = predicted Y – actual Y = Y-y.

Partial slopes (b_1) to (b_i) and intercept b_0 are again selected to minimize the sum of the squared individual errors (Y-y)*(Y-y) at every point of data. For multiple inputs, a key regression requirement is an independent set of input variables for the following reasons.

When inputs X_1 and X_2 affect each other, uncertainties develop in assigning proper and distinct partial coefficients b1 and b2 for the model. Single-variable regressions for X_1 and X_2 yield specific b_1 and b_2 when run separately. Linearity dictates that separate input effects can combine to superpose one output.

Redundant "cross-talk" among input variables is called "multicollinearity." Assessment of correlation between X_1 and X_2 can spot multicollinear risks (R > 0.9, R_{sq} > 0.8). As with single-variable regression, linearity, variable significance, residual inspection, and model validation using a second dataset all need securing.

Multiple regression analysis merits consideration in our research since the experimental heat removal rate (HHR) itself is comprised of measured outdoor air temperature and radiation throughout the solar angular arc. This statistical technique has potential to also unearth the relationship among light transmission and the sun angle or measured solar radiation. Modeling considerations for our research will be presented next.

4.5 Multiple regression models considered for this study

Multiple regression analysis was enlisted as an approach for this research. A few linear regression models were assessed to evaluate the relationship among several factors. The aim was to find the sensitivity and relationship between the dependent and each independent variable in the models. The first model estimated the heat removal rate (HRR) in terms of three candidate variables.

Candidate variables included those directly measured in computing heat removal rate: solar radiation E_t (Btu/hr-sq.ft) and outdoor air temperature T_{oa} (deg F). Solar position represented by altitude angle deserved a look. Pros and cons for each were as follows:

E_t : Dominant input for (HHR), but likely over-represents visible light in LT.

T_{oa} : Direct element in (HHR) while filling a subordinate, yet complicated, role in the heat balance during the experimental study in Blacksburg VA.

$Sun\ Angle$: The horizontal time sweep in the azimuth angle seemed too generic to offer extrapolation insights for hot climate. On the other hand, altitude already well embodies the time-of-day aspect in solar trajectory. Both azimuth and altitude fail to account for sky conditions like Et would in any HRR regression. Sun angle looks much more useful for LT than for HRR.

Of course, correlation testing among Et, Toa and altitude will be required to assure independence for any combination of variables used in multiple regression attempts.

4.5.1 Heat removal rate multiple regression

The candidate multiple regression for heat removal rate (Btu/hr basis) is:

$$\boldsymbol{HRR} = b_0 + b_1\,ALT + b_2\,E_t + b_3\,T_{oa} + error \quad \text{where} \qquad (4.3)$$

HRR = predicted heat removal rate
b_0 = intercept or offset for no inputs, ALT = Et = Toa = 0
$b_1\,ALT$ = partial slope coefficient applied with solar altitude angle
$b_2\,E_t$ = partial slope coefficient applied with solar radiation
$b_3\,T_{oa}$ = partial slope coefficient applied with outdoor air temperature
$error$ = predicted HRR – actual HRR.

Correlation analysis disclosed R_{sq} = 0.93 for radiation E_t versus altitude, an almost one-to-one correlation (results are shown later in page124). Far from being independent variables, angle and radiation were highly correlated. Therefore, only one of the two were to be used. Extrapolation to hot climate and direct use in the eQUEST simulation software favored E_t over altitude.

Correlation analysis for Et versus Toa yielded Rsq = 0.42 to offer a sufficient buffer against multicollinearity. Since DSF conduction comprises 10% of early morning and solar-noon heat transfers, modeling should include T_{oa} :

$$\boldsymbol{HRR} = b_0 + b_1 E_t + b_2 T_{oa} + error \quad \text{where} \qquad (4.4)$$

HRR = predicted heat removal rate
b_0 = intercept or offset for no inputs, Et = Toa = 0
$b_1 E_t$ = partial slope coefficient applied to solar radiation
$b_2 T_{oa}$ = partial slope coefficient applied to outdoor air temperature
$error$ = predicted HRR – actual HRR.

4.5.2 Light transmission multiple regression

The candidate multiple regression for light transmission is:

$$LT = b_0 + b_1 ALT + b_2 E_t + error \quad \text{where} \qquad (4.5)$$

LT = predicted light transmission through DSF
b_0 = intercept or offset for no inputs, ALT = Et = 0
$b_1 ALT$ = partial slope coefficient applied to solar altitude angle
$b_2 E_t$ = partial slope coefficient applied to solar radiation
$error$ = predicted LT – actual LT.

Since altitude and radiation highly correlate, a single-variable regression choice remained using either angle or E_t. The favored model should feature a more linear scatter plot, better-fitting R_{sq} and lower standard error populated with more favorably balanced, random residuals.

4.6 Scatter Plots of Collected Data

A scatter plot is a graph designed to visualize two variables for identifying their potential relationship. Scatter plots for each potential independent variable versus the dependent variable are made. A positive relationship between the two variables is demonstrated by a rising trend in the data. A declining trend indicates a negative association between the variables. Scatter plots provide a picture of the type of relationship between the two variables and its potential linearity.

This section examines DSF thermal and light performance in terms of three variables separately: outdoor air temperature T_{oa}, radiation E_t, and solar altitude angle. Visual reviews of single-variable plots can frame prospects for linearity and slope coefficients. The extent of scatter offers an essential, albeit subjective, check for meeting the OLS regression dictate of linearity. Nonlinear relationships must either be transformed or discarded entirely.

4.6.1 Heat removal rate against outdoor air temperature Toa

The HRR versus outdoor air temperature T_{oa} plot below clearly depicts nonlinearity with T_{oa}. HRR rose as Toa departed either way from a central value of 75F. At Toa < Tin, conduction *out* of the façade *aided* the heat removal of modest dawn radiation. During a hotter solar noon, reflected radiation (small SHGC at higher solar altitudes) limited the overall DSF heat load to again raise HRR. In contrast, hot-air conduction in later afternoons plus more horizontal Et *reduced* HRR to result in data scatter for Toa > 75F.

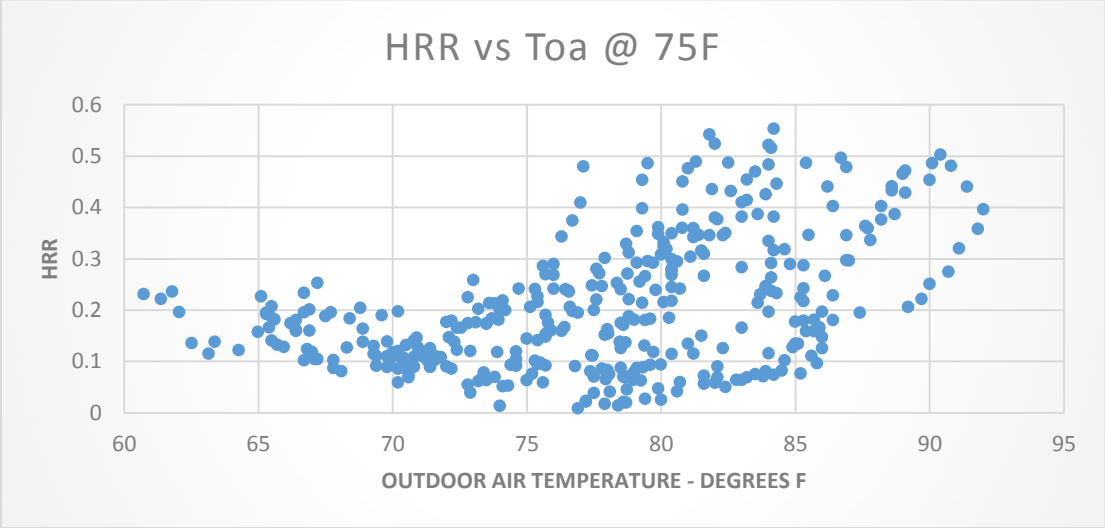

Figure 4.1 Heat removal rate versus outdoor air temperature scatter plot

Framing temperature as an absolute value of $|T_{oa} - \text{Tin}|$ seemed sensible for capturing the effect of bidirectional conduction through the façade.

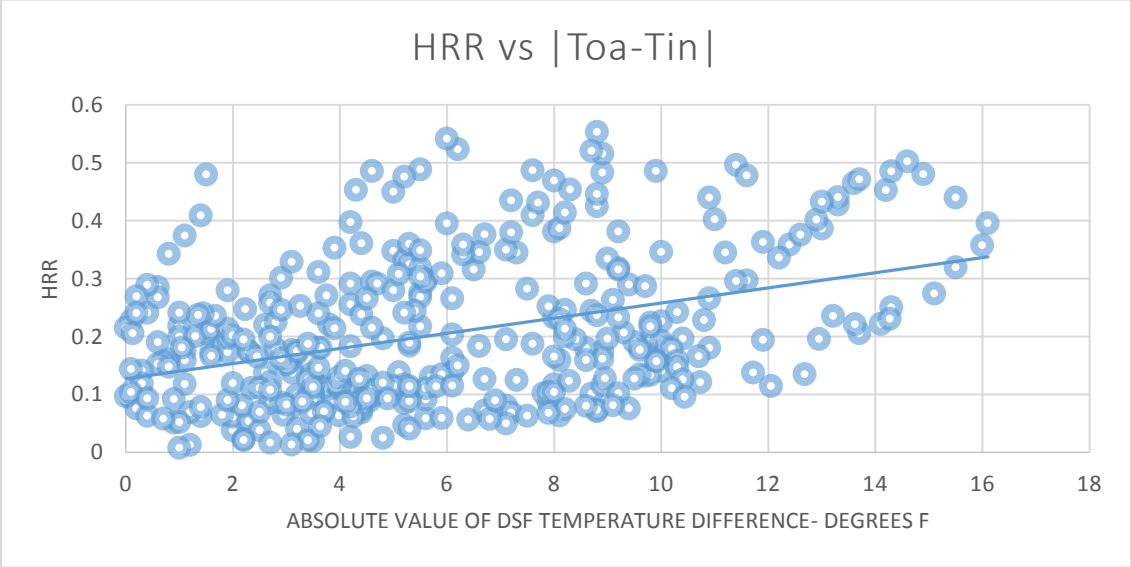

Figure 4.2 Heat removal rate versus |Toa-Tin| scatter plot

When all of HRR is cast as depending only on T_{oa} – based conduction, then the trend line here suggests a sensitivity of 0.10 HRR per 8F for a slope coefficient of 0.0125. For any HRR multiple regression attempts, the slope coefficient for $|T_{oa} - \text{Tin}|$ may well decline into the thousandths range.

4.6.2 Heat removal rate against solar radiation

The HRR versus solar radiation plot appears below. There is little reason to expect a linear relationship here since solar trajectory is not a straight line. The U-shaped trend makes it wise to consider a linear transformation using the square of radiation with the vertex placed at Et = 120. Modest radiant heat transferred to the cool morning air by the DSF cavity and a lower solar-noon SHGC shrinking the heat-load denominator in HRR both likely account for the steepened upswings at each edge of the plot.

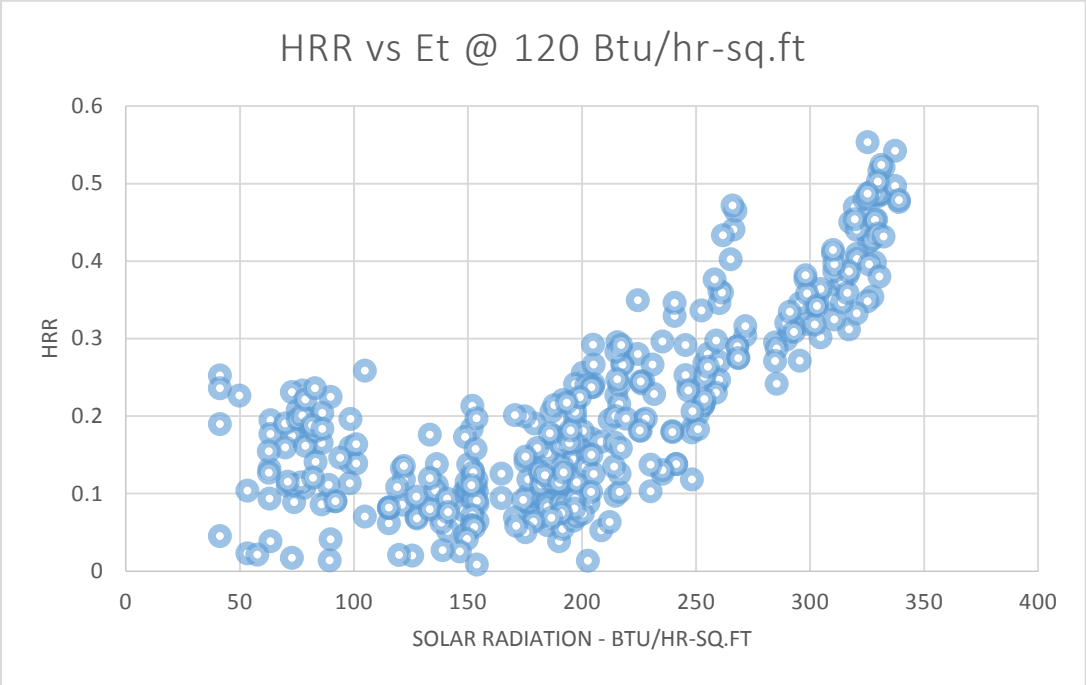

Figure 4.3 Heat removal rate versus solar radiation scatter plot

HRR versus the square of solar radiation offset by 120 offers a better look:

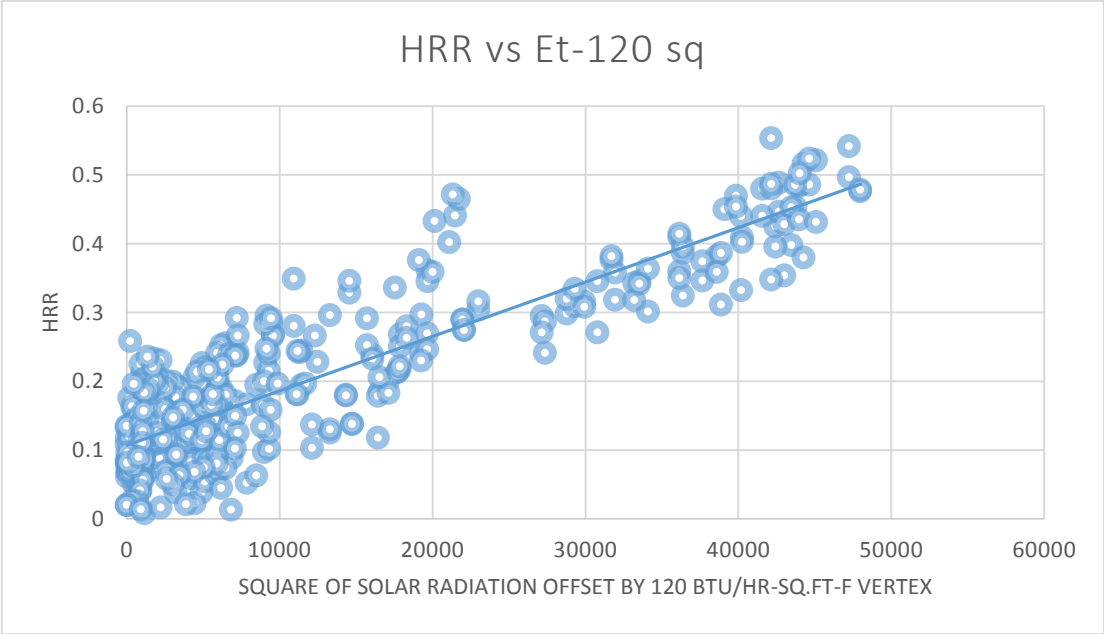

Figure 4.4 Heat removal rate versus square of solar radiation scatter plot

This linear transformation using the square of radiation appears to provide a more centered line with a sensitivity of 0.4 HRR per 50,000 input units for a slope coefficient of 8E-6.

4.6.3 Heat removal rate against solar altitude angle

The *HRR* versus solar altitude plot appears below. There is little reason to expect a linear relationship here since solar trajectory is not a straight line. Indeed, the trend line under-predicts HRR for both low and high angles while over-predicting HRR for midrange altitudes between 25-65 degrees. Any regression usage of altitude in HRR likely requires linear transformation, especially for peak reflective altitudes where SHGC dramatically cuts the radiant heat load in HRR's denominator. Since altitude cannot represent sky conditions or extrapolate to hotter climate like solar radiation can, solar angle seems ill-suited for HRR.

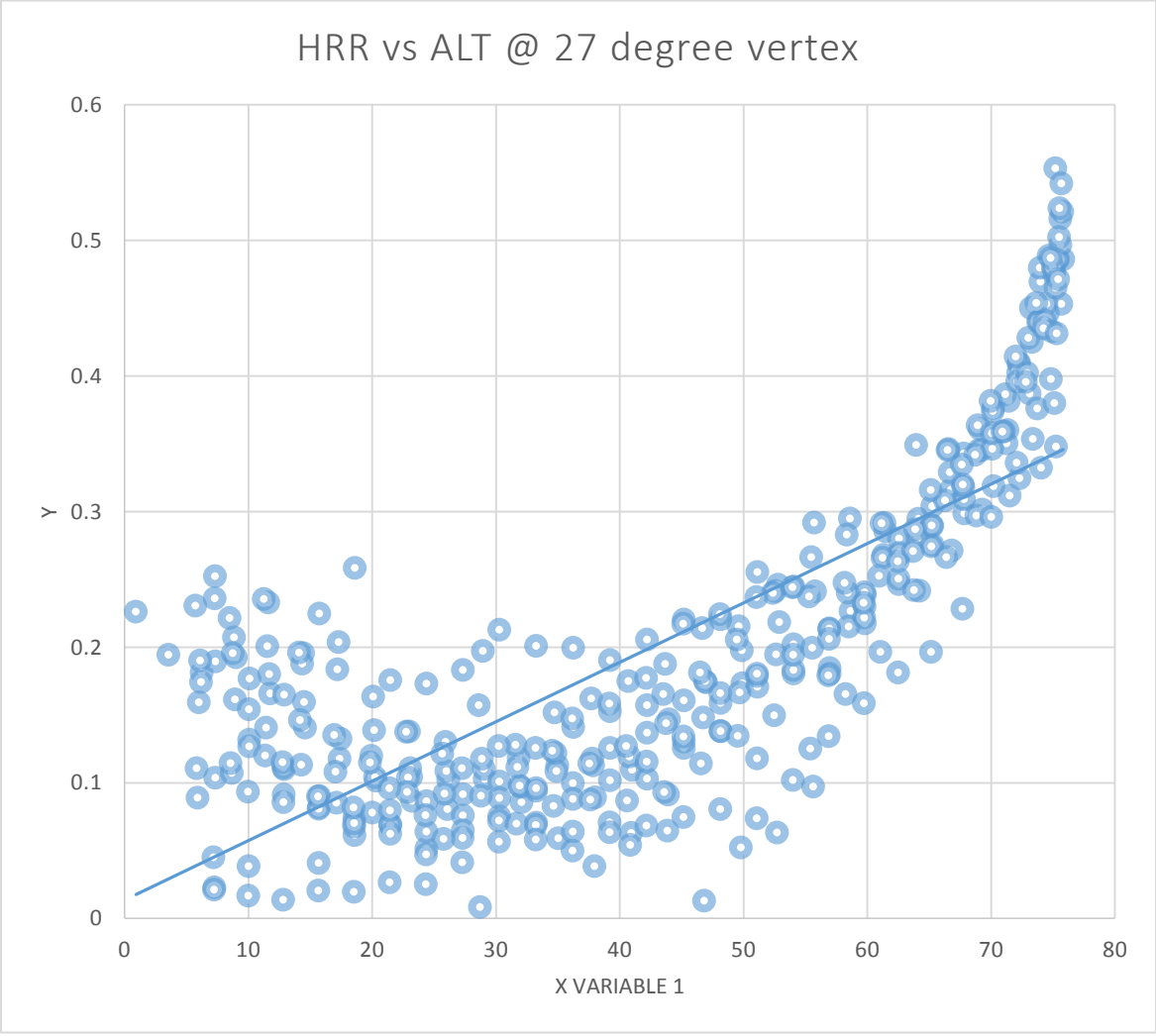

Figure 4.5 Heat removal rate versus solar altitude scatter plot

4.6.4 Light transmission against solar radiation

The light transmission LT versus solar radiation E_t plot below shows a large non-linear drop near the 200 Btu/hr input. Since visible light forms only part of the E_t spectrum, it seems wise to discard this relationship for regression.

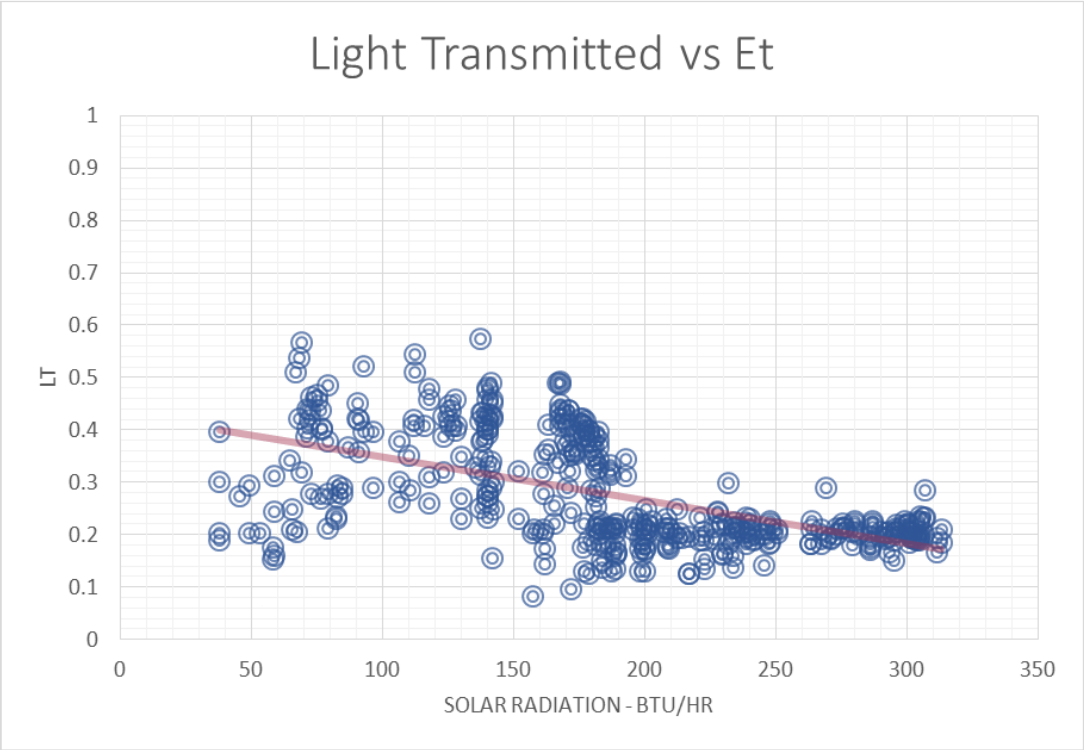

Figure 4.6 Light transmission versus solar radiation scatter plot

4.6.5 Light transmission against solar altitude angle

A nonlinear break appears in the figure below for LT, too, at 50 degrees altitude with notable invariance at higher angles. Perhaps, the slat angle of the shading device reflects a stabilized beam toward indoor lighting.

To avoid clear model over-prediction at 50-60 degrees, either piecewise linearization (LT = 0.2 for SA > 50 degrees) or a modest steepening of the slope may prove suitably conservative for our calculation.

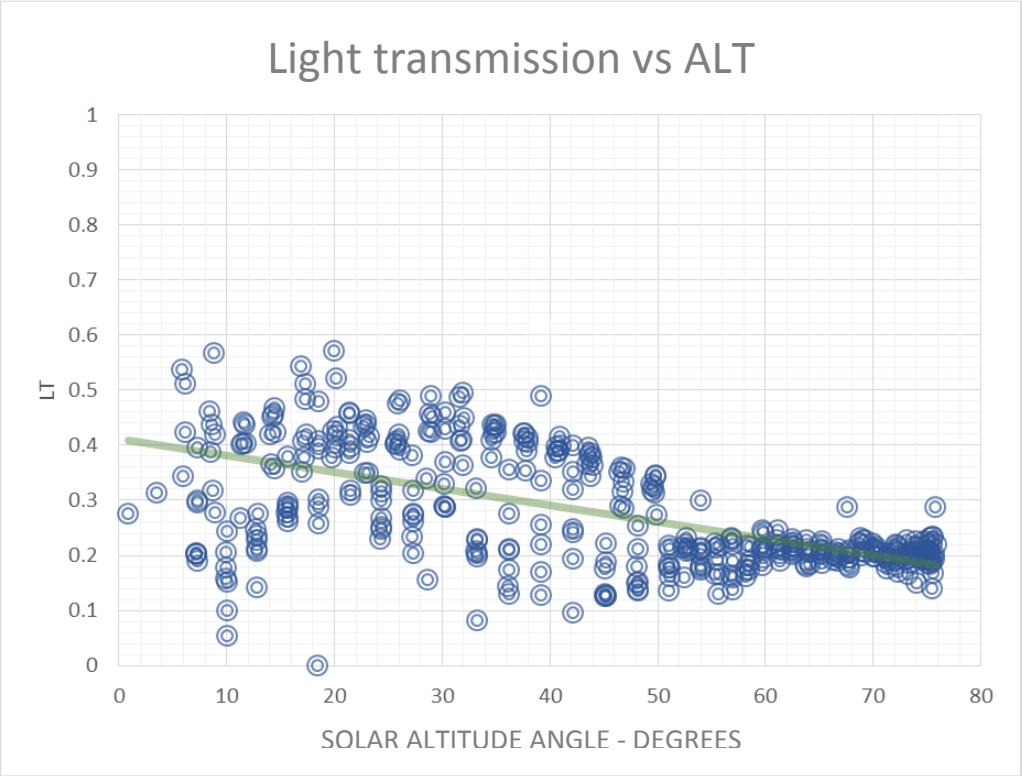

Figure 4.7 Light transmission versus altitude scatter plot

4.7 Multiple regression data analysis

The main task in multiple regression is establishing independent variables. Extremely high correlation (R_{sq} 0.93) was found linking altitude and solar radiation as plotted below, confirming a natural intuition. Since sun angle and E_t redundantly correlate, any multiple regression attempt must enlist

either one or the other, but not both jointly. Radiation and outdoor air temperature showed workable distinction from each other with R_{sq} 0.42, while sun angle and T_{oa} yielded a bit riskier R_{sq} 0.50 (R > 0.70).

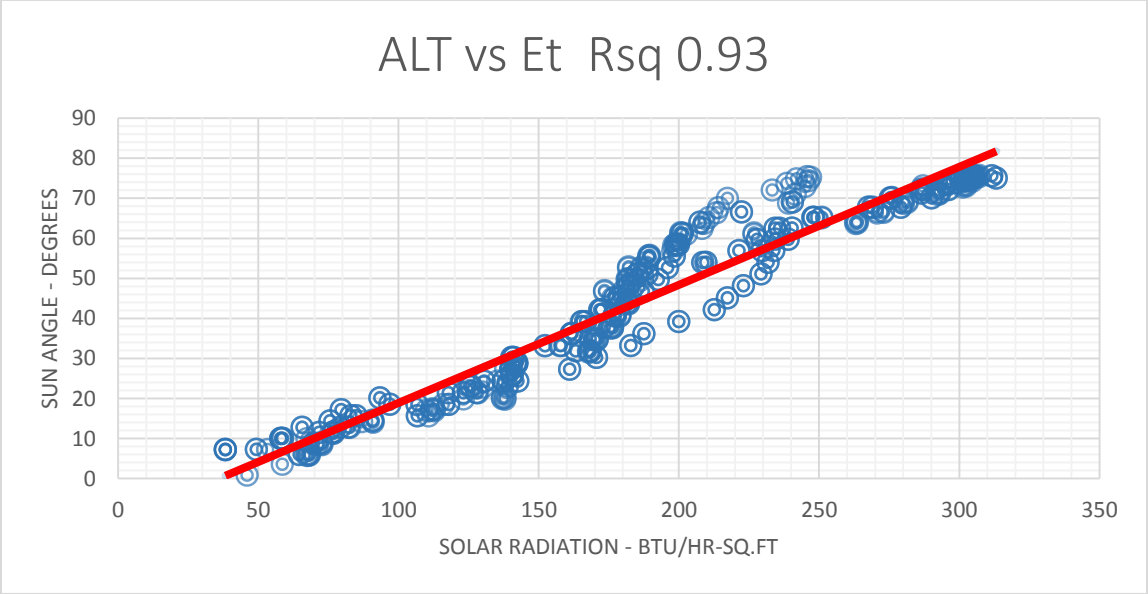

Figure 4.8 Sun angle versus solar radiation scatter plot

The high correlation between sun angle and radiation logically restricts light transmission to single-variable form. Sun angle is selected since visible light photometry comprises only part of the E_t radiation spectrum.

Regression options are next assessed for better fit, tests of significance and for randomly balanced residual errors. Chosen models will finally undergo validation for standard-error performance using a second dataset.

4.7.1 Heat removal rate multiple regression coefficients, p-values & errors

One possible HRR regression enlists altitude and outdoor air temperature. As discussed earlier, both variables require linear transformation to handle V-shaped conduction and U-curve angle effects (vertex at 27 degrees):

$$\boldsymbol{HRR} = b_0 + b_1 |T_{oa} - Tin| + b_2 (ALT - 27)\text{^}2 + error \qquad (4.6)$$

HRR = Heat removal rate
b_0 = intercept or offset for zero inputs where $Toa{=}Tin$ and $ALT{=}27\,deg$
b_1 $|T_{oa} - Tin|$ = partial slope factor acting on outdoor air temperature
b_2 $(ALT\text{-}27)\text{^}2$ = partial slope coefficient applied with altitude angle
$error$ = predicted HRR – actual HRR.

While the Rsq fit of 0.85, low standard error < 0.05 = 25% of average HRR, and p = 0.02 look very alluring, the residual plot suggests under-prediction of HRR for quite a range of altitude inputs. Residual imbalance along with altitude's inability to capture sky conditions, such as cloudiness, or to extrapolate for hotter climate merits caution for this ALT-Toa model.

Regression Statistics	
Multiple R	0.922802974
R Square	0.851565328
Adjusted R Sq	0.850777876
Standard Error	0.04851767
Observations	380

	Coefficients	*Standard Error*	*t Stat*	*P-value*
Intercept	0.085328585	0.004709852	18.11704129	3.22531E-53
ALT-27 sq	0.000144422	3.4326E-06	42.07358813	1.73E-144
|Toa-Tin|	0.001662426	0.000713893	2.328676054	0.020404232

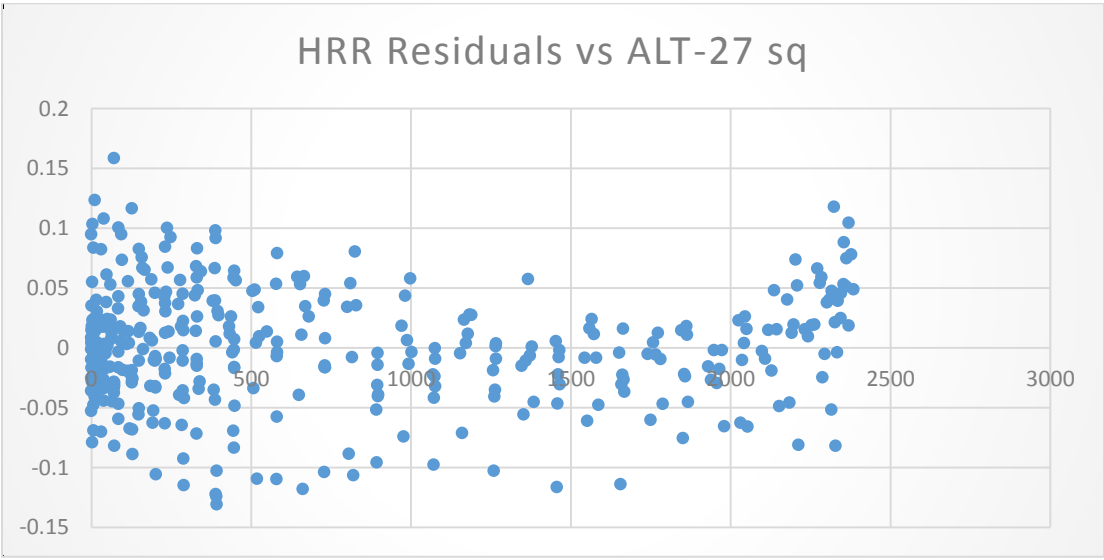

Figure 4.9 HRR versus altitude and Toa – statistical results

Another HRR regression enlists solar radiation with outdoor air temperature. As discussed earlier, both variables require linear transformation to handle V-shaped conduction and U-curve Et effects (vertex at 120 Btu/hr-sq,ft):

$$\boldsymbol{HRR} = b_0 + b_1 |T_{oa} - Tin| + b_2 (Et - 120)^2 + error \qquad (4.7)$$

HRR = Heat removal rate
b_0 = intercept or offset for zero inputs where $Toa{=}Tin$ and $Et{=}120$ units
b_1 $|T_{oa} - Tin|$ = partial slope factor acting on outdoor air temperature
b_2 (***Et***-*120*)^2 = partial slope coefficient applied with solar radiation
$error$ = predicted HRR – actual HRR.

While this Et-Toa model enjoys a bit less Rsq of 0.79 and somewhat greater SE of 0.058 closer to 30% of average HRR, the p-values are excellent, and the residuals across radiation inputs show finer balance and randomness. Extrapolation to hotter climate seems safer with this Et-Toa variable set.

Regression Statistics	
Multiple R	0.88873333
R Square	0.789846932
Adjusted R Sq	0.788732062
Standard Error	0.057729809
Observations	380

	Coefficients	*Standard Error*	*t Stat*	*P-value*
Intercept	0.084567778	0.005621329	15.0440893	2.1427E-40
|Toa-Tin|	0.00466552	0.000824261	5.66024703	2.9975E-08
Et-120 sq	7.5236E-06	2.22869E-07	33.75787941	5.267E-116

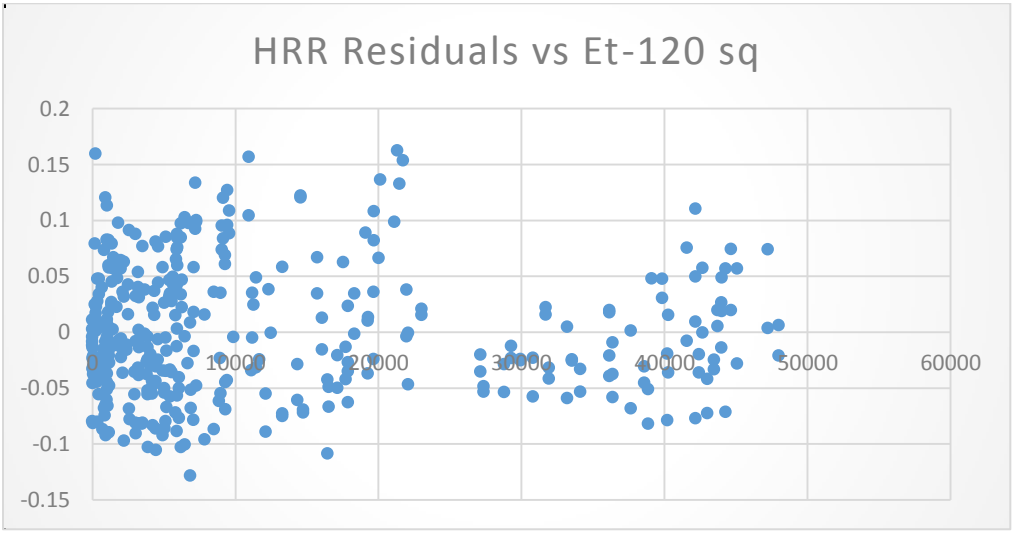

Figure 4.10 HRR versus solar radiation and Toa – statistical results

The HRR residuals across the Toa variable look quite suitable with only about 15 extra points overweighting the +0.1 level. This favored regression model's plot also appears below:

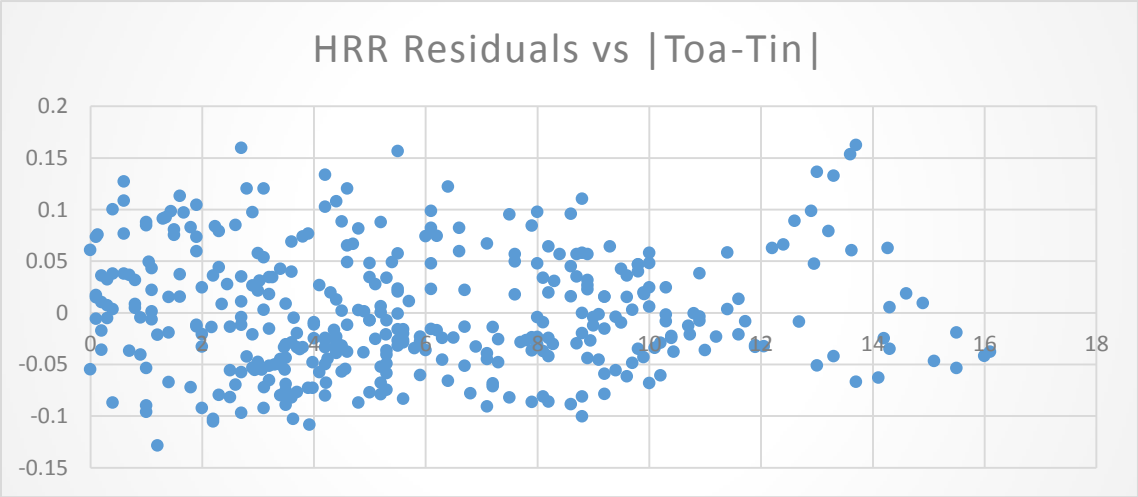

Figure 4.11 HRR residuals versus Toa and regression model plots

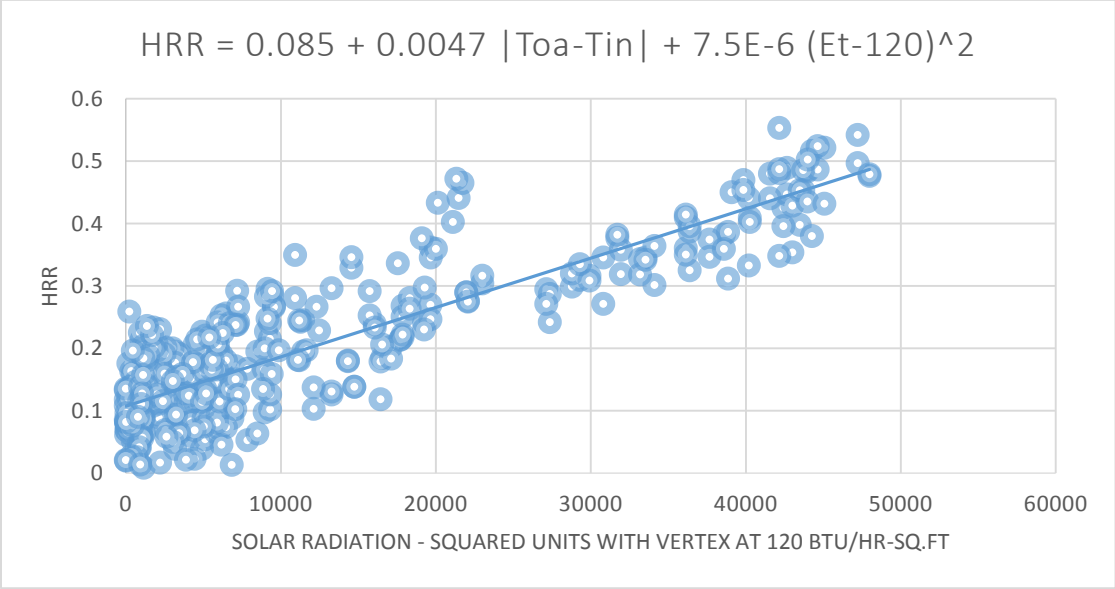

Figure 4.12 HRR residuals versus Toa and regression model plots

The heat removal rate model for our DSF calculations is selected as follows:

HRR = 0.085 + 0.0047 |Toa-Tin| + 7.5E-6 (Et-120)^2 Rsq 0.79, SE 0.058 < 30%

4.7.2 Light transmission single-variable regression

Light transmission ($\mathfrak{I}$) is the percentage of light passing through the DSF into the inner test chamber (office space). The level of total light hitting the south-facing window and the amount of light passing through the shading device and the two layers was recorded. Initially, the general candidate model for light transmission was as follows:

$$\boldsymbol{LT = b_0 + b_1 E_t + b_2 ALT + error} \quad (4.8)$$

$\boldsymbol{LT}$ = transmitted light as a dimensionless fraction of incident light
$\boldsymbol{E_t}$= solar radiation in Btu/hr-sq.ft-F
ALT = altitude (degrees) hinging on time of day
error = departure from actual LT data

Equation (4.8) has two coefficients serving as multipliers for environmental factors represented by b_1 for solar radiation ($\boldsymbol{E_t}$) and b_2 for altitude (***ALT***). In addition, coefficient ($\boldsymbol{b_0}$) represents light transmission when all the environmental factors are zero.

As noted earlier, the solar radiation ($\boldsymbol{E_t}$) is highly correlated with sun angle. Both variables cannot serve together distinctly in the same regression.

The first LT regression form enlists altitude as a single variable:

$$\boldsymbol{LT_{comp} = b_0 + b_1 ALT + error} \quad (4.9)$$

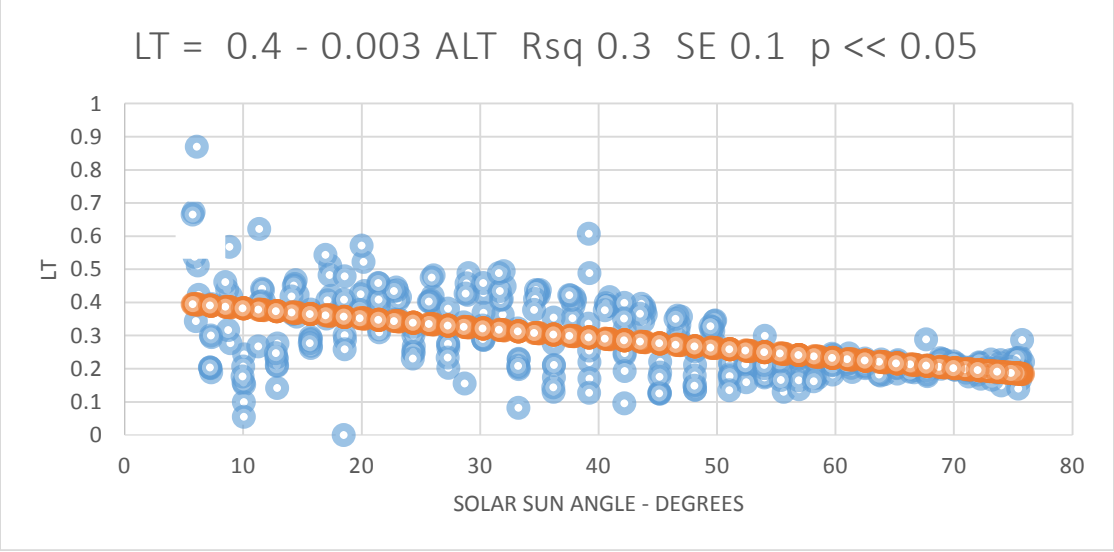

Figure 4.13 Light transmission against sun angle (Altitude) scatter plot

Linear fit characteristics weigh in at R_{sq} 0.32, SE 0.096 (+/-33% of mean LT).

Regression Statistics	
Multiple R	0.564394117
R Square	0.318540719
Adjusted R Square	0.316728327
Standard Error	0.096230834
Observations	378

Coefficient for sun angle amply passes the test of significance (p << 0.05).

	Coefficients	*Standard Error*	*t Stat*	*P-value*	*Lower 95%*
Intercept	0.411994788	0.011070585	37.21526831	3.977E-128	0.390226772
Altitude	0.003005482	0.000226703	-13.25734154	3.5217E-33	0.003451248

Residual plot below depicts a marked kink at 50 degrees altitude:

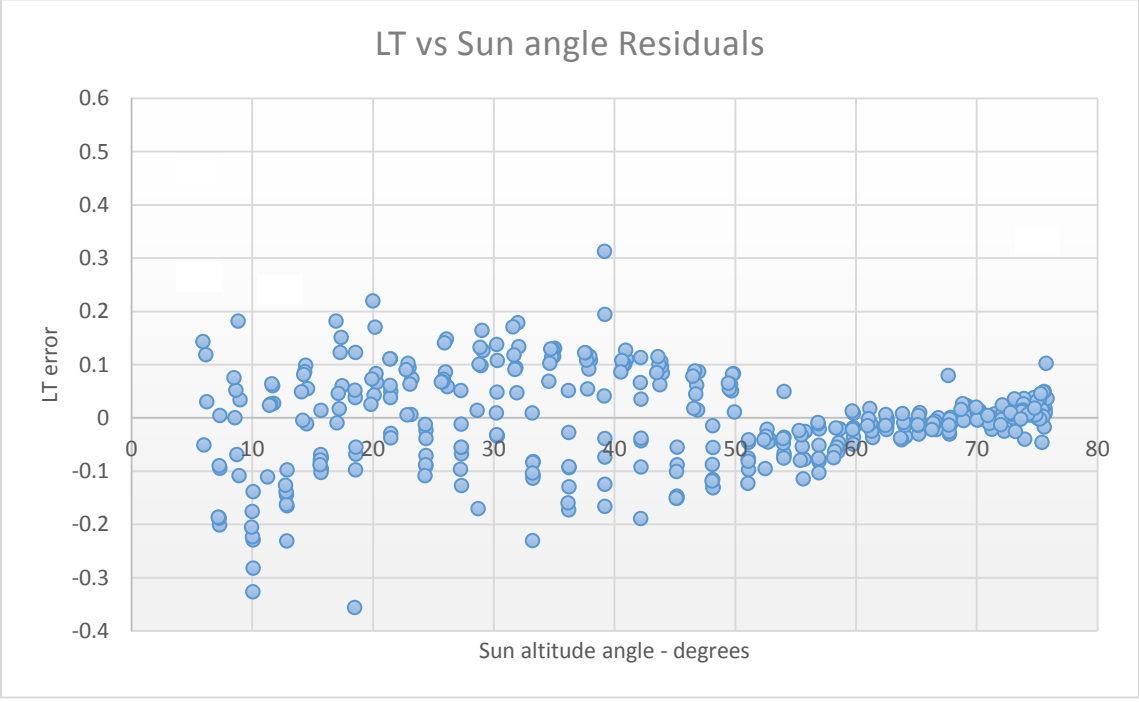

Figure 4.14 Light transmission against sun angle (Altitude) residual plot

The +/- 0.1 error band is exceeded by about 40 points both above and below for decently random error balance at sun angles under 50 degrees. However, notable over-prediction in this model arises for 50-60 degrees.

Another pattern of interest can be seen starting at 44 degrees: errors flip in +/- fashion for each angle sample up to 51 degrees. This discrepancy stems from morning versus afternoon readings logged similar altitudes.

The outdoor photometer was mounted on the DSF glass surface whose temperature (Tcg) varied from 66-110F as compared to an indoor sensor stabilized at 75F. LiCor devices exhibit temperature sensitivity of 0.15% per degree C. A +35F upswing converts to 20C, triggering a 3% error at full scale for the 100 Klux sensor – a 30-60% bias in the middle 5-10 Klux range. The LT with outdoor photometry corrected for temperature plots with a tighter appearance below:

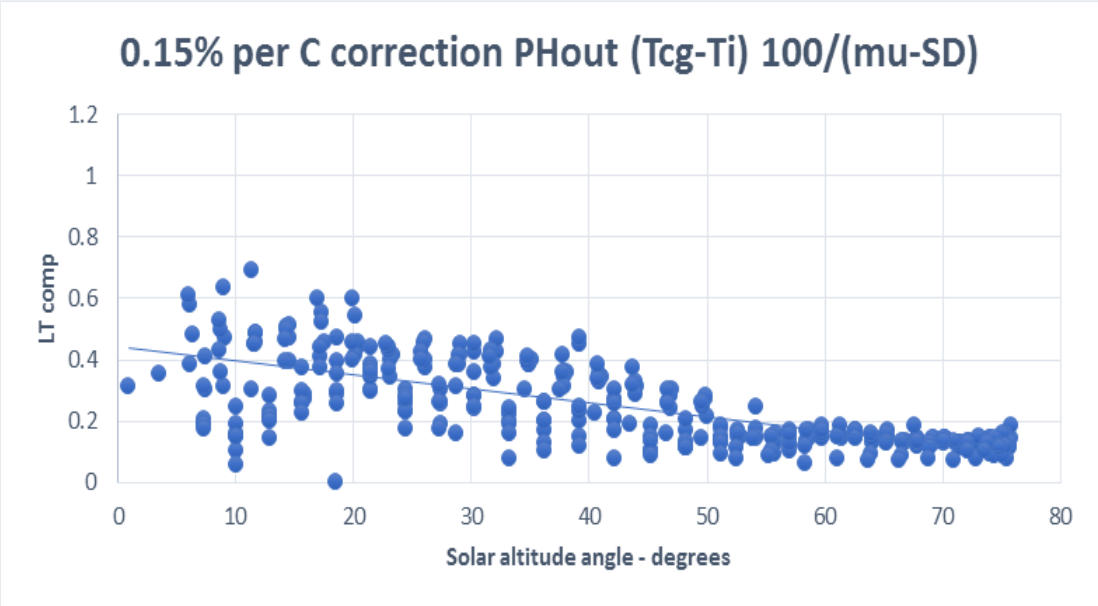

Figure 4.15 Compensated light transmission versus altitude scatter plot

Compensated light transmission against altitude plots the regression form:

$$\boldsymbol{LT_{comp} = b_0 + b_1\, Sun\ angle + error} \qquad (4.10)$$

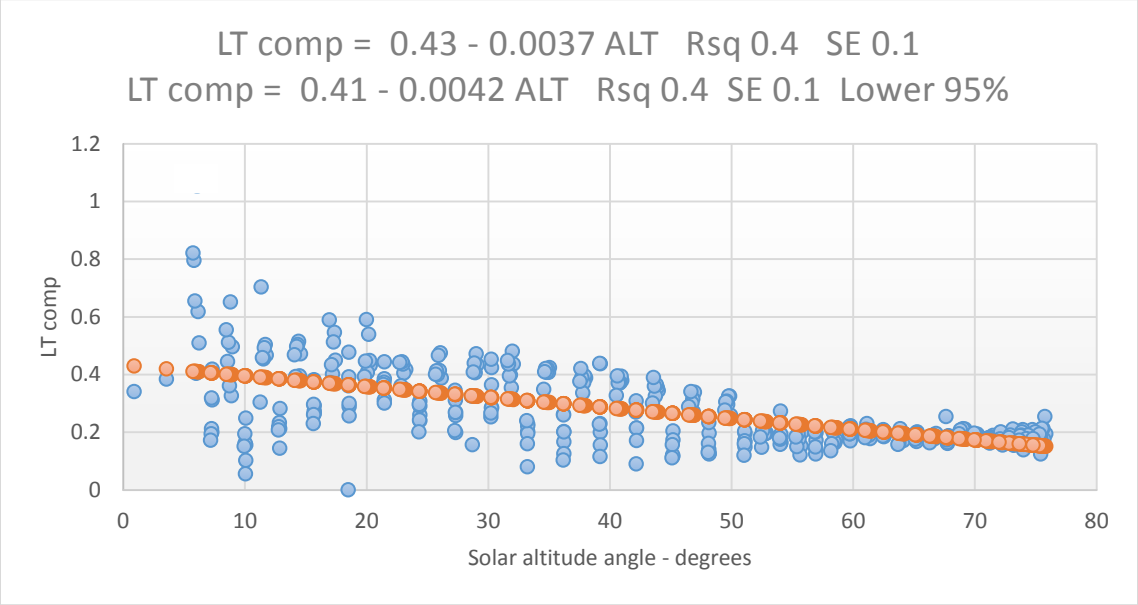

Figure 4.16 Corrected light transmission versus sun angle (Altitude) regression

Linear fit characteristics improve at R_{sq} 0.4, SE 0.1 (+/-37% mean LT comp).

Regression Statistics	
Multiple R	0.62148599
R Square	0.386244836
Adjusted R Square	0.384621145
Standard Error	0.10288841
Observations	380

Coefficient for altitude far better passes the significance test (p << 0.05).

	Coefficients	*Standard Error*	*t Stat*	*P-value*	*Lower 95%*
Intercept	0.432324492	0.011694863	36.96704214	1.358E-127	0.409329355
Altitude	0.003703434	0.000240118	-15.42338372	5.6074E-42	0.004175569

Residual plot depicts a less biased model despite classic low-end scatter:

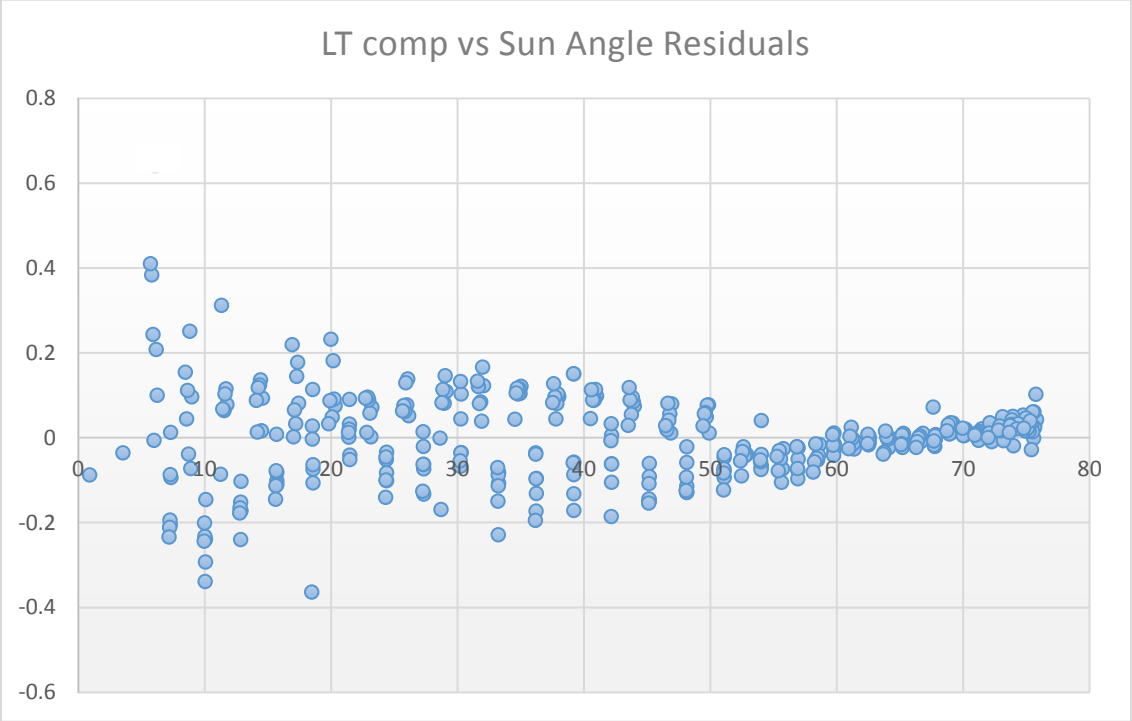

Figure 4.17 Corrected light transmission versus sun angle (Altitude) residual plot

The light transmission model for our DSF calculations is offered as follows:

$$LT_{comp} = 0.43 - 0.0037ALT \quad (4.11)$$

R_{sq} 0.4 SE 0.1 (+/- 37% mean LT) p << 0.05

4.8 Testing for significance

Testing for significance has been used to quantify probabilities of imposing or randomly compiling a linear regression when none may actually exist. Commonly used "t-testing" has been crafted to gauge the departure of actual data from those predicted by linear regression. These departures, called "standard errors", are then accumulated across the range of independent variables, and the t-test assigns likelihood that Y might be completely independent of X. For visually vague datasets, numerical indication is helpful in ruling out the possibility of zero beta coefficients.

For instance, a probability (p-value) can be assigned to the scenario that heat removal rate (***HRR***) or light transmission ($\mathfrak{I}$) might be totally unrelated to sun angle. T-testing quantitatively addresses the concern of how likely that a measured phenomenon may not be cast as a linear relationship.

A t-test "p-value" of 0.50 would suggest a 50% chance that a proposed regression – even one that seems to traverse the middle – may not apply to a selected level of confidence of 95%. Alternatively, p < 0.05 denotes a less than 5% chance of a non-existent linear relationship where Y is totally and randomly detached from X. For our two chosen models, p << 1 ppm!

These t-tests for significance have served as a formal check regarding the validity of our regression variable choices and their linear transformations.

4.9 Final model validations

The comprehensive tests for linearity, variable independence, significance, and randomly balanced residuals have favored these following regression options:

(1) the radiation and temperature inputs for the HRR model, and
(2) the altitude *alone* for LT corrected regarding the Tcg-Tin temperature swings incurred by the outdoor glass-mounted photometer.

$$\boldsymbol{HRR = 0.085 + 0.0047\ |Toa\text{-}Tin| + 7.5E\text{-}6\ (Et\text{-}120)\text{^}2} \quad (4.12)$$

Rsq 0.79, SE 0.058 (< +/- 30% mean HRR) p << 0.05

$$\boldsymbol{LT_{comp} = 0.43 - 0.0037\ ALT} \quad (4.13)$$

R_{sq} 0.4, SE 0.1 (+/- 37% mean LT) p << 0.05

Next was tabulating predicted values from each regression against actual data from another time series. Effort to quantify RMS error between model and actual used a square root of [sum (Y – y)^2 / n]. Validation standard errors (SE') were then checked to lie within each regression model's SE.

4.9.1 Validating HRR against outdoor air temperature and solar radiation

One sunny day on 7/9/2015 following the opening week of the July 2015 dataset was used to validate the HRR regression model.

$$HRR = 0.085 + 0.0047\ |Toa\text{-}Tin| + 7.5E\text{-}6\ (Et\text{-}120)^2 \quad (4.12)$$

Rsq 0.79, SE 0.058 (< +/- 30% mean HRR) p << 0.05

The 7/9 test set included 54 points for 0645-2000. The standard error SE of prediction minus actual was SE 0.04 for 22% of mean HRR << 30% to pass.

Validation values for Predicted HRR vs. Radiation, Error, and Error Squared are tabulated below:

Table 4.3 Validation values for Predicted HRR vs. Radiation

Predict	Et-120 sq	Predict-actual	E square
0.15085	2899	-0.02734	0.00075
0.14579	2445	-0.03649	0.00133
0.13747	1977	-0.04431	0.00196
0.12784	1080	-0.03965	0.00157
0.11376	423	-0.03559	0.00127
0.10627	50	-0.00572	0.00003
0.10132	28	0.02116	0.00045
0.09690	120	0.01052	0.00011
0.09583	295	0.01282	0.00016
0.10223	1062	0.02050	0.00042
0.10926	1990	0.02928	0.00086
0.11697	2752	0.04016	0.00161
0.12670	2952	0.01282	0.00016
0.13241	3442	0.01643	0.00027
0.14193	3652	-0.00189	0.00000
0.15307	4394	-0.00231	0.00001
0.17547	5567	-0.00315	0.00001
0.18995	8051	0.00157	0.00000
0.20123	9857	-0.00140	0.00000
0.22291	10797	-0.01340	0.00018
0.22887	13249	-0.02076	0.00043
0.25085	13794	-0.01740	0.00030

0.29605	16473	-0.03230	0.00104
0.30610	22123	-0.05315	0.00283
Predict	Et-120 sq	Predict-actual	E square
0.33515	24028	-0.04347	0.00189
0.34560	27526	-0.05536	0.00307
0.35579	29044	-0.04864	0.00237
0.35208	30152	-0.06628	0.00439
0.34897	29344	-0.03953	0.00156
0.33895	28428	0.00290	0.00001
0.33511	27468	0.00307	0.00001
0.31904	26830	0.05753	0.00331
0.28569	24374	0.04137	0.00171
0.26921	19866	0.03286	0.00108
0.25012	17481	0.01929	0.00037
0.24066	15060	0.05780	0.00334
0.21453	13235	0.05107	0.00261
0.17756	10126	0.02093	0.00044
0.17365	4947	0.01187	0.00014
0.16883	4112	0.02568	0.00066
0.16057	3470	0.03594	0.00129
0.16056	2618	0.03911	0.00153
0.15067	2053	0.03417	0.00117
0.15803	1674	0.06680	0.00446
0.15239	1403	0.07505	0.00563
0.14426	400	0.06653	0.00443
0.13985	381	0.06138	0.00377
0.14099	295	0.06910	0.00478
0.13702	9	0.05799	0.00336
0.13569	543	0.04714	0.00222
0.13359	1432	0.05536	0.00306
0.14147	1653	0.06007	0.00361
0.14707	3770	0.03737	0.00140
0.19300	5018	0.06264	0.00392

sum Esq	0.08735
Esq/n	0.00162
SE	0.04022
ave HRR	22%

HRR Error plot below (vs. Et-120 sq), depicts an across-the-board balance with 23 of the 54 errors at zero or less for a slight over-prediction bias.

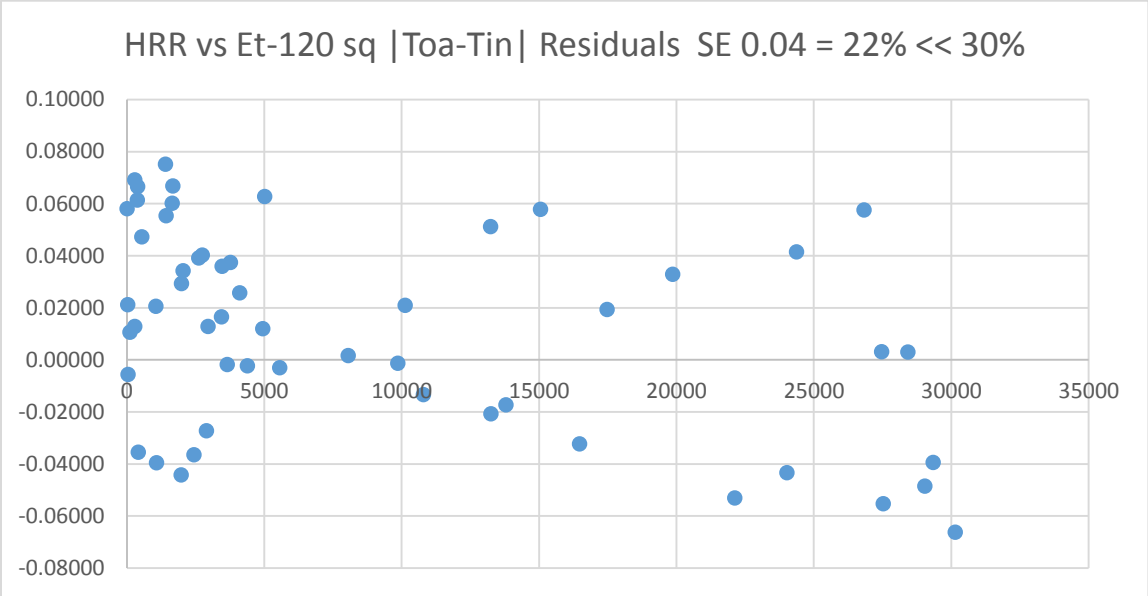

Figure 4.18 Validation heat removal rate residual error plot

4.9.2 Validating LT against altitude

One sunny day 7/9/2015 following the opening week of July dataset was used to validate the LT regression model. The outdoor photometer was compensated for the hot glass temperature at the device's mounting site.

$$\boldsymbol{LT_{comp} = 0.43 - 0.0037\, ALT} \qquad (4.13)$$

R_{sq} 0.4, SE 0.1 (+/- 37% mean LT) p << 0.05

The 7/9 test set included 54 points for 0645-2000. The standard error SE of prediction minus actual was SE 0.097 for 45% of mean LT of 0.22 for a borderline validation. LT model error consistently over-predicted here, too, especially in late afternoon and evening. It may be wise to limit LT model usage to 5pm as office work finishes for the day (41-point dataset). Here, standard error SE of prediction minus actual was SE 0.05 for 20% of mean LT to pass.

Validation values for Predicted LT vs Altitude, Error and Error Squared are tabulated below (n=41 for 5pm cutoff):

Table 4.4 Validation values for Predicted LT vs Altitude

Predict LT	ALT	Predict-Actual	E square
0.409518519	5.53	-0.023542421	2.72682E-05
0.399333333	8.28	-0.005221899	0.01736579
0.389	11.07	-0.131779324	5.24769E-07
0.378518519	13.9	-0.00072441	0.000212427
0.367925926	16.76	-0.014574865	0.000227634
0.357259259	19.64	-0.015087547	0.000157632
0.346444444	22.56	-0.012555166	2.31821E-05
0.335592593	25.49	0.004814778	0.00106744
0.324666667	28.44	-0.032671702	0.001086158
0.313666667	31.41	-0.032956907	0.001600784
0.302666667	34.38	-0.040009803	0.000628025
0.291592593	37.37	-0.025060432	0.000668456
0.280555556	40.35	-0.02585451	2.98723E-06
0.269518519	43.33	0.001728361	5.16614E-05
0.258481481	46.31	-0.007187587	0.001180536
0.247518519	49.27	0.034358923	0.004995479
0.23662963	52.21	0.070678699	0.004883883
0.225888889	55.11	0.069884781	0.003650547
0.215296296	57.97	0.060419753	0.001739487
0.204925926	60.77	0.041707153	0.000855818
0.194888889	63.48	0.029254367	0.000304709
0.185259259	66.08	0.01745593	9.33594E-05
0.176259259	68.51	0.009662265	4.69625E-06
0.168148148	70.7	0.002167084	3.49306E-05
0.161185185	72.58	-0.005910214	0.000118693
0.155888889	74.01	-0.010894625	0.000202954
0.152666667	74.88	-0.014246183	0.000281712
0.151888889	75.09	-0.016784265	9.41166E-05
0.153703704	74.6	-0.009701373	0.000614585
0.157851852	73.48	-0.024790828	0.000306336
0.163925926	71.84	-0.01750247	1.81799E-05
0.171407407	69.82	-0.00426379	0.000124024
0.179925926	67.52	0.011136602	0.000301067
0.189185185	65.02	0.017351286	0.000473772

0.199	62.37	0.021766304	0.001494977
0.209185185	59.62	0.038664931	0.002902999
0.219666667	56.79	0.053879483	0.006215254
0.230333333	53.91	0.078836882	0.00625714
0.241185185	50.98	0.079102087	0.007481383
0.252074074	48.04	0.08649499	0.008833488
0.263074074	45.07	0.09398664	0.022497996

Sum Esq	**0.099082091**
Esq / n	0.002416636
SE	0.049159296
	< 0.103
	OFF 5pm
	n=41 pts

The LT model error plot below, though, shows over-prediction for altitudes between 45-55 degrees. Steepening the slope a bit to -0.004 may offer a modest countermeasure to avoid LT model exaggeration in cost savings.

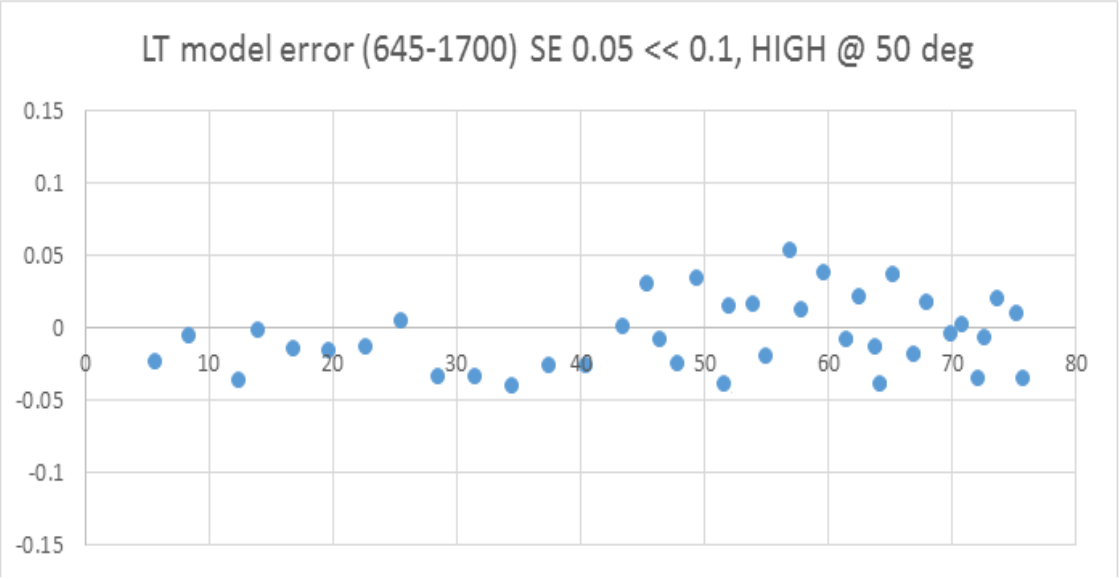

Figure 4.19 Validation light transmission residual error plot

4.10 Conclusion

This concluding section recaps the main line of reasoning in support of the selected regression models capturing DSF thermal and light performance. Ordinary least squares (OLS) linear regression must fulfill basic dictates: linearity, independent set of input variables of significance, and randomly balanced errors from the zero-error line. The HRR variable set required linear transformation to embody bidirectional conduction and U-curve angled-SHGC effects. Better fitting options with lower standard errors were then validated with a second dataset.

Both the fractional heat removal rate (HRR) and percent light transmission (LT) models were formed from measurements logged during the first week of July 2015. This chosen week featured sunny, hot days to ease model extrapolation to hot, sunny climate of the city of Riyadh, Saudi Arabia. Nearly 400 data points (n=378) were logged for seven days from 0645-2000 Eastern Time.

Variables. Inputs for the HRR and LT outputs were outdoor air temperature ($\boldsymbol{T_{oa}}$ degrees F), solar radiation ($\boldsymbol{E_t}$ in W/sq.m), and solar altitude/azimuth (degrees). These were considered for their direct impacts toward heat and light engaging the southern-facing DSF. Altitude more fully captured sun position with its explicit vertical angle as well as the implied timing. Azimuth, on the other hand, is strictly horizontal in its timing sweep.

Linearity. The advantage of Toa was its direct impact on the conduction portion of the DSF's heat balance. However, the nonlinear action of cool-morning conduction inward and hot afternoon conduction outward needed transforming to clone this V-shaped action. |Toa-Tin| was used.

Solar radiation ($\boldsymbol{E_t}$) was nonlinear when accounting for the SHGC value dependency on altitude. This U-curve effect was captured using the Et-transformed variable (Et-120)^2 with a vertex at 120 Btu/hr-sq.ft-F for $\boldsymbol{HRR}$.

For light transmission, all scatter plots displayed a nonlinear "kink" approaching 50 degrees altitude, an issue needing further treatment to meet OLS standards.

Independence. Radiation and altitude could not decouple from the ultra-high correlation seen in the R-squared statistic of 0.93 ($\boldsymbol{R_{sq}}$). This signaled altitude and radiation virtually capturing or expressing 93% of each other. At this point, $\boldsymbol{E_t}$ was favored for HRR extrapolation to hotter climate while LT would use altitude since radiation includes more than just visible light.

Significance. All variables, including those transformed for the HRR model, passed the t-test perfectly. Every chosen linear slope coefficient yielded a p-value under one part in a million (<< 1 ppm) signaling less than 0.0001% chance of any random variable imposter here. Typical p-value thresholds of 0.05 denote 19:1 odds of an improper variable choice.

Residuals. After assessing OLS demands for linearity, independence and significance, model prediction errors from actual data, called "residuals", were plotted versus each input. For both HRR variable transformations, 130 of 380 points (one-third as normal distribution expects) were noted beyond the +/- 0.05 error band, with about 70 above and 55-60 below. Such balance rules out any severe non-normal distribution bias upward or downward for both **($\boldsymbol{E_t}$-120)^2** and **|Toa-Tin|** transformations.

For LT versus angle (chosen over $\boldsymbol{E_t}$ that embodies more than visible light), residuals revealed sensor scatter at low-altitude dimness typical when read far below the photometer's full scale. Low-horizon scatter impact was countered by limiting LT simulation use from 0645-1645 for 5pm cutoff. Another concern was notable over-prediction residuals at higher altitudes. Importantly, LiCor devices are somewhat temperature sensitive, and the outdoor device was mounted on the outer skin where glass temperature would range from 66-110F. Using the 0.15% per C specification, outdoor photometry was corrected to display better linearity and residuals.

The following regression models were selected for the overall optimal fit (high R-squared), low standard error (SE) and extrapolation to hot climate:

$$\boldsymbol{HRR = 0.085 + 0.0047\ |Toa\text{-}Tin| + 7.5E\text{-}6\ (Et\text{-}120)^2} \quad (4.12)$$

Rsq 0.79, SE 0.058 (< +/- 30% mean HRR) p << 0.05

$$\boldsymbol{LT_{comp} = 0.43 - 0.0037\ ALT} \quad (4.13)$$

R_{sq} 0.4 SE 0.1 (+/- 37% mean LT) p << 0.05

The heat removal rate model adds 0.047 to HRR for every 10 difference in outdoor and indoor air temperature. HRR rises 0.075 for an Et departure of 100 from 120 Btu/hr-sq.ft in solar radiation. An Et level of 320 units results in a radiant contribution of 0.30 to HRR.

The compensated LT model reduces light transmission by ten percentage points for every 27 degrees in altitude, leaving about 0.13 LT at an 81-degree altitude angle.

Validation. Used 7/9/2015 data for sunny day one week after original set. HRR tapped n=54 points, 645-2000 Eastern Time. LT ran 645-1645 ET (n=41).

The validation standard error for the HRR test run was SE 0.04 for 22% of mean HRR, less than the model's original 30% from the preceding week.

$$HRR = 0.085 + 0.0047\ |Toa\text{-}Tin| + 7.5E\text{-}6\ (Et\text{-}120)^{\wedge}2 \qquad (4.12)$$

validated SE 0.04 = 22% << 30% mean HRR for 645-2000 ET (n=54)

Validation standard error for LT, corrected for a hot, outer glass-mounted photometer logging n=41 points for 645-1645 ET, was 0.05 (20% mean LT), well within the model's original SE = 0.10 for 645-2000 ET a week earlier!

$$LT = 0.43 - 0.0037\ ALT \qquad (4.13)$$

validated SE 0.05 << 0.1 for 645-1645 ET (n=41)

The next section in Chapter 5 will describe the usage of these regression model results to simulate DSF performance in eQUEST for estimating any potential cost savings offered by the DSF configuration.

5. Chapter Five Building Simulation

5.1 Building simulation usage

This chapter discusses the building energy simulation establishing a base-case electrical usage for a standard window system of an office building. The simulation can predict building energy patterns for planning purposes. For this study, the energy simulation program eQUEST was used to simulate the performance of a hypothetical office building in the city of Riyadh, Saudi Arabia. Next, the heat removal rate regression was extrapolated using Riyadh weather data to compute the energy saved for an individual double skin façade window fixture facing south.

In the Blacksburg experiment, the heat removal rate for the double skin façade system was significantly influenced by outdoor air temperature (Toa), solar radiation (Et), and sun angle (ALT). Correlation findings of the regression analysis indicated sun angle and solar radiation to be collinear. Thus, solar radiation was selected along with Toa for heat removal rate, and sun angle was assigned for light transmission. Regression models detailed in Chapter 4 were used to estimate DSF performance in the hot, arid climate of Riyadh.

In general, various buildings may require different minimum energy usage to attain comfort levels. The focus of every building design is to provide comfortable living conditions and excellent working environments that adapt to the site's immediate surroundings. Behavior and performance of a building depend on the dimensions, orientation, materials, components, and systems (windows, lighting, HVAC, etc.) specified in the design.

The growing number of variables considered for building energy usage in recent years has made it difficult to predict the operational energy performance of buildings. Computer software programs like eQUEST offer fairly accurate forecasts of building energy usage (Crawley et al., 2008). Thermal behavior, lighting, ventilation and other phenomena that occur in a facility modeled by energy simulation tools influence environmental and energy performance. When simulating energy flows, several factors such as internal heat generation and storage, building materials, systems, and climatic factors are treated (Hirsch, 2006). Thus, building energy simulation

serves as a powerful tool for assessing the energy performance effects of construction material and architectural design choices. It can further evaluate and quantify complex design issues, such as opting for a DSF. Energy simulation is useful for designers in developing effective building specifications by analyzing dynamic energy functionality (Rallapalli, 2010). These tools offer multiple investigation methods with visualization features for all design phases from conceptual to schematic to detailed design.

5.2 Introduction to eQUEST/DOE-2

eQUEST® has been a long-standing tool for analyzing building energy using a menu of interfaces to design a structure, compute and tabulate its energy efficiency, and to graphically display the results (Hirsch, 2006). eQUEST also facilitates using the enhanced DOE-2 derived program to develop energy simulations for buildings. In the building creation wizard, a model is specified completing a series of steps, making it possible to

compute hourly building conditions given the windows, glazing, people, electrical outlet loads, ventilation settings and other inputs (eQUEST, 2010). This program can run multiple simulations at the same time with results and charts viewed side-by-side. Moreover, estimates of energy costs, control of daylight and evening lighting systems, and activation of efficiency measures can be implemented and analyzed accordingly.

5.3 Advantages using eQUEST

eQUEST was favored for this study over other simulation programs, such as Energy Plus, mainly for its availability at no cost, courtesy of the State of California's Energy Design Resources program. However, eQUEST has some limitations. The advantages and limitations of eQUEST are as follows.

5.3.1 Integrated energy design

Using other simulation programs, such as Energy Plus, can be complicated and require training. On the other hand, eQUEST provides a free, easy-to-use, comprehensive analysis tool for addressing all design issues such as window type, lighting, architectural properties, mechanical system, etc. This detailed analysis does not require any extensive simulation or modeling experience.

5.3.2 Engine in eQUEST

The engine used in eQUEST is DOE-2, a widely recognized energy analysis program for buildings when U.S. concern emerged for understanding and optimizing the energy needs of buildings. The simulation engine is derived from the latest version of DOE-2 (eQUEST, 2010). In addition, it extends and expands the capabilities of DOE-2 to include dynamic/intelligent defaults, interactive operation, and other fixes to legacy shortcomings in DOE-2. Details of this study's simulation model will follow later in this chapter.

5.3.3 Limitations

One key limitation of eQUEST simulation is that it does not allow reliable direct import of CAD geometries into the system. Dependency on eQUEST also inherits all of its limitations (Jarić et al., 2013). Value analysis for a few database cities is possible in the program, but requires customization of parameters for other sites. For this study, a detailed DOE-2 yearly weather file of hourly data for Riyadh, Saudi Arabia was imported into eQUEST. Finally, since the program's vast documentation was unwieldy and printed in legacy typewriter font from the 1980s, this obscured any practical way to directly import our DSF regression models exclusively for the south face.

5.4 Reason for selecting eQUEST for the simulation

Though inconvenient for simulating DSF performance directly, eQUEST still offered a viable base-case usage model for the single-skin façade (SSF). For this SSF case, the following steps were taken to simulate the base case for comparison with a double skin façade system:

5 4.1 Base case model creation steps

1) Specify site and location of the building in eQUEST.
2) Import weather file from DOE-2 website for Riyadh, Saudi Arabia.
3) Construct base case in eQUEST with building envelope construction, building footprint, exterior window details, exterior doors, daylight zoning, and activity area zoning. Occupancy scheduling was also set. Details of the building will be discussed later in this chapter.
4) Facility mechanical systems were detailed in eQUEST's creation wizard: HVAC system type, temperatures, air flows and fan schedules, cooling and heating equipment, water heating system, and lighting density.

5) Occupancy loads for different zones were set for general lighting, task lighting, and electrical outlet usage.
6) Utility charges were edited to reflect electricity prices in Riyadh, Saudi Arabia for estimating operation costs.
7) Finally, the simulation analyzed building performance for the base-case conventional window system in the hot, arid conditions of Riyadh.

The simulation provided details of the building performance in terms of the amount of electricity used for cooling and lighting inside the building, as well as the overall costs to operate and maintain comfort levels using the single layer window system (SSF) as the exterior façade. Base case results were tabulated monthly and tallied for segment and total annual costs.

5.4.2 Double skin regression models

As previously stated, no energy simulation programs feature the double skin façade as an option in its database to simulate such performance. Instead, the heat removed by a *sole* DSF unit using Riyadh weather data will be computed and multiplied by the number of windows (320) in the south façade of the simulated building. This will allow computing Btu/hr removal and the electrical load of cooling saved. In the Blacksburg test, a working relationship of the variables and their effects on the DSF heat removal rate was regressed. This double skin façade model was next extrapolated by inputting Riyadh's solar radiation and outdoor air temperature to compute heat removed. Electrical kWh saved were cast as a percentage the total energy used in the building and for A/C loads. Thermal and light performance models were regressed as follows.

1) ***HRR = 0.085 + 0.0047 |Toa-Tin| + 7.5E-6 (Et-120)^2*** (5.1)

HRR = heat removal rate as a fraction of incoming heat load.
T_{oa} = outdoor air temperature in Riyadh, degrees Fahrenheit.
T_{in} = indoor air temperature, degrees Fahrenheit.
Et = solar radiation, Btu/hr-ft²

2) ***LT* = 0.43 - 0.0037 *ALT*** (5.2)

LT = light transmission as a fraction of incoming light.
ALT = sun altitude, degrees

As previously detailed in the Chapter 4 analysis, the radiant heat removed is minimized at 120 Btu/hr-sq.ft for a U-shaped model, and heat no longer conducts with zero temperature difference across the window (Toa = Tin). Light transmission in the model drops by ten percentage points for every 27-degree rise in altitude. The diagram below depicts the transmission angle phenomenon:

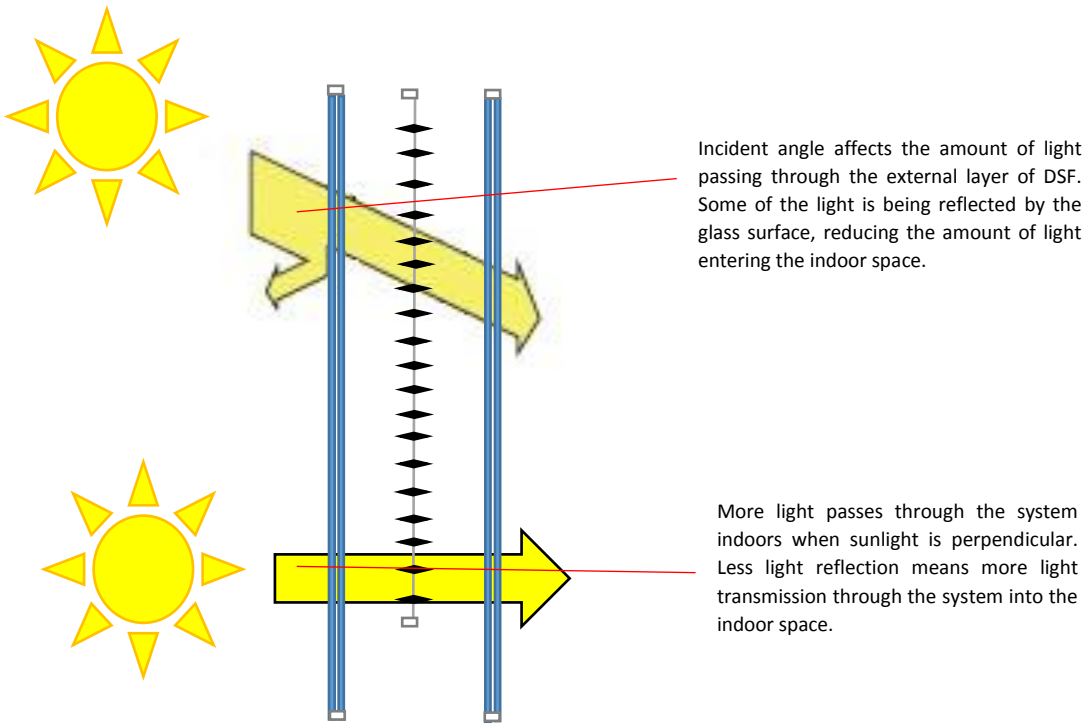

Figure 5.1 Light transmission vs. incident angle

5.5 Energy simulation analysis plan and assumptions

The eQUEST program using DOE-2.2, an advanced version of DOE-2, primarily performs reliable, detailed hourly simulations to support design and energy usage studies. The maximum analysis period is one year with three specific occupancy schedules and two seasons per year as entered in the schematic design wizard (Crawley et al., 2008). In addition, 667 long-term average weather files in different formats are available for use. For this research, a weather file for Riyadh, Saudi Arabia was compiled. The goal was to study the energy performance of an office building using the double skin façade in comparison to a conventional window system. One conventional simulation was performed as a base case, and then the weather file was applied to just one DSF window for its heat removal and eventual upscaling by 320 as a proxy for the entire south façade.

5.5.1 Heat transmission

There are two methods for calculating transmission of heat through opaque exterior surfaces (roofs): the delayed method using conduction transform functions and a quick method enlisting steady-state equations (Attia, 2011). The unit of heat flow is Btu/hr-ft^2, and eQUEST describes its two different methods as follows:

a) Delayed Method: lag time associated with the thermal envelope construction is simulated using transfer functions. It requires using both layer and construction commands; the material command is optional.

b) Quick Method: this requires only U-factors. It should be implemented only for steady-state heat transfer calculations (U.A.T).

For this study, the delayed method was used for the comparison since it best captures thermal storage effects of building mass and its furnishings. Importantly, our HRR regression model did not track any minor thermal storage effects of the small-sized glass, shade and air layers in the DSF.

5.6 Building description and modeling process

This section specifies the building used for simulating the base case for a standard single layer window system typically designed in office buildings.

5.6.1 Building description

As previously mentioned, a hypothetical office building was simulated in the city of Riyadh as a base case to compare the performance of the single layer window system against the double skin façade system to determine the amount of energy saved using DSF.

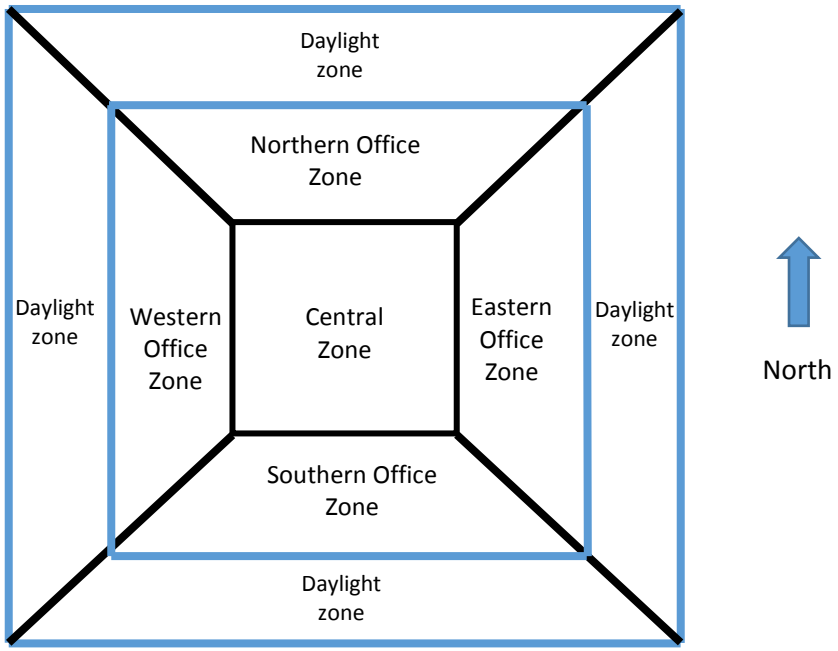

Figure 5.2 Building zone layout for simulation study

The building totals 250,000 square feet in floor space eight stories high (176.80 ft. x 176.80 ft). The day light zone is about 15 feet from each side of the building. The entrance is located at the southern face of the building, and all four façades have eight-foot tall, low-E, double-pane windows installed for all eight floors for the entire elevation. The exterior windows installed in the building are typical of office sites. More details follow later in this chapter.

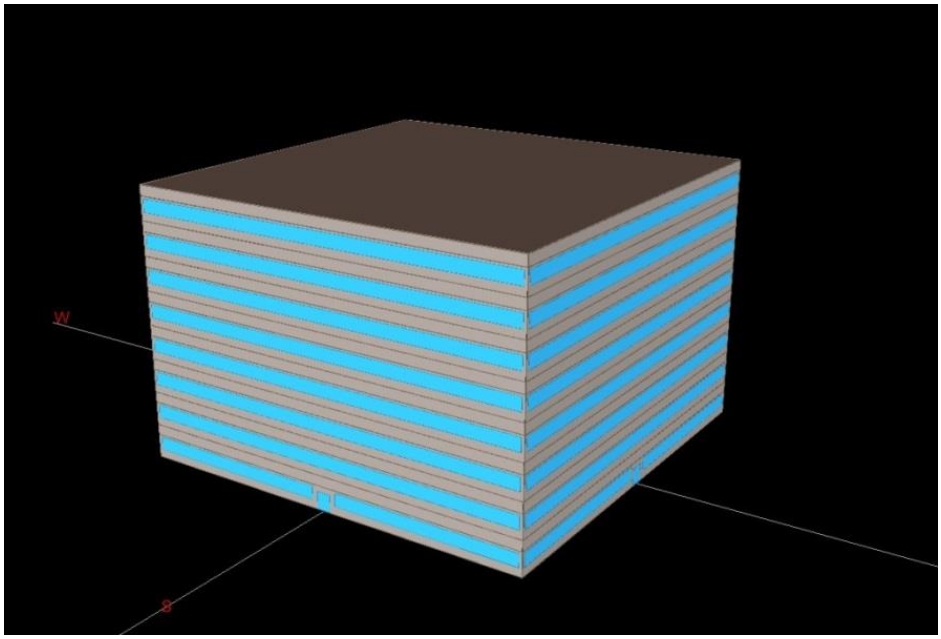

Figure 5.3 Office building 3D model in eQUEST.

Creating a building layout eased the study of facility performance and energy usage for various zones. Façade types see different heat loads depending on sun angle and incident solar radiation. Furthermore, depending on the time of day, temperature difference between the outdoor and indoor air fluctuates to alter the heat conduction through the building façade. The core zone of the building contains service areas and is not affected directly by solar radiation and the façade temperature difference. Partitioning the building into these five zones helped simulate the building properly and ensure that we have accurate results.

5.6.2 Riyadh weather and solar radiation

Riyadh is the capital city of Saudi Arabia, and it sees a hot, arid climate during the summer months due to its geographical location. The city is near the equator at 24.7 N latitude and 46.7 E longitude. Thus, the climate is very hot in summer, reaching 120F with low humidity. Rain and clouds are rare. Riyadh is known for its blinding sandstorms that can last for days.

Table 5.1 Climate data for the city of Riyadh according to the capital development organization, degrees in Fahrenheit, rain in inches.

	Jan	Feb	Mar	Apr	May	Jun	Jul	Aug	Sep	Oct	Nov	Dec
Record High	88.7	94.6	100	108	113	122	126	120	118	111	102	87.8
Average High	68.2	73.4	81.7	93.2	103	109	112	109	106	95	81.7	71.6
Rainfall	0.46	0.33	0.97	0.88	0.18	0	0	0	0	0.4	0.02	13
Humidity	47	38	34	28	17	11	8	4	10	11	14	51

Solar radiation in the city of Riyadh is supremely high. Measures of solar radiation here are among the extreme worldwide. Al-sanea Zedan and Al-ajlan (2004) have noted: "solar radiation in the city of Riyadh is intense and considered one of the highest in the world."

Solar radiation exerts the dominant heat gain on window façade systems in hot climates. When the admitted solar radiation (SHGC * Et) is high, the window allows a significant amount of heat to radiate through the glass. Glass without an insulating air gap also conducts heat. Thus, double-skin façade systems offer a viable solution to trim the amount of heat gained inside the office space by exhausting cavity air that intercepts heat flow. Mechanically ventilated systems can play a significant role in reducing the air conditioning needed to reach comfort levels inside the office area. The simulation calculated the amount of solar radiation striking the glass surface using the city of Riyadh's weather file as a SSF baseline example for evaluating the thermal performance of the double skin façade system.

5.7 Simulation steps

To perform simulation in eQUEST, specification of the building description, mechanical equipment and building materials were input to the program. The eQUEST schematic design wizard was used for this step. In this section, step-by-step details of the settings used for the building will be described.

5.7.1 Building footprint

The shape of the building was set for a square plan oriented north. The building footprint dimensions were 176.80 ft. x 176.80 ft. Each floor rose a total of 13 ft. with 9-foot, floor-to-ceiling clearance. Facility zoning patterns consisted of a building core in the center of the plan with an office-space perimeter 15 ft. deep from the building façade.

5.7.2 Building envelope construction

The building was constructed of metal steel framing with 3-inch exterior insulation (R-18). There was no basement, and the ground floor contacted the earth. Ground floor construction was a 6-inch concrete slab with a ceramic/stone tile finish. Building shell tightness was set for 0.038 cfm/ft^2.

5.7.3 Building interior construction

In this step, the building interior finishes and construction were specified. Walls were set to be frame walls with no insulation. Ceilings had a plaster finish, and the floors were laid in 4-inch concrete slabs with a ceramic/stone tile finish.

5.7.4 Exterior windows and doors

The exterior glass doors and windows determine the amount of heat gain into the building. For the simulation, a conventional type window system was installed to estimate performance for the building. The window was a double-pane, 1/2-inch argon-gapped, low-e, clear-glass window (e2) with 1/4-in. thick panes with no exterior shades or blinds. The building had no roof skylights, and the exterior doors were also made of the same glass.

The specifications of the window included width, height, sill height, area, blind types, glass properties, depth, overhangs, etc. As mentioned in prior chapters, the base case building used a typical window featured in office buildings to simulate its energy usage as a reference for the performance of the double skin façade system. The window used in the experimental

setup was then "exposed" to Riyadh weather for upscaling by 320 to represent the double skin façade system performance.

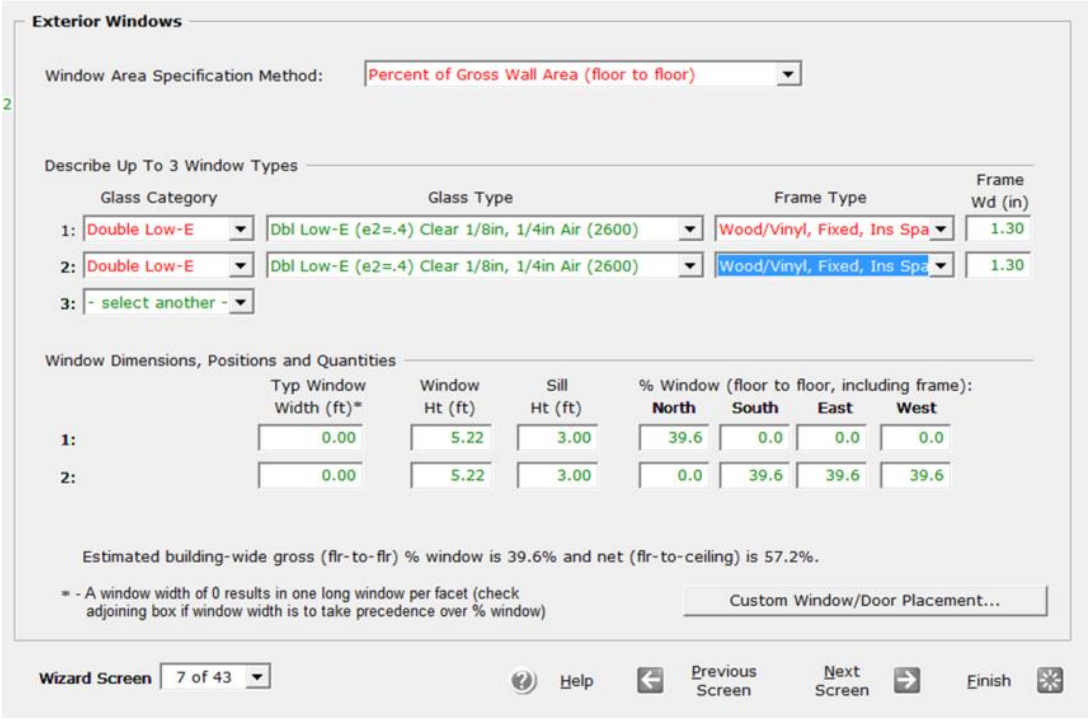

Figure 5.4 Window type selections for base case building using eQUEST 3.65

5.7.5 Activity areas allocation

The office building simulation using eQUEST comprised open-plan office spaces (45% of building area), private office spaces (25%), corridors (10%), lobby and office reception/waiting areas (5%), conference room (4%), copy room (2%), restrooms in the core of the facility (5%), and mechanical and electrical closets (4%).

5.7.6 Occupied loads by activity

To ensure an accurate building simulation, loads for different task types needed setting during office occupation. To attain comfort levels, the ASHRAE 90.1 standard was implemented to satisfy requirements for lighting in different areas in the facility. Table 5.2 lists area type and load.

Table 5.2 Occupied loads by activity

Area Type	Percent area (%)	Lighting (W/sq.ft)	Task light (W/sq.ft)	Plug loads (W/sq.ft)
Office (open plan)	45%	1.10	0.40	1.50
Office (private)	25%	1.10	0.0	1.50
Corridor	10%	0.50	0.0	0.20
Lobby	5%	1.30	0.0	0.50
Conference room	4%	1.30	0.0	1.00
Copy rooms	2%	1.50	0.0	0.20
Restrooms	5%	0.90	0.0	0.20
Mechanical rooms	4%	1.50	0.0	0.20

5.7.7 Unoccupied loads by activity

When the building is not occupied, the load levels drop since there is less need for lighting and equipment operation during this time. This schedule occurs after hours when the building is not occupied. Table 5.3 describes the unoccupied percentage of full load by area.

Table 5.3 Unoccupied loads by activity

Area Type	Percent area (%)	Lighting (%)	Task light (%)	Plug loads (%)
Office (public)	45%	2.0	0.0	20.0
Office (private)	25%	0.0	0.0	20.0
Corridor	10%	10.0	0.0	0.0
Lobby	5%	10.0	0.0	0.0
Conference room	4%	0.0	0.0	0.0
Copy rooms	2%	0.0	0.0	20.0
Restrooms	5%	0.0	0.0	0.0
Mechanical rooms	4%	0.0	0.0	20.0

5.7.8 Main schedule information

This function defines the operating schedule for the building that activates loads when the site is occupied during certain hours to compute lighting, task lights and equipment loads. One parameter that reflects uncertainty in the simulation called "occupancy schedule" (Rallapalli, 2010) varies the model input over time, e.g. seasonally, quarterly and hourly. It helps in modulating building loads as needed. Each modeling program focuses on improving the definitions of lighting schedules, occupancy schedules, thermostat-setting schedules, etc. for a more precise energy usage profile by applying realistic factors for HVAC system operation and its demand for electricity (Azar & Menassa, 2012). Inaccurate scheduling assumptions can still arise from unforeseen human behavior. Occupancy schedules can be simple or complex depending on the situation. It usually contains a fractional value varying from 0 to 1 for use as a multiplier depending on peak values or user-input design. For the building simulation, a simplified schedule for the office building was selected and applied.

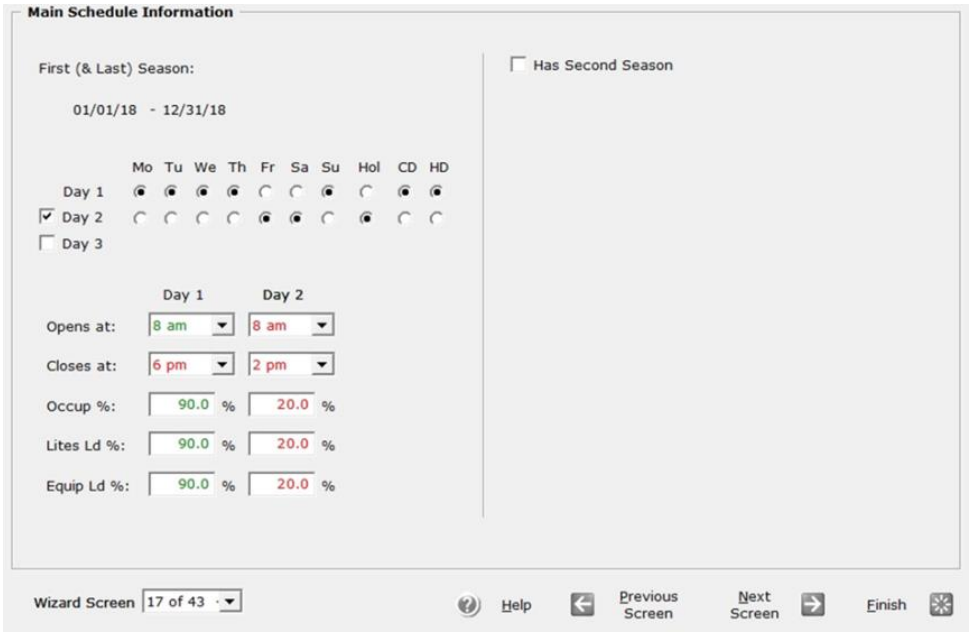

Figure 5.5 Main schedule of the simulated office building information using eQUEST 3.65

The goal was to keep the schedule accurate and simple to demonstrate daily HVAC and light usage. The office schedule was set for 8 am to 6 pm weekdays (Sunday-Thursday), and 8 am to 2 pm Friday with Saturday off. In eQUEST, the user can select occupancy options from default/simplified schedules to quite detailed hourly profiles. Occupied hours are identified by defining inputs for 'opens at' and 'closes at' while 'rest' is deemed as unoccupied hours. To form the occupancy schedule, three assumptions were applied.

1) Simplified schedules were selected to provide access to the Main & Alternate schedule screens within the wizard.
2) The Alternate activity area screen was selected for office buildings, and loads were specified on the activity area screen.
3) One season was selected for describing the operations of the building over the entire year.

5.7.9 HVAC system definitions and operating hours

Wide-ranging functions, supply sources and products comprise the control settings for the heating, ventilating and air conditioning systems (HVAC). eQUEST defines control as a start point, end point or regulator for all the HVAC functions. Our HVAC system was standard VAV with HW reheat.

A) Fan Power: this term refers to the electric power required to drive a fan per amount of air circulating through the fan. The fan power was set to 3.50 inches of H20 with auto-size flow.

B) Air Flow: this is the measurement of air flow through a reference area per minute. It varies with the change in temperature with a minimum of 0.50 cfm/ft². See Fig. 5.8 below.

To simulate the HVAC system's amount of energy needed for cooling and heating, a few following assumptions were applied.

1) The schematic HVAC wizard has two HVAC system types based on the building type and HVAC equipment type. Depending on the system type, the number of actual systems varies. On the screen, the appropriate coil type for heating and cooling sources were selected along with the preferred system type.

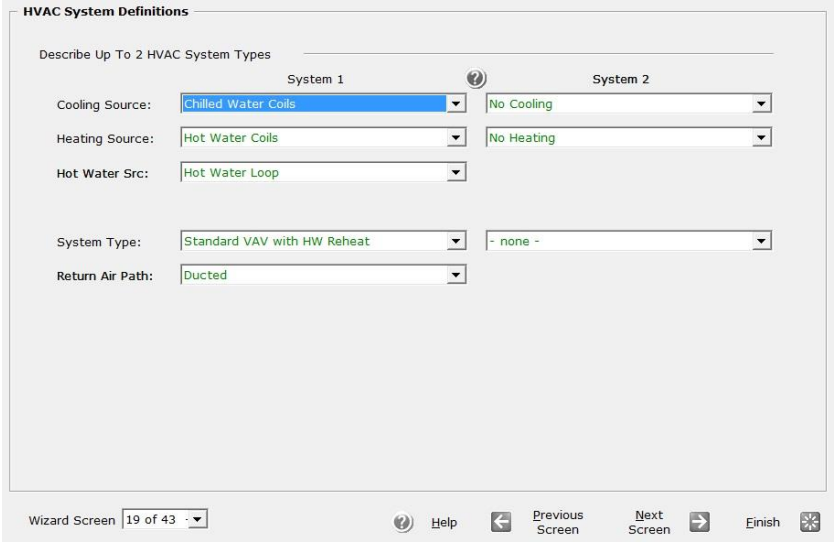

Figure 5.6 Type of HVAC system used in the building simulation using eQUEST 3.65

2) HVAC zone temperatures and air flow, thermostat set points, and design temperatures were also chosen for the simulation as follows:

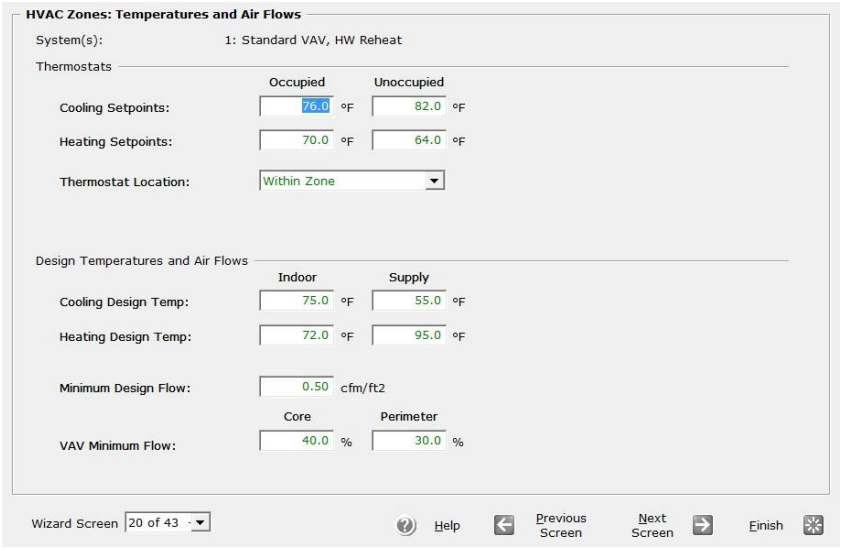

Figure 5.7 Type of HVAC system zone temperature setup using eQUEST 3.65

3) In the next step, packaged HVAC equipment is displayed only when such package is previously selected for one or both systems.

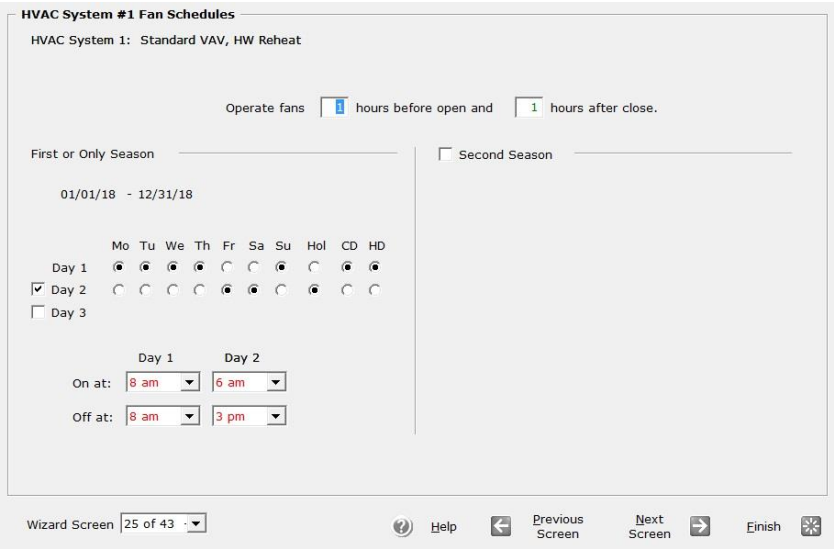

Figure 5.8 HVAC schedule setup using eQUEST 3.65

4) The next wizard screen specifies the HVAC system fans by selecting fan power, fan motor efficiency, fan type and flow.

5) In the next step, HVAC fan schedules were defined by specifying one-hour lead and lag times for fan operation. Negative inputs can also be used in this section.

5.7.10 Cooling and heating primary equipment

The chiller type used for our simulation was an electrical centrifugal motor (hermetically sealed) with a water-cooled condenser. Motor efficiency was set to 0.676 kW/ton and temperature to 44F°. For the heating system, an electric water-heater boiler with high efficiency was used with the temperature set to 180F°.

5.7.11 Lighting power density

Lighting power density refers to the watts of lighting per square foot for all the zones within the proposed building structure (W/sf). Two major terms in eQUEST define lighting power density: ambient lighting power density and actual hourly lighting power density (eQUEST, 2010). The former refers to the average peak ambient lighting power density, and the latter is the actual lighting density during any given hour. The ambient lighting power density does not include task lighting when calculated. Ballast energy is included even when not using 100% lighting. Control of ambient lighting may use daylight photo-sensors to adjust gross loads, but not task lighting.

Different building types need tailored levels of light. For our simulation, the office building had a 30% dimming strategy and design light level of 30 fc. To compute Ambient Lighting Power Density, defining activity area types is essential. Any change in the activity type will adjust the ambient lighting power density. For this simulation, the base-case office building in Riyadh, Saudi Arabia used the minimum amount of light per ASHRAE standards for the office space. Nevertheless, the facility's other public areas such as restrooms and hallways demand different light densities. There are nearly fifty options in eQUEST for selecting one or more activity type. This requires specifying building areas and their activity types. Certain parameters, including ventilation rates, occupant density loads, equipment density loads, etc., have default settings depending on its type of activity area. Actual hourly ambient lighting power density is calculated by multiplying the ambient lighting power density with the fractional value assigned by the lighting schedule for a particular zone at a given hour.

5.7.12 Utility rates

Utility rates set by a government regulatory agency allows a public utility to earn a specific rate of return based on asset values. Utilities may include electricity, water and gas. A list of utility providers and their rates based on building locations in common residential/commercial areas of California and in Seattle, Washington is given in eQUEST (Hirsch, 2009).

Users outside these jurisdictions create their own utility rate descriptions using the predefined syntax and format of DOE-2's Building Description Language (BDL). Such descriptions are saved in text-file format in eQUEST.

Table 5.4 Electricity prices in Saudi Arabia provided by the Saudi Electric Company

Slab in KWh	Residential Tariff in Halala/KWh	Commercial Tariff in Halala /KWh	Government Tariff in Halala /KWh	Industrial Tariff in Halala /KWh
1001 -2000	5	5	5	12
2001-3000	10	10	10	12
3001-4000	10	10	10	12
4001-5000	12	12	12	12
5001-6000	12	12	12	12
6001-7000	15	15	15	12
7001-8000	20	20	20	12
8001-9000	22	22	22	12
9001-10000	24	24	24	12
Over 10000	26	26	26	12

For the building simulation, rates for electricity in Saudi Arabia were used. Electricity in Saudi Arabia is provided only by the Saudi Electric Company, owned principally by the government and supported by Saudi Aramco. Saudi utility rates are low compared to other regions in the Middle East. Table 5.4 lists the bulk rates for different building types. For our simulation, the commercial tariff was applied in Saudi Riyal currency.

5.8 Energy simulation

eQUEST computes the total annual energy used in the building and presents monthly energy usage and costs by segment. Energy simulation results help compare window system performance in terms of energy usage and costs to see how much the double skin façade system can improve energy efficiency for potential cost savings.

5.8.1 Base case single-layer window office building energy performance

The building performance of the base case model estimated 100-200 kWh of monthly energy needed for space cooling seen in dark blue at bar top. Peak usage reflects the mechanical air conditioning needed for comfort levels in hot summer months. Ambient area lighting usage of 70-80 kWh monthly is depicted in yellow at bar bottom. Below in Figure 5.10 is the building's comprehensive energy consumption profile.

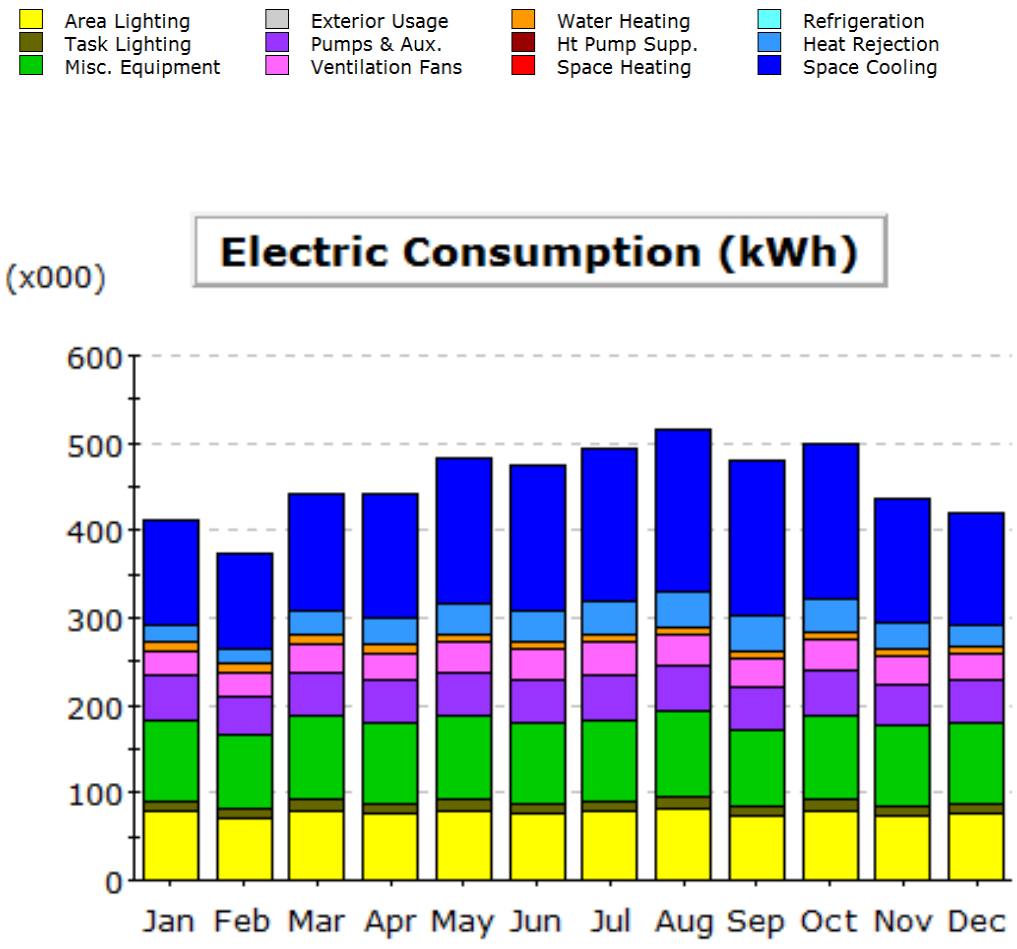

Figure 5.9 Annual energy consumption in base case model according to eQUEST program

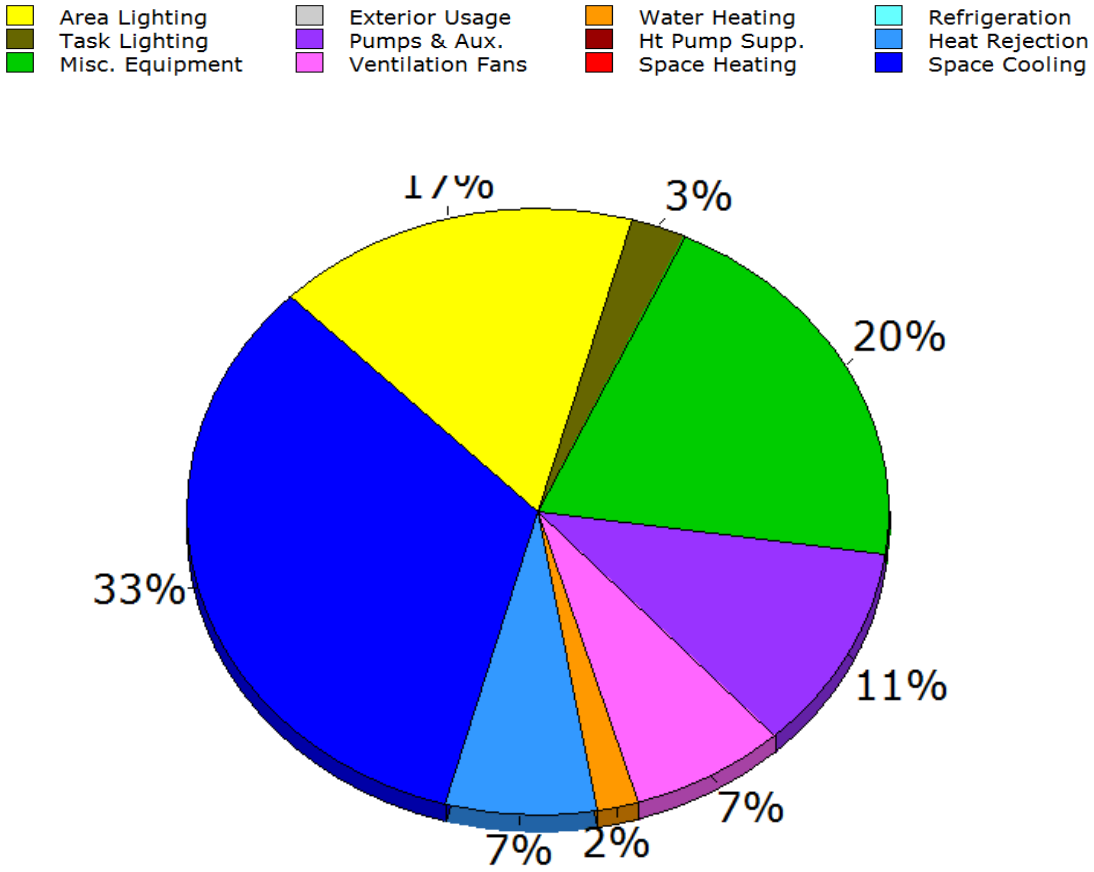

Figure 5.10 Percentage of annual energy consumption in base case model according to eQUEST program

The largest category of energy consumed to reach comfort levels was for space cooling. Space cooling, when coupled with heat rejection, comprised nearly 40% of the total annual energy budget, reflecting the impact of large glass window facades in hot, arid weather conditions. Due to the Riyadh's latitude, solar radiation is the main cause of office space increases in temperature. The temperature difference between the outdoor and indoor air driving conduction is a secondary factor. Therefore, indoor spaces require mechanical air conditioning to reach comfort levels and to counteract window glazing gains in temperature. Energy needed for ambient lighting is 17% of the annual energy usage. Of course, light passing through the window into the office reduces the daytime demand for ambient illumination.

Electric Consumption (kWh x000)

	Jan	Feb	Mar	Apr	May	Jun	Jul	Aug	Sep	Oct	Nov	Dec	Total
Space Cool	117.7	107.8	136.0	141.7	164.5	166.5	177.0	186.2	177.4	176.9	141.8	127.2	1,820.6
Heat Reject.	21.0	18.9	27.0	30.0	35.8	36.0	38.3	40.2	39.5	38.3	30.4	24.7	380.1
Refrigeration	-	-	-	-	-	-	-	-	-	-	-	-	-
Space Heat	-	-	-	-	-	-	-	-	-	-	-	-	-
HP Supp.	-	-	-	-	-	-	-	-	-	-	-	-	-
Hot Water	9.3	8.6	9.8	9.3	9.3	8.5	8.3	8.5	7.5	8.5	8.2	8.7	104.5
Vent. Fans	29.4	27.4	32.1	30.3	34.0	34.8	36.7	36.0	32.8	36.8	31.6	29.7	391.6
Pumps & Aux.	49.9	45.0	49.9	48.9	50.4	48.8	51.1	52.1	49.9	51.4	47.8	49.9	595.1
Ext. Usage	-	-	-	-	-	-	-	-	-	-	-	-	-
Misc. Equip.	94.1	85.1	96.1	92.5	96.1	92.5	94.1	98.1	88.5	96.1	90.5	92.2	1,115.9
Task Lights	11.6	10.5	11.9	11.4	11.9	11.4	11.6	12.3	10.7	11.9	11.1	11.2	137.4
Area Lights	77.8	70.4	80.0	76.8	80.0	76.8	77.8	82.2	72.5	80.0	74.6	75.7	924.6
Total	410.8	373.7	442.8	440.9	482.0	475.2	494.9	515.5	478.8	500.0	436.0	419.2	5,469.8

Figure 5.11 Total monthly energy segments in base case model according to eQUEST program

This base-case building with a single layer window system used a total of 5470 kilowatt-hours to maintain comfort levels. Monthly energy usage also exhibits seasonality for electricity consumption in kWh. Here are notable simulation results.

1) Space cooling is the single most significant energy-consuming task with a total of 1820.6 kWh for the whole year. Space cooling ranges from February's 108 kWh to August's 186 kWh, reflecting nearly 30 percent to 40 percent of total usage, respectively.

2) Ambient lighting energy remains virtually constant throughout the year ranging from 70.4 kWh to 82.2 kWh for an average of 77 kWh (+/-10%). Even though the single layer window allows light to penetrate outer-edge office zones, the core central zone still requires artificial light to attain comfortable vision levels.

3) Operating energy for fans, pumps and other equipment as a whole demanded nearly 2100 kWh of annual electricity for nearly 40% of the building total. In round terms, 40% of usage was allocated for seasonal A/C and heat rejection, 40% for constant equipment operation, and 20% for task and ambient lighting that did not change much monthly.

The building simulation also tallied utility bills and monthly expenses to operate the building and reach comfort levels. The annual electricity bill was 1.01 million Saudi Riyals, equivalent to 270,000 USD (five cents / kWh). Higher costs ran from April through October as air conditioning peaked to maintain office comfort, adding about 20% to off-season billing amounts.

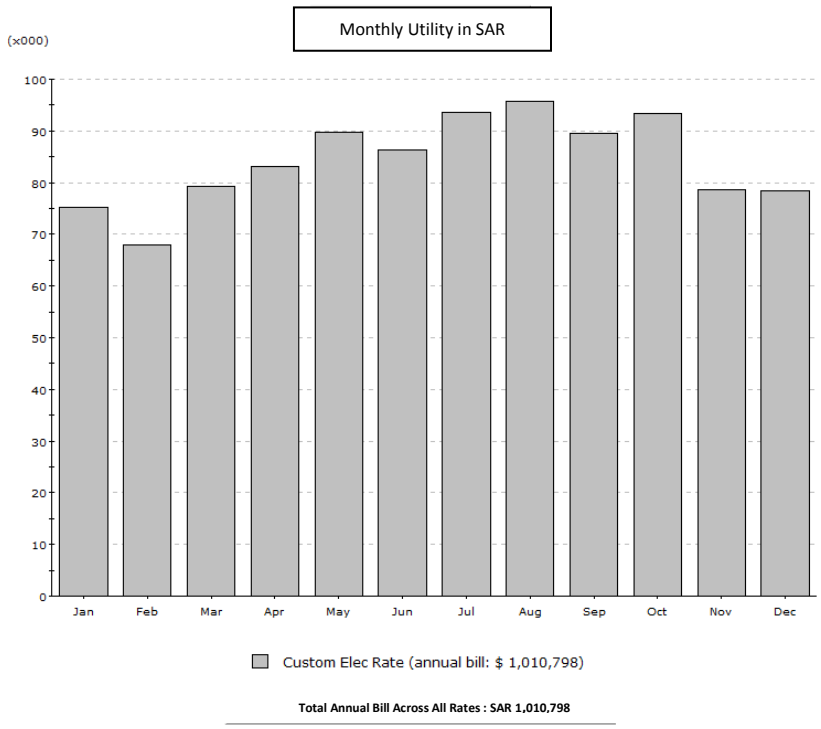

Figure 5.12 Total monthly energy usages in base case model.

5.8.2 Double skin façade system window calculations and savings

Since eQUEST simulates only single skin facades, this study needed a direct and practical method for capturing DSF heat removed with reference to the base-case Riyadh simulation. It was decided to expose the models for DSF performance from Blacksburg test regressions to a Riyadh weather file.

This climate extrapolation applied to a single window fixture of 4'x 8' was next amplified by area for the 320-window base case façade facing south to aggregate the facility's potential energy savings. Such a process could be replicated for various designs at another site by applying its location's weather file to both the eQUEST base case and the 4'x 8' DSF boxplot for heat removed per window area. This procedure promises a fair estimate without any uncertain, complex tampering within eQUEST's internal code.

Riyadh's major solar radiation component undergoes this basic treatment:

1) Riyadh's weather file Et engages the DSF's angle-dependent solar heat gain coefficient (SHGC typically 0.4) for entry into the window's nearly three square-meter area.
2) Solar radiation entering the DSF is combined with heat conduction flowing due to air temperature gradients across the DSF for total Qin.
3) Riyadh's hourly Et and difference in outdoor-indoor air temperatures are also fed into the HRR regression model to compute Riyadh's HRR.
4) One DSF unit's heat removed (Btu/hr) = Riyadh's HRR * Riyadh's Qin.
5) Heat removed is then rescaled for 320 windows, converted to kWh of heat, translated into electrical consumption via an air-conditioning coefficient of performance (CoP=3), and cast as a percentage of the building's base-case A/C energy consumption and of the site's total electrical usage.

Sample results of this process are presented in the next section.

5.8.2.1 Heat removal rate

To sense extrapolation from a summer test day in Blacksburg to Riyadh's hot, arid climate, Tables 5.5 through 5.8 list descriptive statistics and sample thermal data for each. First, a 7/2 test in Blacksburg (Table 5.6) saw a solar flux of 332 Btu/h-SF with peak HRR=0.57 and heat removed of 1296 Btu/hr. July in Riyadh (Table 5.8) shows 400, 0.81 and 2824 for each, respectively.

Table 5.5 Blacksburg DSF Descriptive Statistics 6:45-20:00 July 1-7, 2015

Variable	*S. Dev.*	*count*	*sq rt*	*Std. E*	*Mean*	*Min*	*Max*
Et (Btu/h-SF)	78.14	380	19.49	4.01	198.4018	41.3498	339.0433
Toa	6.68	380	19.49	0.34	77.5493	60.7300	92.0000
T cav in	0.29	380	19.49	0.01	75.1862	73.9000	75.9000
T cav out	2.18	380	19.49	0.11	77.7810	75.1000	83.1000
Q removed	356.47	380	19.49	18.29	448.4346	17.2800	1296.0000
SHGC Et A	566.63	380	19.49	29.07	2154.0461	563.0218	*3020.9153*
U A |To-Ti|	51.93	380	19.49	2.66	18.6848	-112.8285	127.2978
HRR	0.13	380	19.49	0.01	0.1995	0.0083	0.5654

Table 5.6 Blacksburg DSF July 2, 2015 Sample Thermal Performance Data 12:00-14:45

Qs	Qc	Q removed	HRR	SHGC	ALT	Toa-Tin	Et Btu/h SF
2755.59	51.39	898.56	0.32	0.30	66.75	6.50	293.00
2652.98	57.72	950.40	0.35	0.28	69.20	7.30	303.15
2562.25	63.25	1019.52	0.39	0.26	71.42	8.00	316.47
2441.09	69.58	1088.64	0.43	0.24	73.31	8.80	325.98
2305.62	70.37	1173.57	0.49	0.22	74.75	8.90	329.72
2208.02	70.37	1202.04	0.53	0.21	75.61	8.90	330.42
2202.39	68.79	1209.60	0.53	0.21	75.76	8.70	332.32
2222.65	69.58	1296.00	0.57	0.22	75.20	8.80	325.34
2319.91	63.25	1140.48	0.48	0.23	73.99	8.00	319.64
2426.94	60.09	1036.80	0.42	0.25	72.28	7.60	310.12
2524.67	52.97	984.96	0.38	0.27	70.18	6.70	298.07
2657.75	46.65	846.72	0.31	0.29	67.82	5.90	291.16

Conduction driver *Toa-Tin* hovered near 9F for the Blacksburg test with the conduction component near 70 Btu/hr. Riyadh has triple the temperature difference and conduction (Table 5.8) of 29F and 229 Btu/hr.

As expected, radiation (Qs) dominates the total heat load (over 90%) at both locations, except at dusk in Riyadh and when its noon sun's near-vertical ALT plunges SHGC to 5%. Maximum radiant heat load Qs in Riyadh in Table 5.7 below nears 4200 Btu/hr – 40% above Blacksburg's peak of about 3000 (Table 5.5).

Table 5.7 Riyadh DSF Performance Descriptive Statistics Using 1980 Hourly DOE-2 Weather File: lower-than-Blacksburg Means reflect Riyadh's 24-hour annual data vs. summer daylight-only test in Blacksburg.

Variable	*S. Dev.*	*count*	*sq rt*	*Std. E*	*Mean*	*Min*	*Max*
Et (Btu/hr-sq.ft)	129.96	8760	93.59	1.39	96.69396066	0	409.877118
Toa	8.52	8760	93.59	0.09	86.56883562	62	109
T cav in	1.99	8760	93.59	0.02	78.16666667	76	80
Qs = SHGC Et A	1391.96	8760	93.59	14.87	1072.93451599	0	4201.837723
Qc = UA|To-Ti|	76.55	8760	93.59	0.82	66.43336969	-142.32047	260.9208661
model HRR Et,dT	0.14	8760	93.59	0.00	0.26508598	0.085000314	0.852703484
model HRR*Qi	667.01	8760	93.59	7.13	431.53041918	-9.9920144	3025.837581

Table 5.8 Riyadh DSF July 16, 1980 Sample Near-Maximum Thermal Performance Data 6:00-17:00

Toa-Tin	Et W/sq.m	ALT	Et Btu/h-SF	HRR	Q solar	Q conduct	Qin	HRR*Qin	SHGC
11.00	181.21	8.99	57.46	0.17	782.37	86.97	869.34	144.34	0.43
13.00	470.10	22.02	149.07	0.15	2022.38	102.79	2125.17	323.96	0.43
14.00	759.80	35.34	240.93	0.26	3200.98	110.69	3311.68	862.65	0.42
20.00	999.98	48.85	317.09	0.47	3934.66	158.13	4092.80	1925.04	0.39
27.00	1175.63	62.46	372.79	0.69	3872.39	213.48	4085.87	2824.06	0.33
29.00	1263.52	76.02	400.66	0.79	2616.66	229.29	2845.96	2311.14	0.21
29.00	1263.44	86.73	400.64	0.78	*645.78*	*229.29*	875.07	710.54	*0.05*
26.00	1167.43	75.63	370.19	0.68	2471.10	205.57	2676.67	1811.23	0.21
27.00	994.73	62.07	315.43	0.50	3301.73	213.48	3515.21	1751.77	0.33
26.00	749.11	48.45	237.54	0.31	2956.84	205.57	3162.41	982.95	0.39
26.00	457.91	34.94	145.20	0.21	1931.26	205.57	2136.84	452.93	0.42
27.00	171.24	21.62	54.30	0.24	*736.87*	*213.48*	950.35	232.15	0.43

As surveyed in Table 5.8, Riyadh's 7/16 median HRR and heat removed during office hours (omitting the first 6am line) are 0.47 and 983 Btu/hr, respectively – twice the Blacksburg averages of 0.2 and 448 (Table 5.5).

Does the doubling of heat removed extrapolating to Riyadh make sense? Recall the HRR regression model's dominant term: the square of Et-120. Peak Et in Riyadh of 410 yields a 410-120 gap of 290, and the Blacksburg maximum Et of 340 yields a difference of 220 Btu/h-SF. The ratio of *Et-120* differences is 290/220 ~ 4/3. Squaring 4/3 yields 16/9 for a near double. Since heat removed is mainly HRR * Et, and maximum Et increases another 20% in Riyadh from 340 to 410, then heat removed should surpass 19/9 for more than double. Tripling the minor conduction component boosts both HRR and heat removed a bit further to confirm the Riyadh extrapolation.

Totaling all 8760 system operation hourly heat removed per one DSF unit using Riyadh's 1980 annual weather file for comparison with base case usage is shown next:

Table 5.9 Total annual DSF heat removed as a percentage of base case usage: A/C and whole building.

One DSF annual heat removed		***3780206***	***Btu/hr***
		1108	*kWh*
A/C Electricity saved per DSF		369	kWh
Electricity cost savings per DSF unit	*SAR*	*18*	

A/C CoP	SAR per kWh
3	0.05

eQUEST base usage MWh per year		5500	MWh/yr
A/C Electricity usage / year @ 40%		2200	MWh/yr
320 DSF windows annual savings		118	MWh
% A/C usage saved		5%	
% Building usage saved		2%	

Clearly, DSF offers very limited energy savings. The nearly 4 MBtu/hr of heat removed per one DSF unit converts to 1100 kWh of annual heat removal. Since air-conditioning (A/C) exploits the evaporative power of refrigerants, A/C takes less than 1/3 W of electricity to counter every Btu of heat load. Electricity saved for cooling drops below 400 kWh per DSF yearly in Riyadh. At this city's utility rate of five cents per kWh, less than $20 is saved per DSF window unit each year.

Multiplying the annual 400 kWh utility savings per DSF by a 300-window south façade totals about 120 MWh. When scaled against the yearly base-case A/C usage of 2200 MWh, 5% savings is observed. This 120 MWh represents only 2% of eQUEST's total base usage near 5500 MWh annually.

A final check of the figures may use a global annual solar flux map placing Riyadh in the 2500 kWh/sq.m area:

1) 4'x 8' DSF unit area of about three sq.m captures 7500 kWh.
2) SHGC of 0.4 reduces radiant heat load to 3000 kWh.
3) HRR averaging 0.4 yields heat removed of 1200 kWh.
4) A/C coefficient of performance (CoP=3) confirms 400 kWh savings per DSF.

5.8.2.2 Light transmission effect on energy usage

Since the DSF thermal performance offered no significant energy savings, and since reduced light transmission through the DSF only worsens utility bills for greater ambient lighting needs, LT merits no further discussion here.

5.9 Results and conclusion

Could a change in the aspect ratio of the building plus a heightened HRR improve DSF energy savings in hot, arid climates? Even 100% HRR by closing the shades to boost energy savings by a factor of 2.5 recovers only about 15% of A/C and 5% of the total base usage. A tall, thin tower facing south may emphasize a southern façade's impact while reducing rooftop and sidewall effects so that half of the tower's skin is DSF. Perhaps another twofold enhancement here? When starting at such a low of 2-5% savings, even exaggerated gestures seem modest.

While DSF captures sunlight efficiently for heating European winter offices, it seems the well-designed SHGC (0.4) itself nicely shields even a hot, arid site from high A/C usage. Future thermal performance is more likely to come from glass-coating innovation and better A/C coefficients of performance than from DSF exploits. Lastly, ambient lighting efficiency is gaining ground with LED fixtures in ways that make DSF light transmission loss more and more irrelevant in any analysis of HRR vs. LT trade-offs for double skin arrays.

Only if utility rates skyrocket in Riyadh (very unlikely) may site orientation and amazing DSF cavity-shade maneuvers be considered for removing enough heat to justify DSF installation – even in hot, arid climates.

6. Chapter Six Conclusion and Future Work

6.1 Summary

In today's architecture, the aesthetic demand for large glazing areas may be adversely affecting the quality of office spaces in hot, arid climates. Glass as a building material has relatively low insulation properties with higher heat transfer rates. Glass buildings in hot, arid weather conditions are thus mechanically air-conditioned to maintain comfort environments. In a hot, arid city like Riyadh, Saudi Arabia, office buildings have been designed with sizable window areas without a quantitative consideration of climate conditions and how comfort levels in the facility are impacted. Office buildings with high glazing areas can consume significant energy for cooling in hot, arid climates. As a result, government agencies in Saudi Arabia have recently been studying the energy usage in these buildings and are seeking fresh solutions to conserve energy needed to achieve comfort levels.

In this research, the goal was to study the double skin façade system as a potential innovative solution for controlling energy consumption and electricity use in office buildings. Prior to this research, there had been no clear quantitative understanding of precisely how the double skin façade system performs in hot, arid climate conditions.

Double skin façade systems were thought to offer the desired glass facades while balancing the environmental effects of electricity production to meet energy demands. This study, however, showed quantitatively that double skin façade systems, regardless of configuration, do not improve a building's façade performance enough to decrease heat loads in office spaces to significantly lower the electrical energy needed to mechanically air-condition the space for comfort.

A full-scale single facade base case model was simulated as a reference for energy usage comparison with double skin facade unit performance. Testing the relationship among sun angle, solar radiation, outdoor temperature, light transmission and heat removal rate favored regression of test findings for extrapolation to an office building in hot, arid climate conditions to quantify the DSF system thermal performance potential.

The double skin façade has not been available in any simulation program. Studying double skin performance thus required a workable procedure to compare the double skin façade system performance to a single-layer window base model. An experimental test located in Blacksburg, VA was conducted to evaluate the effects of solar radiation and outdoor air temperature on the heat gained in the double skin façade system cavity. Then, calculation and regression analysis allowed us to quantify the heat removal rate inside the cavity for extrapolation to Riyadh's climate.

The performance of the double skin façade and the regression analysis from experimental data allowed comparison with a hypothetical base-case office building in the city of Riyadh, Saudi Arabia. The weather file of Riyadh, Saudi Arabia was applied to the DSF regression model for heat removal rate. Thermal performance of one double skin façade unit was next multiplied by the total southern façade area for comparison to a typical single layer window system used in Riyadh, Saudi Arabia. The energy simulation results provided a clear reference for assessing the potential benefits of using the double skin façade system for removing heat captured in the DSF cavity.

6.2 Conclusive finding

This study's simulation analysis clearly rejects any hypothesis that the double skin façade system used for this study can be useful in hot, arid climates in reducing energy consumption versus the traditional single layer double panel window base case. The double skin façade system showed a minimal 2-5% reduction in baseline energy usage needed to reach comfort levels inside the building.

6.3 Research limitations

This research began with an experimental setup in Blacksburg, VA to study the performance of the double skin façade system. The testing involved building a full-scale double skin façade unit in a test chamber to measure

the performance of the system during hot summer months. The goal was to quantify key variables affecting the performance of the DSF system: sun angle, solar radiation, outdoor air temperature, light transmission and heat removal rate in the cavity. The following limitations constrained our study:

1) Location: the experimental setup was conducted in Blacksburg, VA. Temperatures in this location rise to about 90ºF in hot summer months. Blacksburg summer weather cannot represent a hot, arid climate. With the goal of identifying the influence of sun angle, solar flux and outdoor air temperature on heat removal rate, test data for the warmest and sunniest days were collected to create a regression model permitting extrapolation of DSF performance in hot, arid climate for comparison with base-case facility simulation in eQUEST.
2) Double skin model: literature review findings forged the decision to build a one-story test chamber installed with a double skin façade unit aimed south served by mechanical ventilation. One constraint was the inability to study more than one double skin façade system with different cavity widths. Tight resources limited our study to one double skin façade unit, mechanically ventilated with a wide cavity.
3) Case Study: for this research, a hypothetical office building was simulated per ASHRAE 90.1 standards to compare the performance of the double skin façade system to a traditional baseline office building using the single layer façade system. Difficulties obtaining blueprints and utility bills for an existing office building in Riyadh, Saudi Arabia forced the hypothetical simulation.

In conclusion, the experimental setup data effectively yielded multiple regression models approximating the relationships among key variables, the heat removal rate and light transmission for comparison with simulated base case energy usage. The energy simulation clear indicated that the double skin façade system offers virtually no savings at current utility prices.

6.4 Proposed future studies

This research examined the performance of the double skin façade system in hot, arid climate conditions using a combination of experimental testing, regression analysis and building energy simulation. The aim was to quantify how much the double skin façade system improves the quality of indoor space while reducing energy usage to reach comfort levels. Based on our findings from this research, some additional studies may ensue if utility rates rise exponentially in the future:

1) Cavity-width, shade-angle investigation:
   Research can study multiple double-skin façade system performance with various cavity widths and shade-angle settings to configure the best array for better heat removal rate in hot, arid weather conditions. A bigger cavity, actively shaded, may intercept more of the inbound heat load without much loss in light transmission.

2) Existing building energy simulation where kWh rates exceed 30 cents:
   Current buildings with a traditional window type can be simulated as a base case while applying this study's DSF-HRR regression model with local weather data for comparing performance and energy savings.

3) Double skin façade system comprehensive cost-savings analyses:
   Research can focus on itemized installation and operating costs of a double skin façade system compared to single layer façade systems. Determination of a price point for DSF benefits in the context of future kWh rate hikes and low interest rates may truncate the payback time.

References

Al-Senea, S. A., Sedan, M. F., & Al-Ajlan, S. A. (n.d.). *Adjustment factors for the ASHRAE clear-sky model based on solar-radiation measurements in Riyadh*(79th ed., Vol. 4, Ser. 2).

Alnaser, N.W (2005, August, 26). The Need of Sustainable Buildings Construction In the Kingdom of Bahrain . Building and environment. 495-506.

Alnaser, WE, & Alattar, R (1999). simple models for estimating the total diffuse, direct and normal solar irradiation in Bahrain. Renewable Energy. 18, 417-434.

Baden, S., et al., (2006).Hurdling Financial Barriers to Lower Energy Buildings: Experiences from the USA and Europe on Financial Incentives and Monetizing Building Energy Savings in Private Investment Decisions. Proceedings of 2006 ACEEE Summer Study on Energy Efficiency in Buildings. 8-5, 8-6, 8-7.

Bartak, M., Dunovska, T., & Hensen, J. (2001). Design support simulations for a double-skin facade . 01,

Brainard , J. (2010, March 18). The Eyes and vision . Retrieved from http://www.ck12.org/ck12/images?id=293643

Brown, G., DeKay, Mark, Library, British, & Architects, Royal. (2001). Sun, wind& light. John Wiley & Sons Inc.

Compagno, Andrea. (1995). Intelligente glasfassaden. Birkhauser.

Daniels, Klaus. (1997). The Technology of ecological building. Berlin: Birkhauser.

Fischer, Volker, Grüneis, Horst, & Richter, Ralph. (1997). Sir norman foster and partners. Edition Axel Menges.

Gavan, V., Woloszyn, M., Kuznik, F., & Roux, J. (2009). Experimental study of a mechanically ventilated double-skin facade with venetian sun-shading device: a full-scale investigation in controlled environment. Solar Energy, (84), 183-195.

Gratia, E., & Herde, A. (2004). Natural ventilation in a double-skin facade. Energy and Buildings, (36), 137-146.

Gratia, E, & Herde, A. (2004). Natural cooling strategies efficiency in an office building with a double-skin façade. Energy and Buildings, 1(36), 1139–1152.

Gratia, E., & Herde, A. (2006). Guidelines for improving natural daytime ventilation in an office building with a double-skin facade. Solar Energy, 81, 435-448.

Groat, I. N., & Wang, D. (2004). Architectural research methods. Wiley.

Haase, M, & Amato, Alex. (2006). Ventilated facade design for hot humid climate. 1,

Hensen, J, Bartak, M, & Drkal, F. (2002). Modeling and simulation of double-skin facade system. American Society of Heating, Refrigerating and Air-Conditioning Engineers, 108(2),

Klems, J. H. (2011). The mobile window thermal test facility (mowitt). Retrieved from http://escholarship.org/uc/item/30g2t4p4

Konya, Allan (1984). Design Primer for hot climates. London, UK: Architectural Press.

Oesterle, Eberhard. (2001). Double-skin facades. Prestel Pub.

Ott, L., & Longnecker, M. (2010). *An introduction to statistical methods and data analysis*. Belmont, CA: Brooks/Cole Cengage Learning.

Mostaedi, Arian. (2002). Facades. Links Internacional.

Saeed, ARS (2001).Energy savings using bioclimatic architecture with special reference to Bahrain. Architecture Since Review. 44, 277-284.

Stec, W., & Passen, D. (2003). Defining the performance of the double skin facade with the use of the simulation model. Building simulation, 2,

TSI 8475-03 Air Velocity Transducer 3" Omni Directional Probe [Web Photo]. Retrieved from http://www.mitchellinstrument.com/air-velocity-transducer-tsi-8475-03-air-flow.html

US Department of Energy. Annual Energy Review 2006 27 June 2007. Accessed 26 Oct 2008.

Wong, P.C, Prasad, D, & Behania, M. (2008). A new type of double-skin facade configuration for the hot humid climate. 1.